DEPARTMENT OF CIVIL ENGINEERING

UNIVERSITY OF SOUTHERN CALIFORNIA

PRELIMINARY EMPIRICAL MODELS FOR SCALING RELATIVE VELOCITY SPECTRA

by

Mihailo D. Trifunac and John G. Anderson

Report No. CE 78-05

A Report on the Research Conducted Under a
Contract from the U.S. Nuclear Regulatory Commission

Los Angeles, California

August, 1978

ABSTRACT

This report presents two empirical models for estimation of Relative Velocity Spectrum amplitudes (SV), for scaling in terms of (i) earthquake magnitude and epicentral distance, or (ii) Modified Mercalli Intensity (MMI), at the recording station. These models also present dependence of SV amplitudes on geologic site conditions, horizontal or vertical direction of motion and on the selected confidence level that the chosen spectrum amplitudes will not be exceeded.

INTRODUCTION

This report is the last in a series devoted to characterization of strong earthquake ground motion in terms of geologic site classification. It presents two empirical scaling functions for relative velocity spectrum amplitudes, SV. This series of reports was initiated with the analysis of duration of strong shaking (Trifunac and Westermo, 1976a,b) and continued with empirical scaling models for Fourier amplitude spectra (Trifunac, 1976, 1978), absolute acceleration spectra, SA (Trifunac and Anderson, 1977), and pseudo relative velocity spectra, PSV (Trifunac and Anderson, 1978). In this report, we employed the same scaling functional forms as in all our previous work to derive the empirical dependence of spectral amplitudes on (1) magnitude, M, epicentral distance, R, or (2) Modified Mercalli Intensity, MMI, at the recording station.

The essential common link in this series is the characterization of the recording site conditions in terms of a rough site classification, s, with essentially two groups: (1) alluvium and sediments (s=0) and (2) sound igneous rock (s=2). For the site which cannot be unequivocally grouped into s=0 or s=2, typically corresponding to consolidated sedimentary rock or to a complex geologic environment (Trifunac and Brady, 1975), we have selected an "intermediate" classification, s=1. Current research by the authors has shown that a more refined site characterization is possible in terms of the depth of sediments at each recording station. In numerous circumstances, however, little is known about the

depth of alluvium and sedimentary layers at a site so that the scaling in terms of s=0, 1 and 2 remains a useful approach to the scaling of amplitudes and the duration of strong shaking.

The data on SV spectra which represent the basis for empirical models presented here consists of the same 186 records studied in our previous work. For completeness of this presentation, we summarize the distribution of this data among different magnitudes, Modified Mercalli intensities and site classification groups. The distribution of data among magnitude intervals is as follows: 3.0 to 3.9, 1 record; 4.0 to 4.9, 5 records; 5.0 to 5.9, 40 records; 6.0 to 6.9, 129 records; and 7.0 to 7.9, 7 records; unknown, 4 records. The distribution of data among seven intensity levels is as follows: MMI = III, 1 record; MMI = IV, 3 records; MMI = V, 34 records; MMI = VI, 66 records; MMI = VII, 75 records; MMI = VIII, 6 records; and MMI = X, 1 record. The majority of recordings (117) were registered on stations located on alluvium and sedimentary deposits (classified under s=0; see Trifunac and Brady, 1975, for a detailed description of this classification and examples of assigning s=0, 1 or 2 to selected sites), 52 records came from stations located on intermediate type rocks (s=1), and 13 records came from stations on basement rocks (s=2).

To describe the effects of digitization and processing noise on the amplitudes of SV spectra we employed the data on hand-digitized straight line (Trifunac, 1976, 1978) to calculate SV spectra that would result from digitization and processing noise only. The spectra that result from this noise, for durations of noise record equal to 15 sec,

30 sec, 60 sec, and 100 sec are presented in this report in all figures which deal with SV amplitudes. Following the procedures described by Trifunac (1976), 13 individual digitizations were used to compute SV spectrum amplitudes. Figures in this report then present the average and average plus one standard deviation of SV amplitudes for these 13 records.

MODELS FOR SCALING SA SPECTRA

Following the previous work on scaling Fourier amplitude spectra, (Trifunac, 1976, 1978), absolute acceleration spectra, SA (Trifunac and Anderson, 1977), and pseudo relative velocity spectra, PSV (Trifunac and Anderson, 1978), we write the empirical equations for scaling the relative velocity spectra, SV, at an undamped period, T, of a single-degree-of-freedom, viscously damped, oscillator as

$$\log_{10}[SV(T)_{,p}] = M + \log_{10}A_o(R) - a(T)p - b(T)M - c(T) - d(T)s - e(T)v - f(T)M^2 - g(T)R \quad (1)$$

and

$$\log_{10}[SV(T)_{,p}] = a(T)p + b(T)I_{MM} + c(T) + d(T)s + e(T)v \ . \quad (2)$$

In (1), M represents published earthquake magnitude, which for most data points in this work (consisting of 57 earthquakes), corresponds to the local magnitude scale M_L (Richter, 1958). $\log_{10}A_o(R)$ (Table I) describes amplitude attenuation with distance, R, between the station and earthquake epicenter. Parameter p, between 0.1 and 0.9, approximates the probability that $SV(T)_{,p}$ will not be exceeded. s describes local geologic site classification (Trifunac and Brady, 1975) with s=0 for alluvium sites, s=1 for "intermediate" sites, and s=2 for basement rock sites. v stands for component direction, with v=0 used for horizontal and v=1 for vertical spectral amplitudes. In (2), I_{MM} represents numerical values assigned to the MMI levels with I_{MM} = 3, 4, 5,... corresponding to MMI = III, IV, V,... . The meaning of p, s and v in (2) is identical to that in equation (1).

TABLE I

$\log_{10}A_o(R)$ Versus Epicentral Distance R*

R (km)	$-\log_{10}A_o$	R (km)	$-\log_{10}A_o(R)$	R (km)	$-\log_{10}A_o(R)$
0	1.400	140	3.230	370	4.336
5	1.500	150	3.279	380	4.376
10	1.605	160	3.328	390	4.414
15	1.716	170	3.378	400	4.451
20	1.833	180	3.429	410	4.485
25	1.955	190	3.480	420	4.518
30	2.078	200	3.530	430	4.549
25	2.199	210	3.581	440	4.579
40	2.314	220	3.631	450	4.607
45	2.421	230	3.680	460	4.634
50	2.517	240	3.729	470	4.660
55	2.603	250	3.779	480	4.685
60	2.679	260	3.828	490	4.709
65	2.746	270	3.877	500	4.732
70	2.805	280	3.926	510	4.755
80	2.920	290	3.975	520	4.776
85	2.958	300	4.024	530	4.797
90	2.989	310	4.072	540	4.817
95	3.020	320	4.119	550	4.835
100	3.044	330	4.164	560	4.853
110	3.089	340	4.209	570	4.869
120	3.135	350	4.253	580	4.885
130	3.182	360	4.295	590	4.900

* Only the first two digits may be assumed to be significant.

As in our previous work dealing with empirical scaling of Fourier, absolute acceleration, and pseudo relative velocity spectrum amplitudes, the functional form of equation (1) has been motivated by the definition of local magnitude scale (Richter, 1958) which states that the logarithm of response amplitude on a standard instrument and corrected for attenuation with R ($\log_{10}A_o(R)$) is equal to M. The terms $a(T)p + b(T)M + c(T) + d(T)s + e(T)v + f(T)M^2 + g(T)R$ then represent an empirical correction function in M, s, v and R. The terms $b(T)M$ and $f(T)M^2$ are motivated by previous approximate source spectrum analysis (Trifunac, 1973) and by direct observation of spectral amplitudes computed from recorded accelerograms (Trifunac, 1976). Anelastic amplitude attenuation with distance, R, is often described by $\exp\left\{-\frac{\pi R}{TQ\beta}\right\}$ where Q is attenuation constant and β is shear wave velocity. g(T) does not correspond directly to $(\pi/TQ\beta)\log_{10}e$, however, since anelastic attenuation is also included in $\log_{10}A_o(R)$. Functions d(T) and e(T) model frequency dependent changes of spectral amplitudes with respect to geologic site conditions and direction of motion, respectively.

To derive scaling functions a(T), b(T) through g(T), all data was partitioned into groups corresponding to magnitude ranges 4.0 to 4.9, 5.0 to 5.9, 6.0 to 6.9 and 7.0 to 7.9. These groups were further divided into three sub-groups corresponding to site classification s=0, s=1 and s=2. Each of these sub-groups was finally subdivided into two parts corresponding to v=0 and v=1. Within each of these parts, n data points on $\log_{10}[SV(T)] - M - \log_{10}A_o(R)$ were rearranged to create a monotonically decreasing sequence. With m = integer part of (pn) and $0.05 \leq p \leq 0.95$,

the m^{th} point then represents an estimate of an upper bound on $\log_{10}[SV(T)] - M - \log_{10}A_o(R)$ for which 100p percent of the corresponding data set is less than that value. In subsequent regression calculations, at most 19 values of p = 0.05, 0.10, 0.15, ..., 0.90 and 0.95 were used to eliminate strong dependence of the final regression model on those earthquakes which contribute most to the present data set. For instance, the San Fernando, California, earthquake of 1971 contributed 98 to the total of 187 records available for this study. The above method of data screening eliminated about 70 percent of San Fernando records before regression analysis at each T is performed to compute a(T), b(T), ..., and g(T).

For computation of a(T), b(T), ..., e(T) in equation (2), a similar procedure was adopted. The data on $\log_{10}SV(T)$ were first distributed into groups corresponding to intensity levels III, IV, V, VI, VII, VIII and X and then into sub-groups and parts, as above, corresponding to site classification and component direction. From that point on, and prior to regression analysis, the same procedure of eliminating data from different groups and parts, to diminish undue influence of earthquakes which generated numerous records, was followed.

a. Correlations in Terms of M, R, p, s and v

Figure 1 presents the functions a(T), b(T), ..., f(T) and g(T) in equation (1) that resulted from regression analysis at 91 selected periods T and for five fractions of critical damping ζ = 0.0, 0.02, 0.05, 0.10 and 0.20. It shows coefficient functions smoothed by an Ormsby filter along $\log_{10}T$ axis. Table II

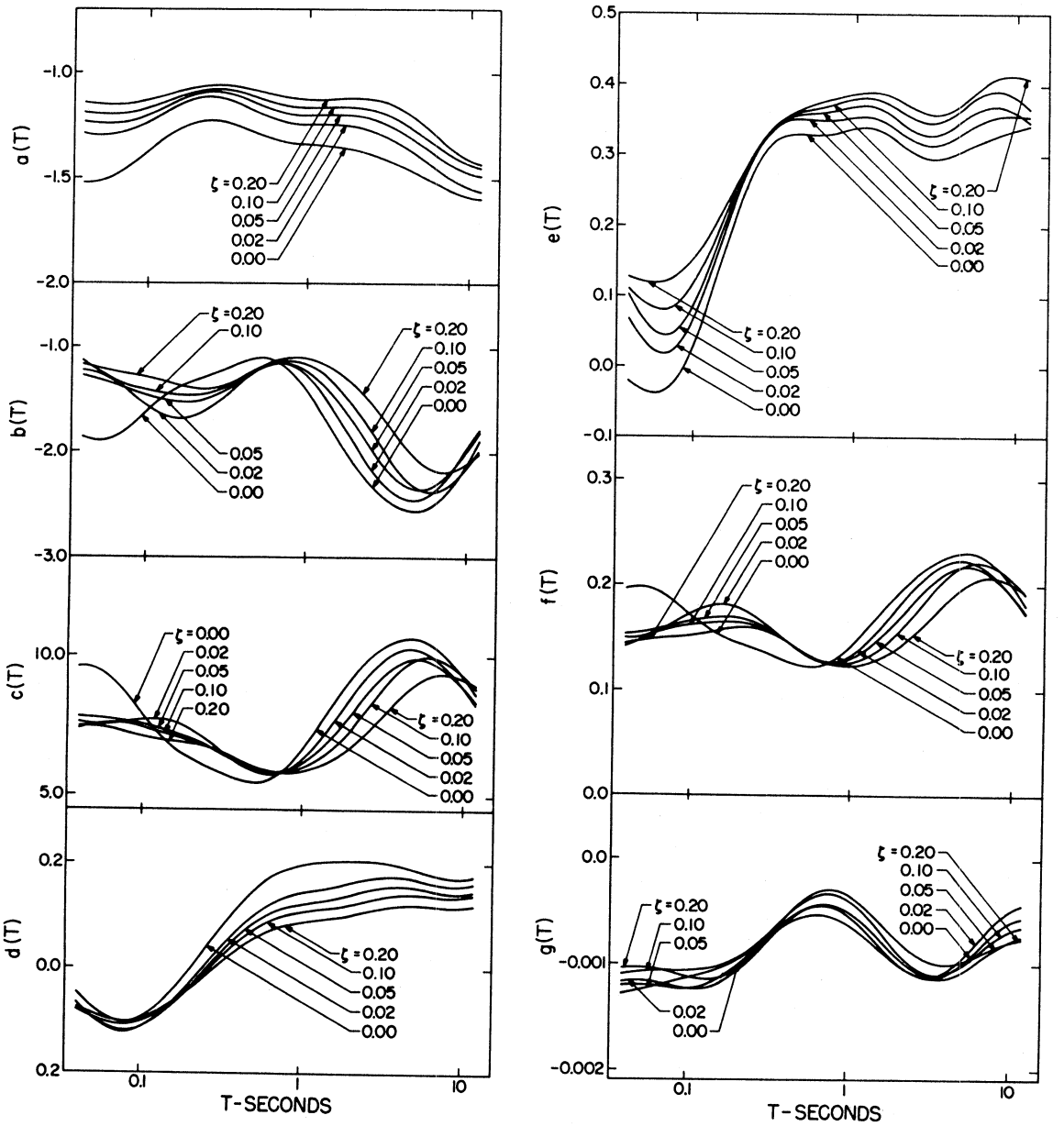
a(T)
-1.0
-1.5
-2.0
ζ = 0.20
0.10
0.05
0.02
0.00
b(T)
-1.0
-2.0
-3.0
ζ = 0.20
0.10
0.05
0.02
0.00
c(T)
10.0
5.0
ζ = 0.00
0.02
0.05
0.10
0.20
d(T)
0.2
0.0
0.2
0.1
1
10
T-SECONDS
e(T)
0.5
0.4
0.3
0.2
0.1
0.0
-0.1
f(T)
0.3
0.2
0.1
0.0
g(T)
0.0
-0.001
-0.002
0.1
1
10
T-SECONDS

FIGURE 1

TABLE II

Regression Parameters for Equation (1) and $\alpha(T)$, $\beta(T)$ and $N(T)^*$ at Eleven Selected Periods

$\log_{10}T$(sec)	-1.398	-1.168	-0.938	-0.708	-0.478	-0.247	-0.017	0.213	0.443	0.673	0.903
ζ = 0.0											
a(T)	-1.521	-1.469	-1.340	-1.241	-1.247	-1.310	-1.343	-1.359	-1.405	-1.479	-1.566
b(T)	-1.857	-1.836	-1.539	-1.327	-1.195	-1.105	-1.365	-1.905	-2.363	-2.549	-2.339
c(T)	9.629	9.059	7.491	6.365	5.753	5.502	6.490	8.419	10.041	10.645	9.975
d(T)	-0.047	-0.099	-0.083	-0.011	0.079	0.157	0.194	0.202	0.203	0.191	0.173
e(T)	-0.020	-0.033	0.065	0.227	0.321	0.329	0.338	0.330	0.297	0.307	0.330
10f(T)	1.961	1.912	1.644	1.456	1.332	1.227	1.390	1.781	2.126	2.304	2.169
1000g(T)	-1.203	-1.214	-1.219	-1.049	-0.749	-0.542	-0.600	-0.872	-1.111	-1.045	-0.721
$\alpha(T)$	1.142	1.135	1.143	1.198	1.273	1.501	1.803	2.299	2.646	3.973	4.387
$\beta(T)$	0.669	0.662	0.653	0.636	0.595	0.309	-0.081	-0.711	-1.205	-2.577	-2.799
N(T)	20	20	20	20	19	11	6	3	2	1	1
ζ = 0.02											
a(T)	-1.290	-1.286	-1.213	-1.130	-1.138	-1.212	-1.250	-1.253	-1.294	-1.391	-1.511
b(T)	-1.225	-1.357	-1.612	-1.664	-1.435	-1.181	-1.241	-1.691	-2.219	-2.447	-2.199
c(T)	7.627	7.583	7.736	7.393	6.499	5.810	6.189	7.745	9.509	10.283	9.545
d(T)	-0.066	-0.118	-0.104	-0.037	0.043	0.108	0.141	0.155	0.170	0.172	0.159
e(T)	0.068	0.019	0.100	0.251	0.339	0.350	0.354	0.345	0.316	0.332	0.356
10f(T)	1.490	1.579	1.770	1.791	1.575	1.315	1.309	1.640	2.047	2.236	2.059
1000g(T)	-1.173	-1.181	-1.236	-1.102	-0.769	-0.478	-0.510	-0.837	-1.104	-1.000	-0.630
$\alpha(T)$	1.160	1.132	1.120	1.181	1.280	1.536	1.849	2.342	2.688	3.990	4.358
$\beta(T)$	0.661	0.665	0.674	0.657	0.598	0.289	-0.116	-0.746	-1.235	-2.595	-2.781
N(T)	20	20	20	20	19	11	6	3	2	1	1
ζ = 0.05											
a(T)	-1.235	-1.239	-1.186	-1.108	-1.106	-1.172	-1.207	-1.203	-1.237	-1.331	-1.445
b(T)	-1.275	-1.376	-1.487	-1.523	-1.392	-1.187	-1.207	-1.541	-2.039	-2.342	-2.175
c(T)	7.796	7.700	7.450	7.050	6.427	5.875	6.116	7.272	8.913	9.914	9.439
d(T)	-0.067	-0.115	-0.105	-0.044	0.031	0.091	0.120	0.132	0.150	0.155	0.144
e(T)	0.102	0.044	0.118	0.255	0.342	0.359	0.369	0.360	0.330	0.350	0.369
10f(T)	1.533	1.594	1.672	1.691	1.556	1.332	1.294	1.538	1.923	2.169	2.048
1000g(T)	-1.283	-1.202	-1.111	-0.987	-0.731	-0.467	-0.475	-0.773	-1.081	-1.103	-0.869
$\alpha(T)$	1.159	1.133	1.127	1.186	1.288	1.545	1.868	2.385	2.764	4.104	4.457
$\beta(T)$	0.662	0.667	0.669	0.650	0.592	0.284	-0.129	-0.775	-1.279	-2.654	-2.835
N(T)	20	20	20	20	19	11	6	3	2	1	1

ζ = 0.10

a(T)	-1.190	-1.195	-1.156	-1.097	-1.087	-1.139	-1.170	-1.166	-1.191	-1.279	-1.400
b(T)	-1.132	-1.337	-1.426	-1.458	-1.367	-1.174	-1.150	-1.392	-1.876	-2.318	-2.299
c(T)	7.377	7.598	7.327	6.950	6.441	5.899	5.976	6.810	8.373	9.799	9.781
d(T)	-0.080	-0.105	-0.095	-0.044	0.023	0.078	0.106	0.115	0.130	0.141	0.136
e(T)	0.110	0.081	0.141	0.261	0.343	0.366	0.379	0.374	0.348	0.367	0.391
10f(T)	1.409	1.565	1.629	1.644	1.543	1.332	1.259	1.430	1.813	2.163	2.156
1000g(T)	-1.097	-1.065	-1.052	-0.969	-0.710	-0.397	-0.365	-0.698	-1.051	-1.049	-0.781
α(T)	1.151	1.131	1.130	1.190	1.288	1.550	1.877	2.418	2.830	4.206	4.537
β(T)	0.659	0.671	0.671	0.649	0.593	0.281	-0.133	-0.791	-1.306	-2.688	-2.855
N(T)	20	20	20	20	19	11	6	3	2	1	1

ζ = 0.20

a(T)	-1.144	-1.152	-1.120	-1.076	-1.068	-1.103	-1.132	-1.130	-1.138	-1.223	-1.368
b(T)	-1.165	-1.245	-1.307	-1.391	-1.350	-1.165	-1.103	-1.247	-1.593	-2.031	-2.174
c(T)	7.450	7.351	7.055	6.871	6.507	5.952	5.870	6.377	7.481	8.863	9.377
d(T)	-0.074	-0.099	-0.090	-0.046	0.013	0.061	0.086	0.096	0.110	0.121	0.117
e(T)	0.127	0.122	0.171	0.264	0.342	0.372	0.386	0.385	0.360	0.374	0.412
10f(T)	1.445	1.494	1.535	1.594	1.534	1.331	1.235	1.332	1.601	1.951	2.066
1000g(T)	-1.043	-1.057	-1.138	-1.077	-0.744	-0.371	-0.323	-0.615	-0.925	-0.986	-0.847
α(T)	1.136	1.129	1.141	1.204	1.300	1.552	1.879	2.437	2.889	4.324	4.616
β(T)	0.672	0.668	0.663	0.642	0.585	0.278	-0.136	-0.800	-1.334	-2.749	-2.889
N(T)	20	20	20	20	19	11	6	3	2	1	1

---

* See section entitled, "Distribution of Spectral Amplitudes" for definition of α(T), β(T) and N(T).

presents amplitudes of a(T) through g(T) at eleven selected periods. These coefficients yield SV in units of inches/second.

It has been suggested that close to an earthquake source, strong motion amplitudes cease to grow with magnitude, M (Trifunac, 1973). Several studies which dealt with empirical scaling of epicentral amplitudes (Trifunac, 1976; Trifunac and Anderson, 1977, 1978) have further confirmed that this interpretation is not contradicted by the data so far available. For this reason and to maintain consistency with our previous work, we re-write equation (1) as follows:

$$\log_{10}A_o(R) - \log_{10}[SV(T),_p] =$$

$$\begin{cases} -M_{max} + ap + bM_{max} + c + ds + ev + fM_{max}^2 + gR & M \geq M_{max} \\ -M + ap + bM + c + ds + ev + fM^2 + gR & M_{min} \leq M \leq M_{max} \\ -M + ap + bM_{min} + c + ds + ev + fM_{min}^2 + gR & M \leq M_{min} \end{cases}$$

Here, $M_{min} = b/2f$ and $M_{max} = (1-b)/2f$. It can be seen then that with these modifications, (1) assumes linear growth of $\log_{10}[SV(T),_p]$ with M for $M \leq M_{min}$, parabolic growth for $M_{min} \leq M \leq M_{max}$ and no growth for $M \geq M_{max}$. Figure 2 presents the plot of M_{max} versus T and for ζ = 0.0, 0.02, 0.05, 0.10 and 0.20. It shows that this analysis suggests that SV amplitudes cease to grow for $M \geq 7.5$ to 8, in agreement with analogous correlations of pseudo relative velocity spectra, PSV (Trifunac and Anderson, 1978), absolute acceleration, SA (Trifunac and Anderson, 1977), and Fourier amplitude spectra (Trifunac, 1976).

Functions a(T), d(T) and e(T) are very similar to those presented previously for scaling of PSV and SA spectra. The short period part

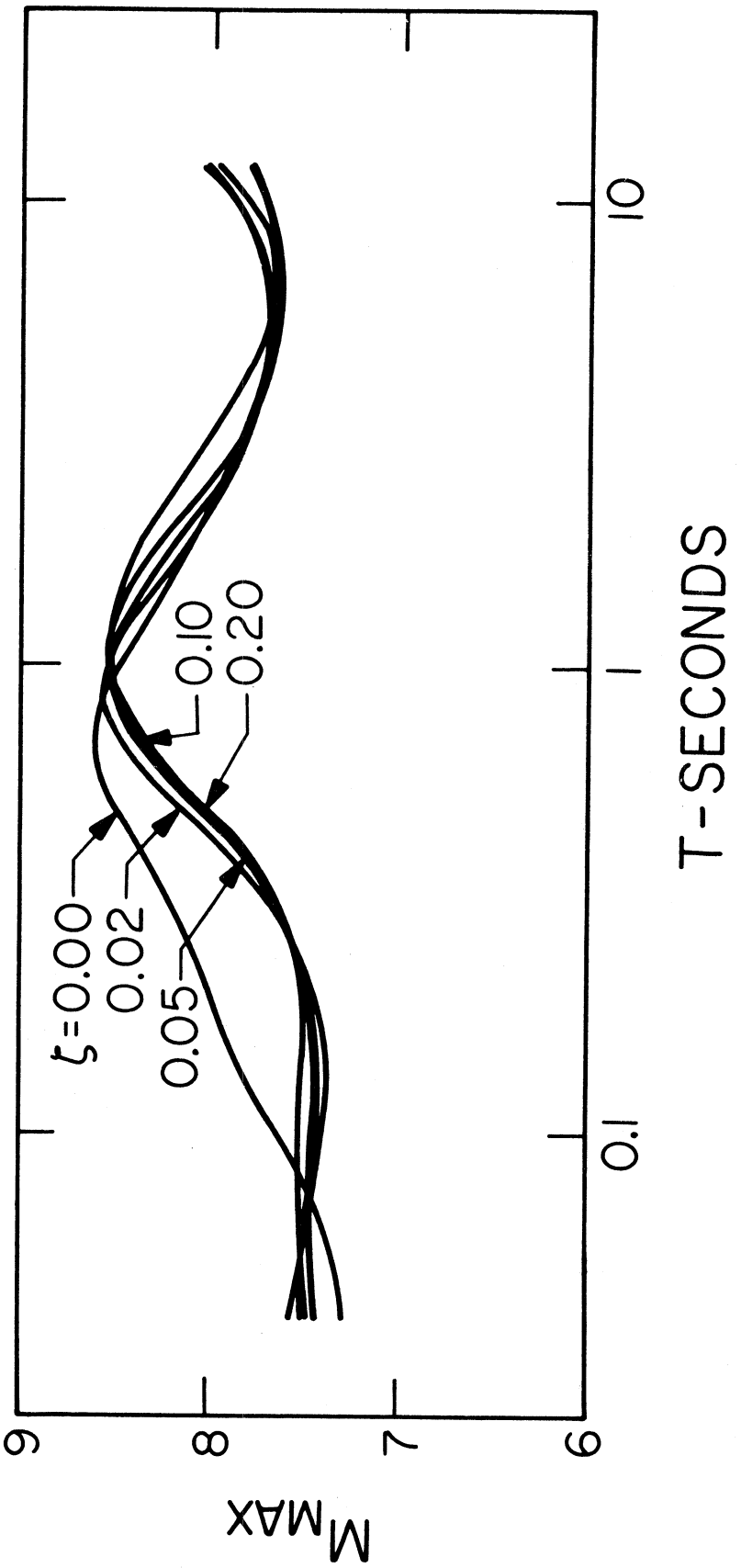

FIGURE 2

of e(T) is also very similar to e(T) for PSV and SA spectra. However, for long periods in Figure 1, e(T) is larger than in previous analyses suggesting greater differences between vertical and horizontal SV spectra relative to the corresponding differences for PSV and SA spectra. Functions b(T), c(T), and f(T), if compared with our previous work (Trifunac and Anderson, 1977, 1978) reflect differences in units employed in scaling different spectra as well as frequency dependent variations of different spectral amplitudes.

Figures 3 through 12 show horizontal and vertical SV amplitudes plotted for ζ = 0.0, 0.02, 0.05, 0.10 and 0.20, for p = 0.5, R = 0 km for the five magnitudes (M = 4.5, 5.5, 6.5, 7.5 and 8.5) and two geologic site classifications (s=0 for alluvium and s=2 for basement rock). For completeness in presentation, though outside the magnitude range for which data is now available, spectra for M = 8.5 have been plotted to show that, according to these correlations, maximum SV amplitudes are essentially recorded for M = 7.5+. All Figures 3 through 12 also present the average and average plus one standard deviation of SV amplitudes computed from digitization and processing noise.

The approximate noise elimination scheme used by Trifunac and Anderson (1977) has been used in this work as well. However, some distortions in a(T) through g(T) are inevitable for T > 2 sec and T < 0.05 sec. Consequently, equation (1) should not be used for T > 2 sec and for small magnitudes, typically M < 5.0. Spectral amplitudes from

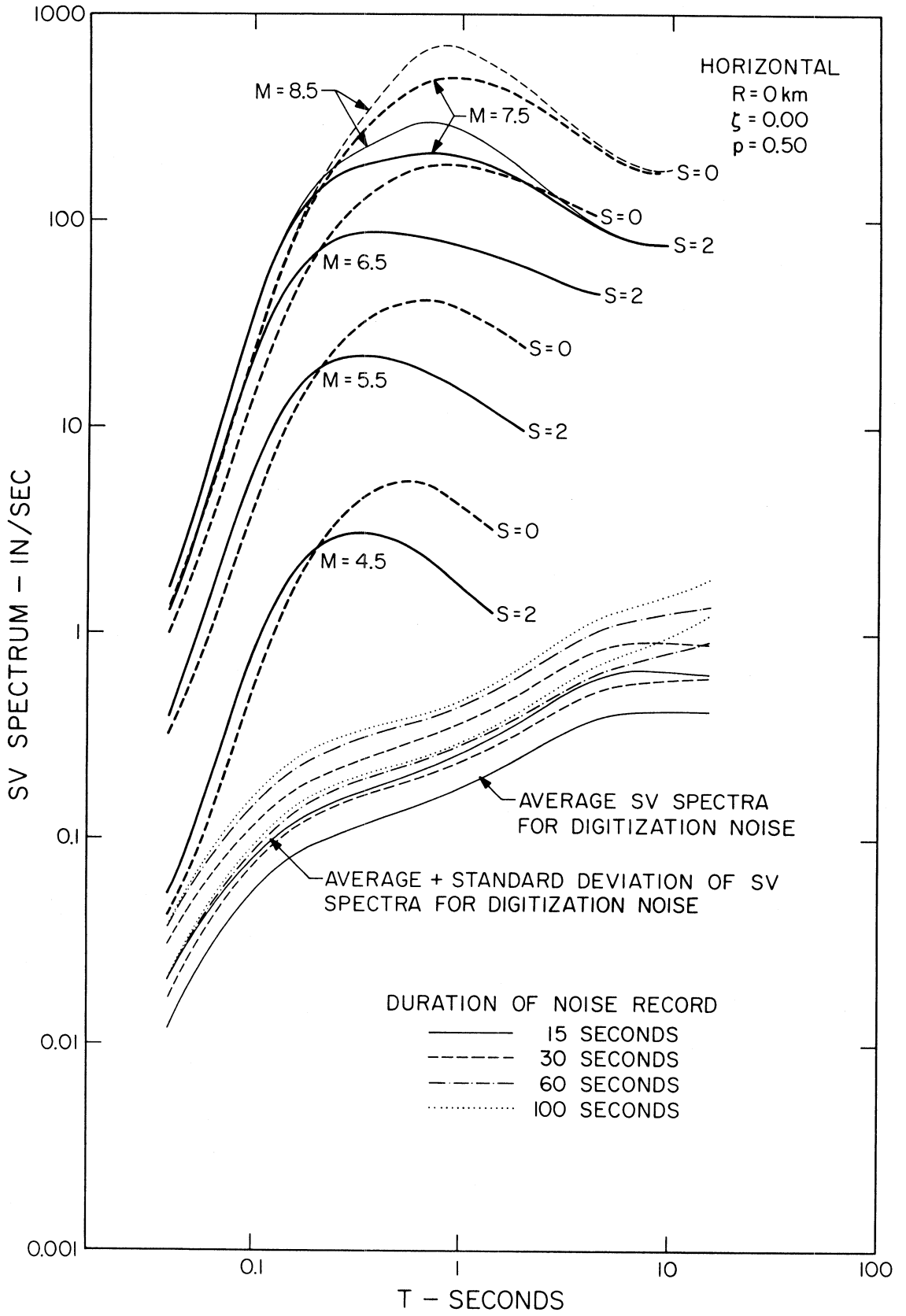
HORIZONTAL
R = 0 km
ζ = 0.00
p = 0.50
M = 8.5
M = 7.5
S = 0
S = 0
S = 2
M = 6.5
S = 2
S = 0
M = 5.5
S = 2
S = 0
M = 4.5
S = 2
AVERAGE SV SPECTRA FOR DIGITIZATION NOISE
AVERAGE + STANDARD DEVIATION OF SV SPECTRA FOR DIGITIZATION NOISE
DURATION OF NOISE RECORD
15 SECONDS
30 SECONDS
60 SECONDS
100 SECONDS
SV SPECTRUM – IN/SEC
1000
100
10
1
0.1
0.01
0.001
0.1
1
10
100
T – SECONDS

FIGURE 3

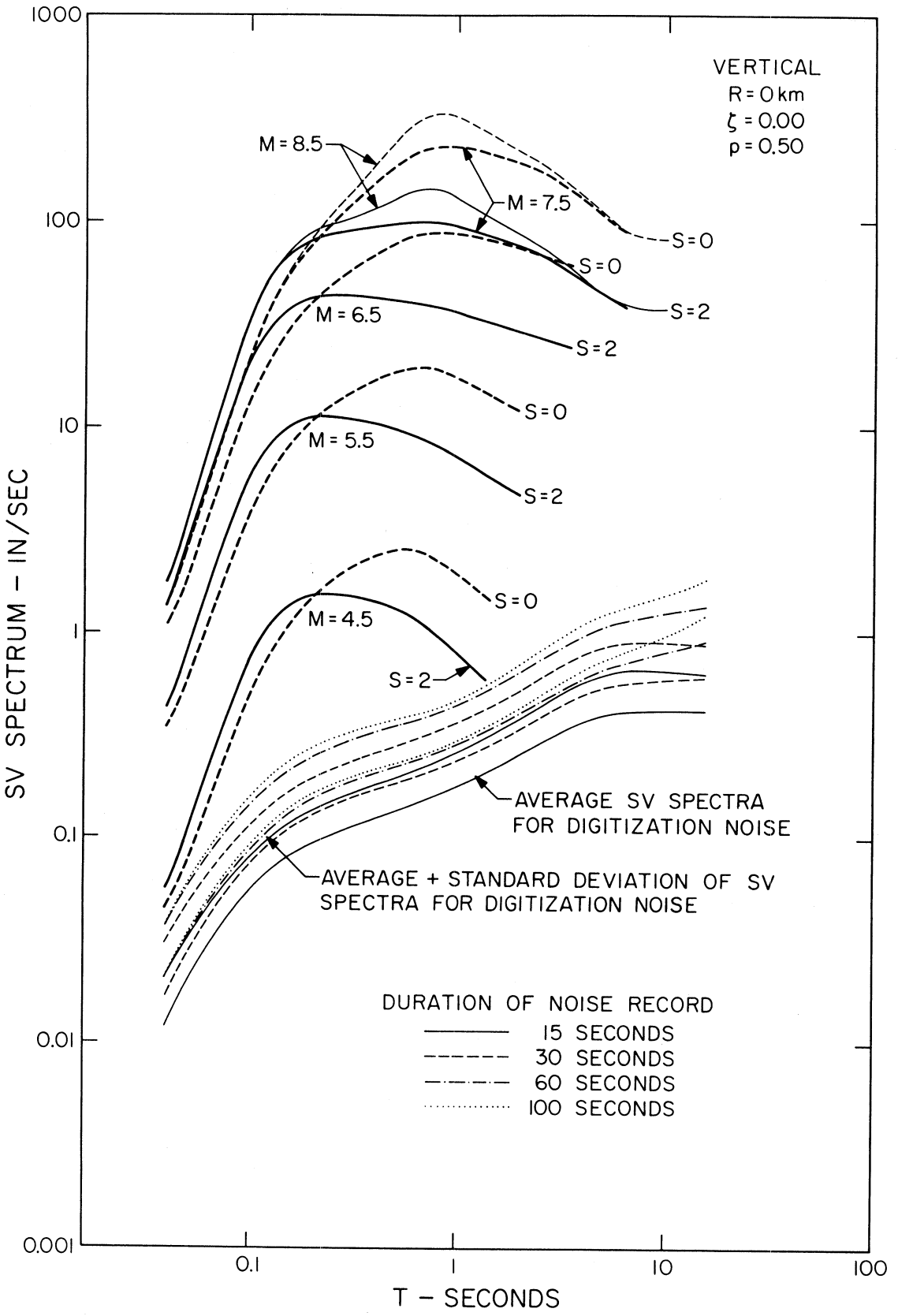
VERTICAL
R = 0 km
ζ = 0.00
p = 0.50
M = 8.5
M = 7.5
M = 6.5
M = 5.5
M = 4.5
S = 0
S = 2
AVERAGE SV SPECTRA FOR DIGITIZATION NOISE
AVERAGE + STANDARD DEVIATION OF SV SPECTRA FOR DIGITIZATION NOISE
DURATION OF NOISE RECORD
15 SECONDS
30 SECONDS
60 SECONDS
100 SECONDS
SV SPECTRUM – IN/SEC
T – SECONDS
1000
100
10
1
0.1
0.01
0.001
0.1
1
10
100

FIGURE 4

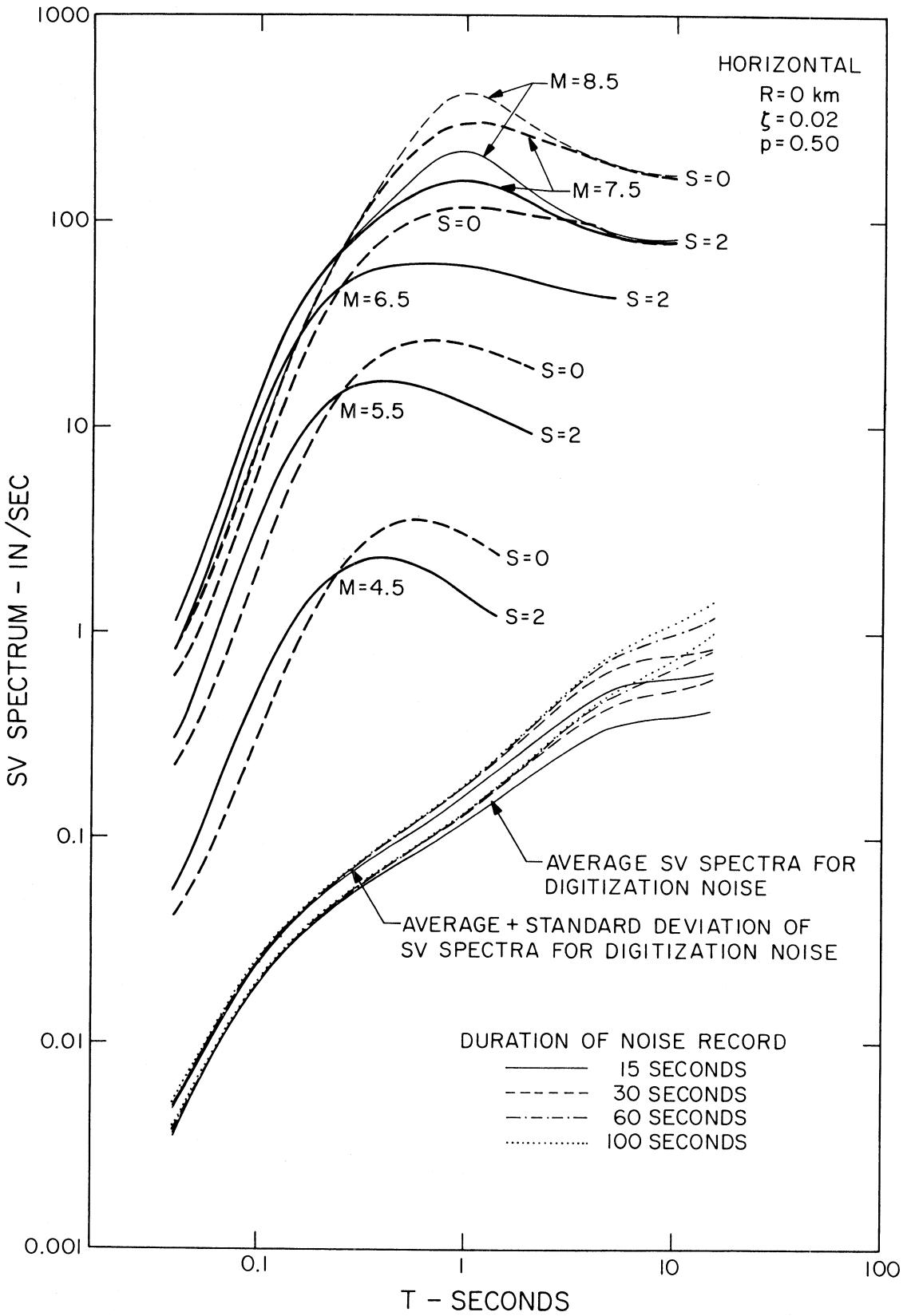
HORIZONTAL
R = 0 km
ζ = 0.02
p = 0.50
M=8.5
M=7.5
M=6.5
M=5.5
M=4.5
S=0
S=2
AVERAGE SV SPECTRA FOR DIGITIZATION NOISE
AVERAGE + STANDARD DEVIATION OF SV SPECTRA FOR DIGITIZATION NOISE
DURATION OF NOISE RECORD
15 SECONDS
30 SECONDS
60 SECONDS
100 SECONDS
SV SPECTRUM - IN/SEC
T - SECONDS
1000
100
10
1
0.1
0.01
0.001
0.1
1
10
100

FIGURE 5

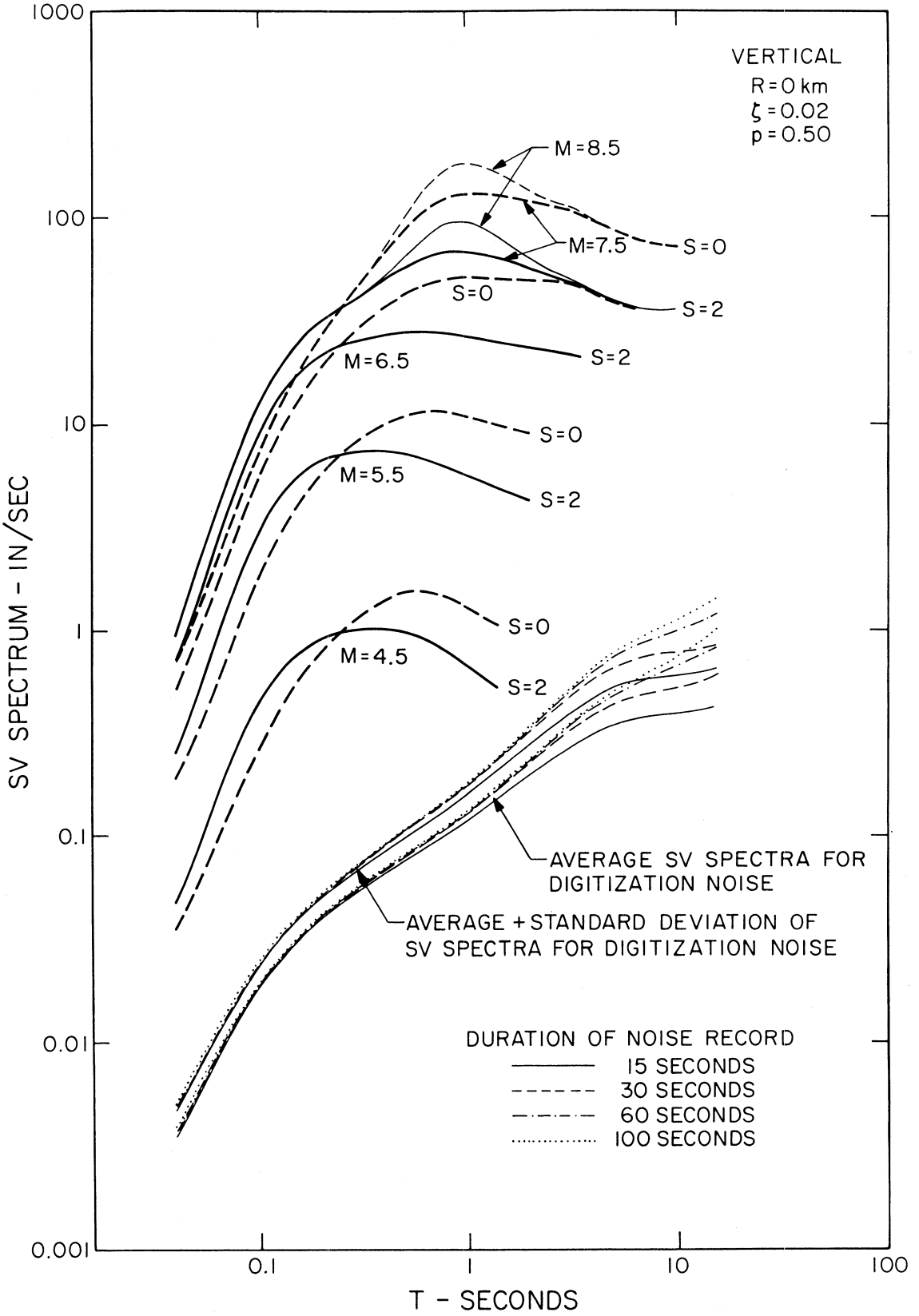
VERTICAL
R = 0 km
ζ = 0.02
p = 0.50
M=8.5
M=7.5
S=0
S=2
S=0
S=2
M=6.5
S=0
M=5.5
S=2
S=0
M=4.5
S=2
AVERAGE SV SPECTRA FOR DIGITIZATION NOISE
AVERAGE + STANDARD DEVIATION OF SV SPECTRA FOR DIGITIZATION NOISE
DURATION OF NOISE RECORD
15 SECONDS
30 SECONDS
60 SECONDS
100 SECONDS
SV SPECTRUM - IN/SEC
1000
100
10
1
0.1
0.01
0.001
0.1
1
10
100
T - SECONDS

FIGURE 6

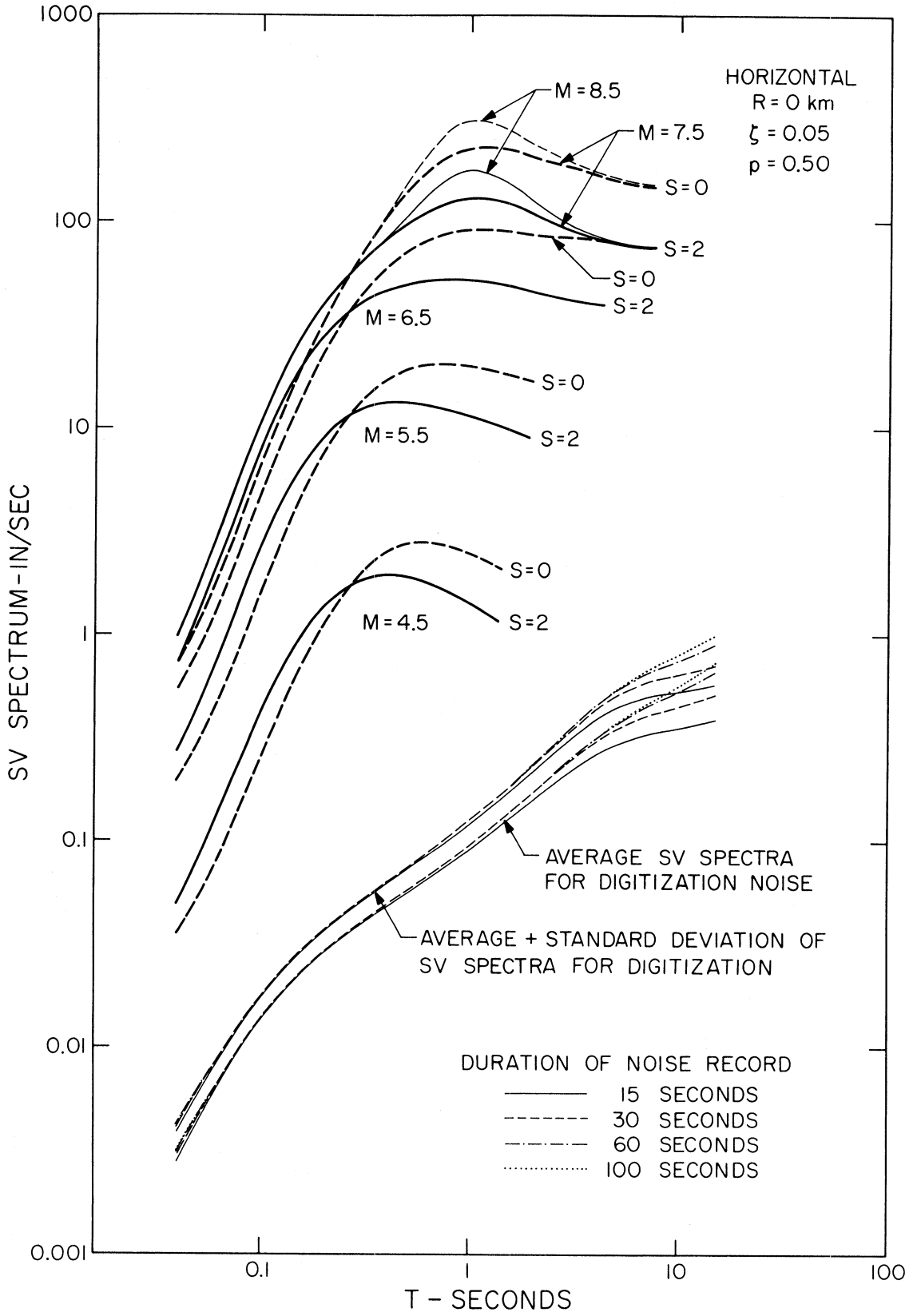
HORIZONTAL
R = 0 km
ζ = 0.05
p = 0.50
M = 8.5
M = 7.5
S=0
S=2
S=0
S=2
M = 6.5
S=0
M=5.5
S=2
S=0
M=4.5
S=2
AVERAGE SV SPECTRA
FOR DIGITIZATION NOISE
AVERAGE + STANDARD DEVIATION OF
SV SPECTRA FOR DIGITIZATION
DURATION OF NOISE RECORD
15 SECONDS
30 SECONDS
60 SECONDS
100 SECONDS
SV SPECTRUM-IN/SEC
1000
100
10
1
0.1
0.01
0.001
0.1
1
10
100
T - SECONDS

FIGURE 7

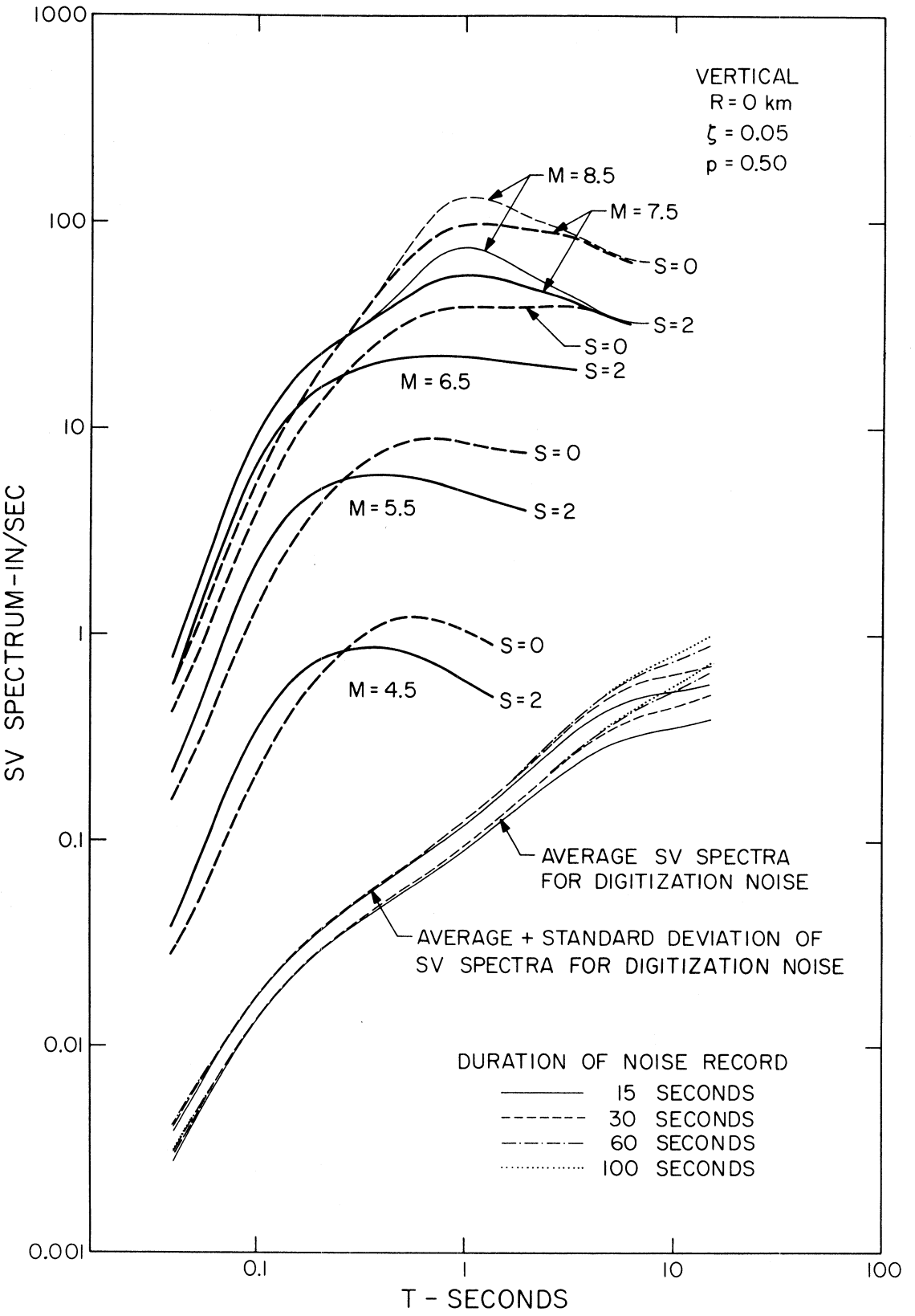
VERTICAL
R = 0 km
ζ = 0.05
p = 0.50
M = 8.5
M = 7.5
S = 0
S = 2
S = 0
S = 2
M = 6.5
S = 0
M = 5.5
S = 2
S = 0
M = 4.5
S = 2
AVERAGE SV SPECTRA
FOR DIGITIZATION NOISE
AVERAGE + STANDARD DEVIATION OF
SV SPECTRA FOR DIGITIZATION NOISE
DURATION OF NOISE RECORD
15 SECONDS
30 SECONDS
60 SECONDS
100 SECONDS
SV SPECTRUM-IN/SEC
1000
100
10
1
0.1
0.01
0.001
0.1
1
10
100
T - SECONDS

FIGURE 8

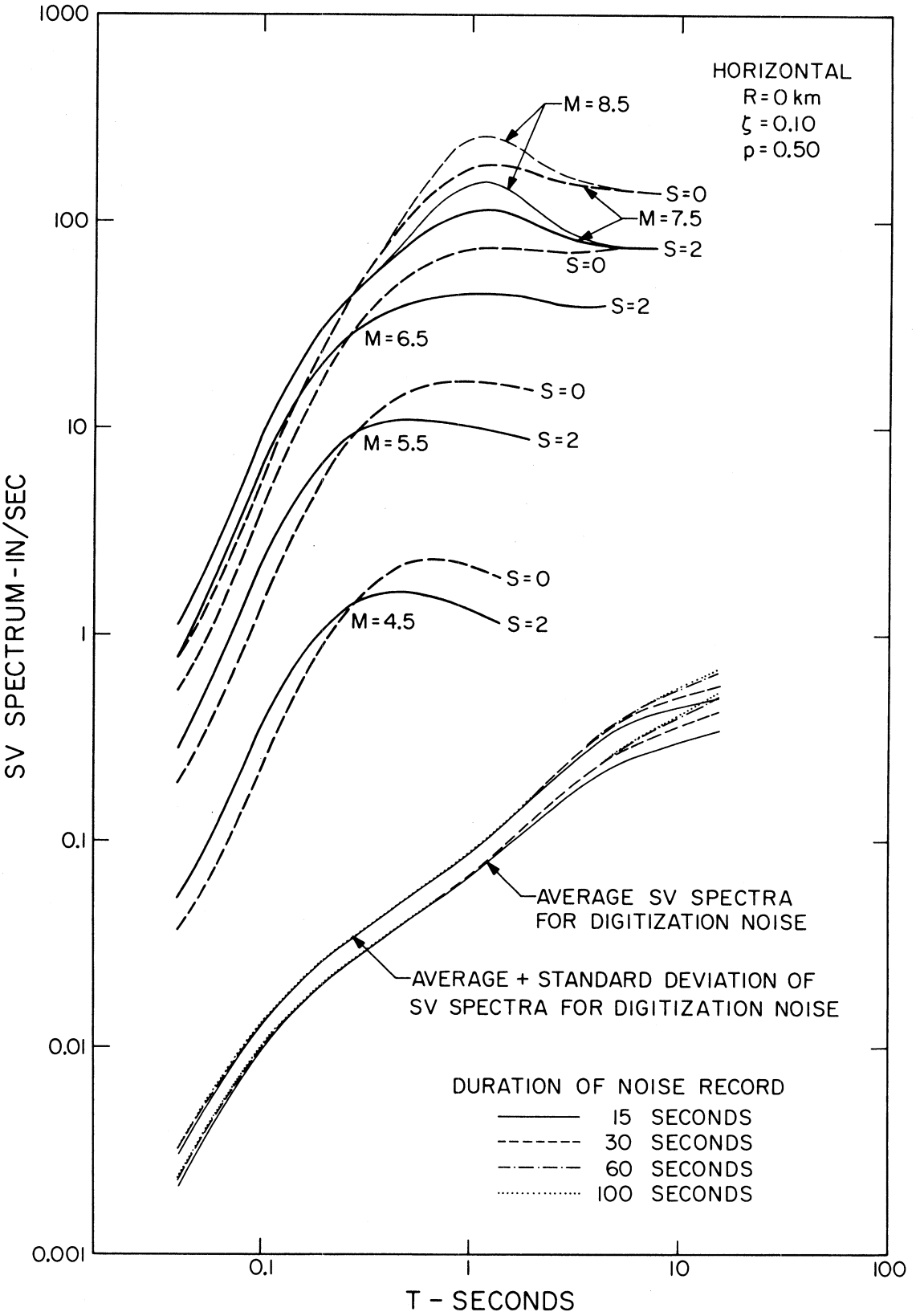
HORIZONTAL
R = 0 km
ζ = 0.10
p = 0.50
M = 8.5
S = 0
M = 7.5
S = 2
S = 0
S = 2
M = 6.5
S = 0
M = 5.5
S = 2
S = 0
M = 4.5
S = 2
AVERAGE SV SPECTRA
FOR DIGITIZATION NOISE
AVERAGE + STANDARD DEVIATION OF
SV SPECTRA FOR DIGITIZATION NOISE
DURATION OF NOISE RECORD
15 SECONDS
30 SECONDS
60 SECONDS
100 SECONDS
SV SPECTRUM - IN/SEC
1000
100
10
1
0.1
0.01
0.001
0.1
1
10
100
T - SECONDS

FIGURE 9

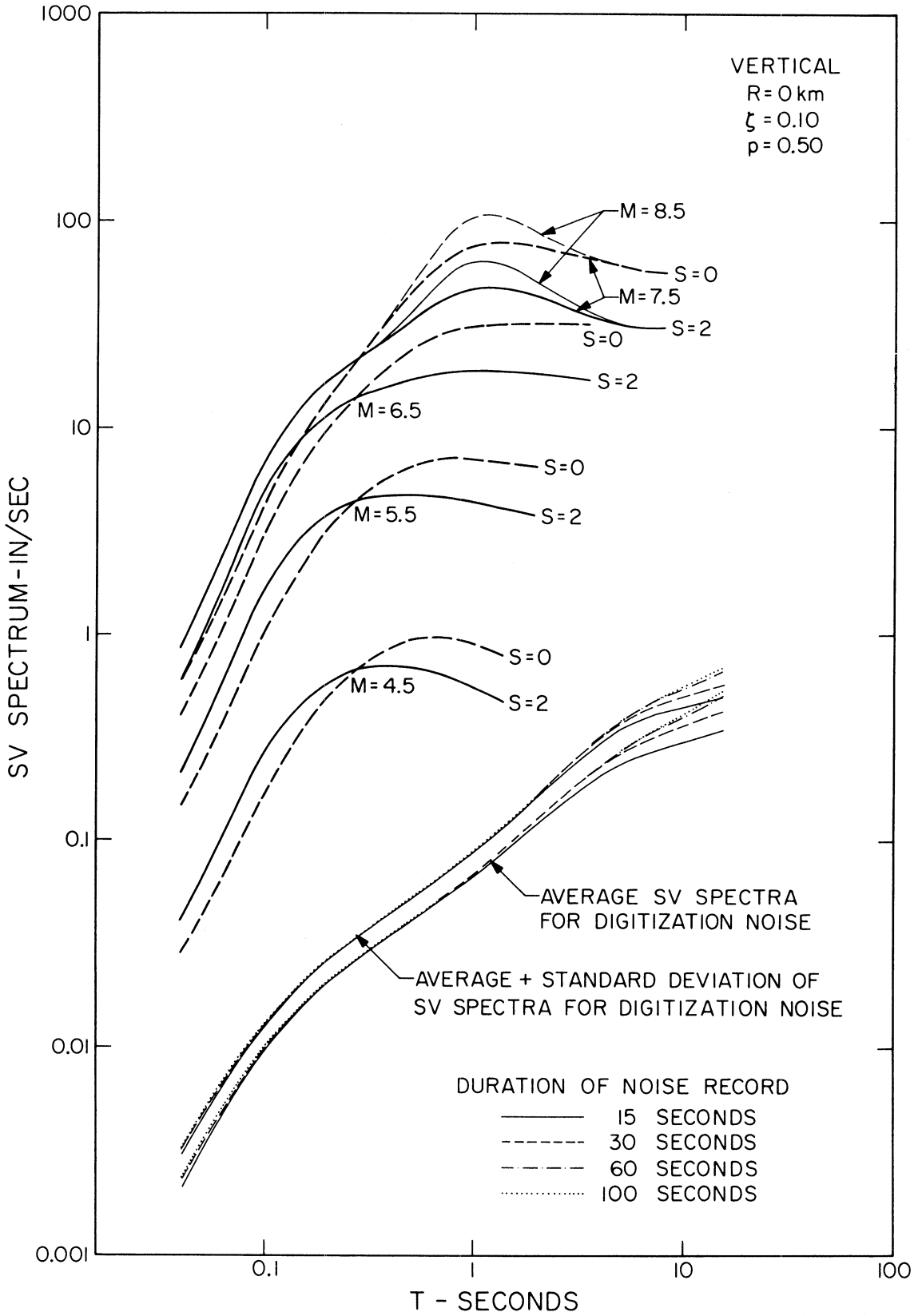
VERTICAL
R = 0 km
ζ = 0.10
p = 0.50
M = 8.5
S = 0
M = 7.5
S = 2
S = 0
S = 2
M = 6.5
S = 0
M = 5.5
S = 2
S = 0
M = 4.5
S = 2
AVERAGE SV SPECTRA
FOR DIGITIZATION NOISE
AVERAGE + STANDARD DEVIATION OF
SV SPECTRA FOR DIGITIZATION NOISE
DURATION OF NOISE RECORD
15 SECONDS
30 SECONDS
60 SECONDS
100 SECONDS
SV SPECTRUM-IN/SEC
1000
100
10
1
0.1
0.01
0.001
0.1
1
10
100
T - SECONDS

FIGURE 10

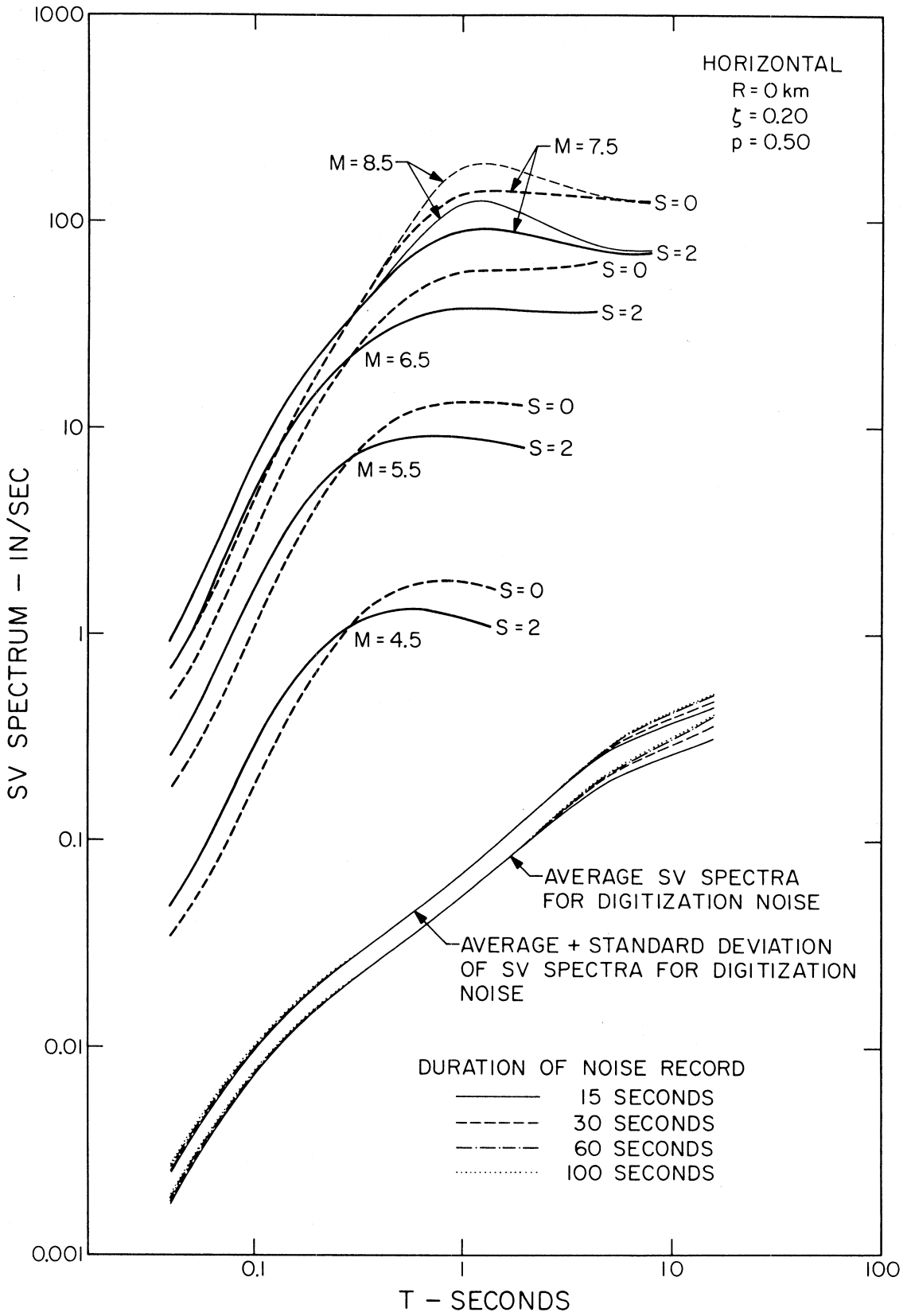
HORIZONTAL
R = 0 km
ζ = 0.20
p = 0.50
M = 8.5
M = 7.5
S = 0
S = 2
S = 0
S = 2
M = 6.5
S = 0
S = 2
M = 5.5
S = 0
S = 2
M = 4.5
AVERAGE SV SPECTRA FOR DIGITIZATION NOISE
AVERAGE + STANDARD DEVIATION OF SV SPECTRA FOR DIGITIZATION NOISE
DURATION OF NOISE RECORD
15 SECONDS
30 SECONDS
60 SECONDS
100 SECONDS
SV SPECTRUM – IN/SEC
1000
100
10
1
0.1
0.01
0.001
0.1
1
10
100
T – SECONDS

FIGURE 11

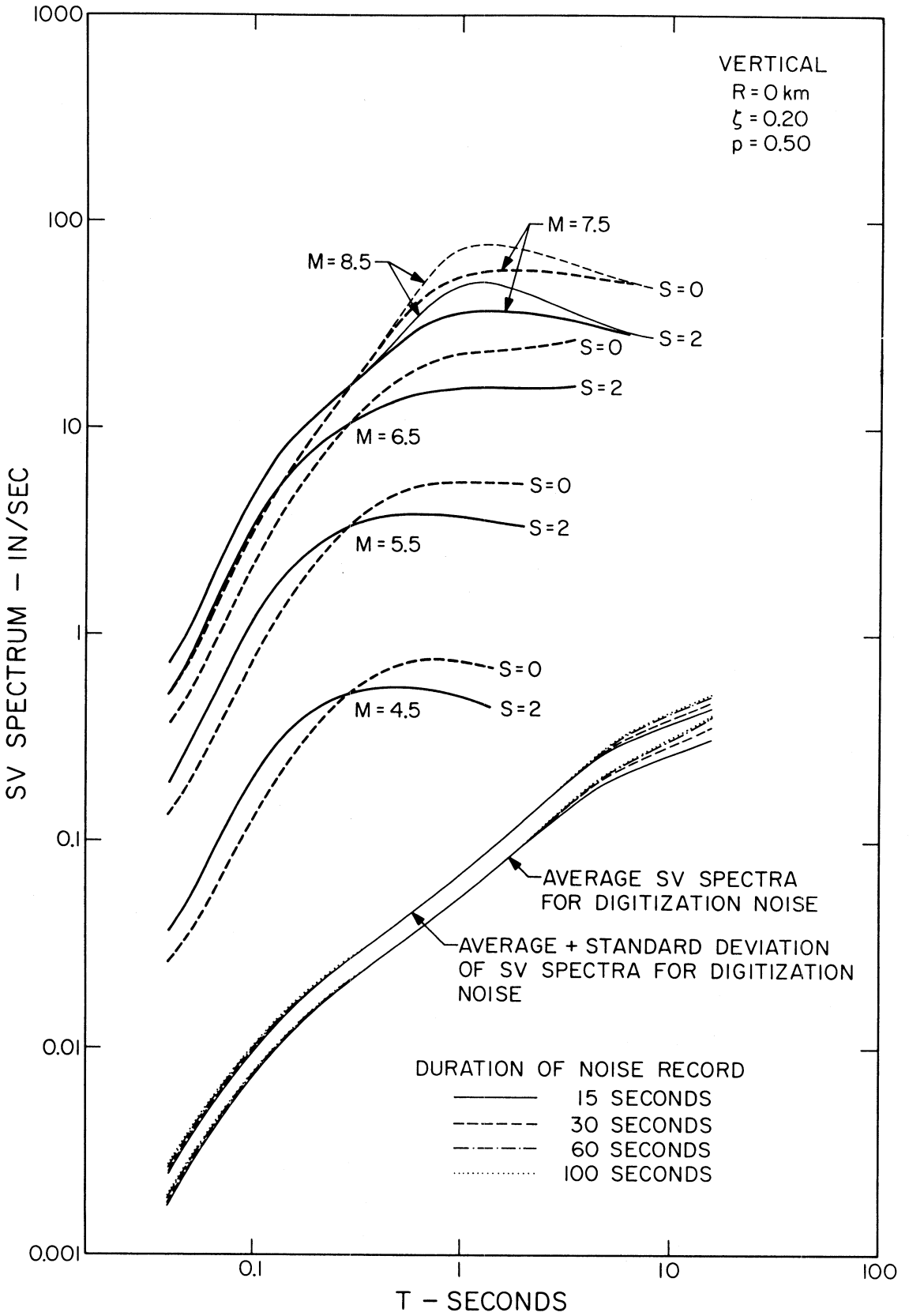
VERTICAL
R = 0 km
ζ = 0.20
p = 0.50
M = 8.5
M = 7.5
S = 0
S = 2
S = 0
S = 2
M = 6.5
S = 0
S = 2
M = 5.5
S = 0
S = 2
M = 4.5
AVERAGE SV SPECTRA FOR DIGITIZATION NOISE
AVERAGE + STANDARD DEVIATION OF SV SPECTRA FOR DIGITIZATION NOISE
DURATION OF NOISE RECORD
15 SECONDS
30 SECONDS
60 SECONDS
100 SECONDS
SV SPECTRUM – IN/SEC
1000
100
10
1
0.1
0.01
0.001
0.1
1
10
100
T – SECONDS

FIGURE 12

equation (1) should be relatively free of noise distortion at those periods, selected separately for each magnitude, which are plotted in Figures 3 through 12.

Figures 13 through 18 present a comparison of recorded with computed SV spectra. Spectra were computed for $p = 0.9$ and 0.1, for $\zeta = 0.0$, 0.02, 0.05, 0.10 and 0.20, and for M, R, and s corresponding to recording conditions at the Pacoima Dam site (Figures 13, 14 and 15) during the San Fernando, California, earthquake of 1971 and at the El Centro Site (Figures 16, 17 and 18) during the Imperial Valley, California, earthquake of 1940. The interval between SV spectra for $p = 0.9$ and 0.1 represents approximately the 80 percent confidence interval where the spectra of recorded motions would be expected to be. As can be seen from these figures, more than 80 percent of recorded spectral amplitudes are within the predicted 80 percent confidence interval. Different figures in this group show various degrees of agreement between predicted and computed SV amplitudes.

b. Correlations in Terms of I_{MM}, p, s and v

Figure 19 and Table III present scaling functions a(T), b(T), c(T), d(T), and e(T) which result from regression analysis in terms of equation (2). As for scaling in terms of M, R, s, v and p, these scaling functions have been smoothed by an Ormsby low-pass filter along $\log_{10}T$ axis. Table III presents a(T) through e(T) at eleven selected periods and for five fractions of critical damping ζ.

Consistent with previous correlations, equation (2) assumes

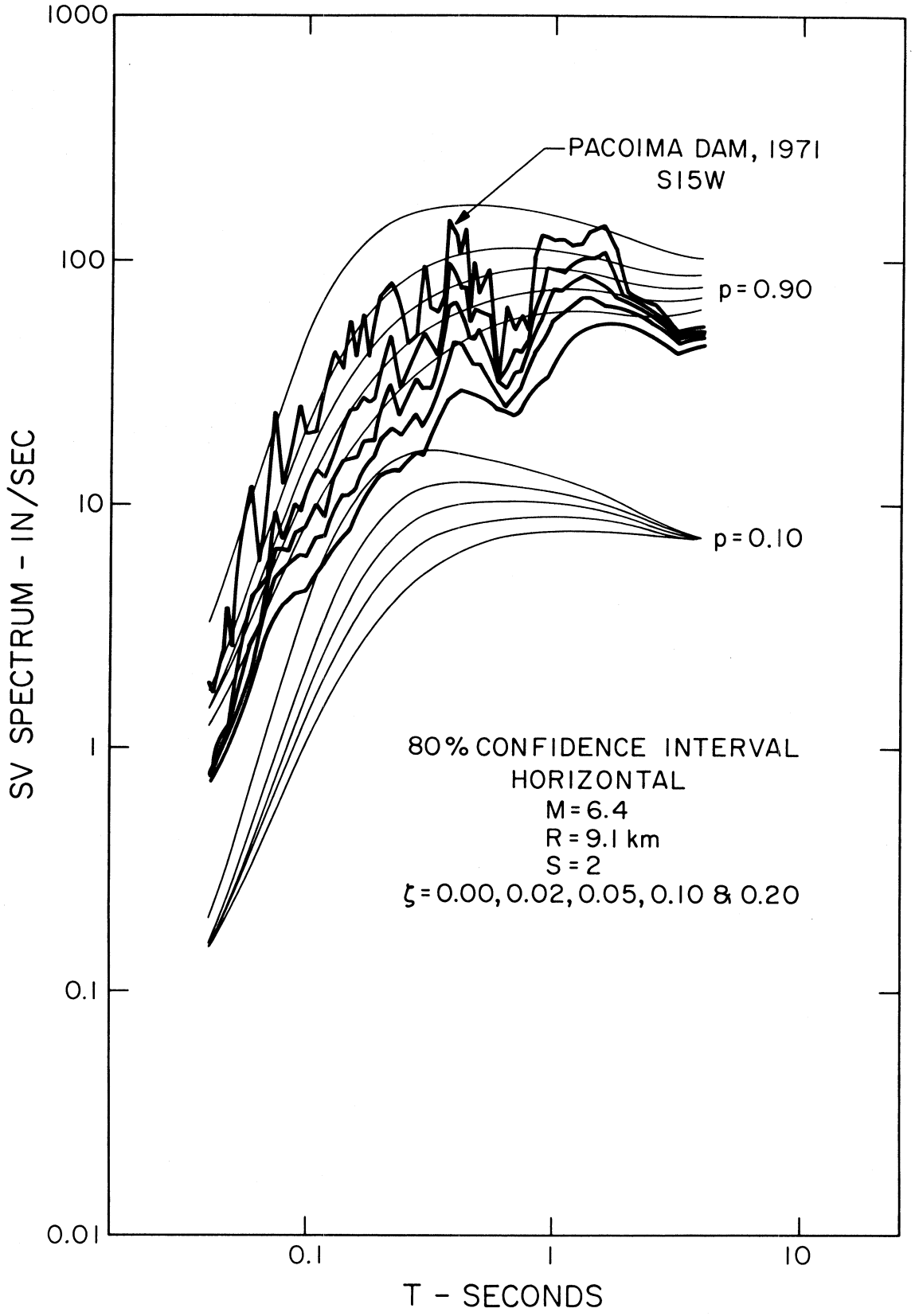
1000
100
10
1
0.1
0.01
SV SPECTRUM - IN/SEC
PACOIMA DAM, 1971
S15W
p = 0.90
p = 0.10
80% CONFIDENCE INTERVAL
HORIZONTAL
M = 6.4
R = 9.1 km
S = 2
ζ = 0.00, 0.02, 0.05, 0.10 & 0.20
0.1
1
10
T - SECONDS

FIGURE 13

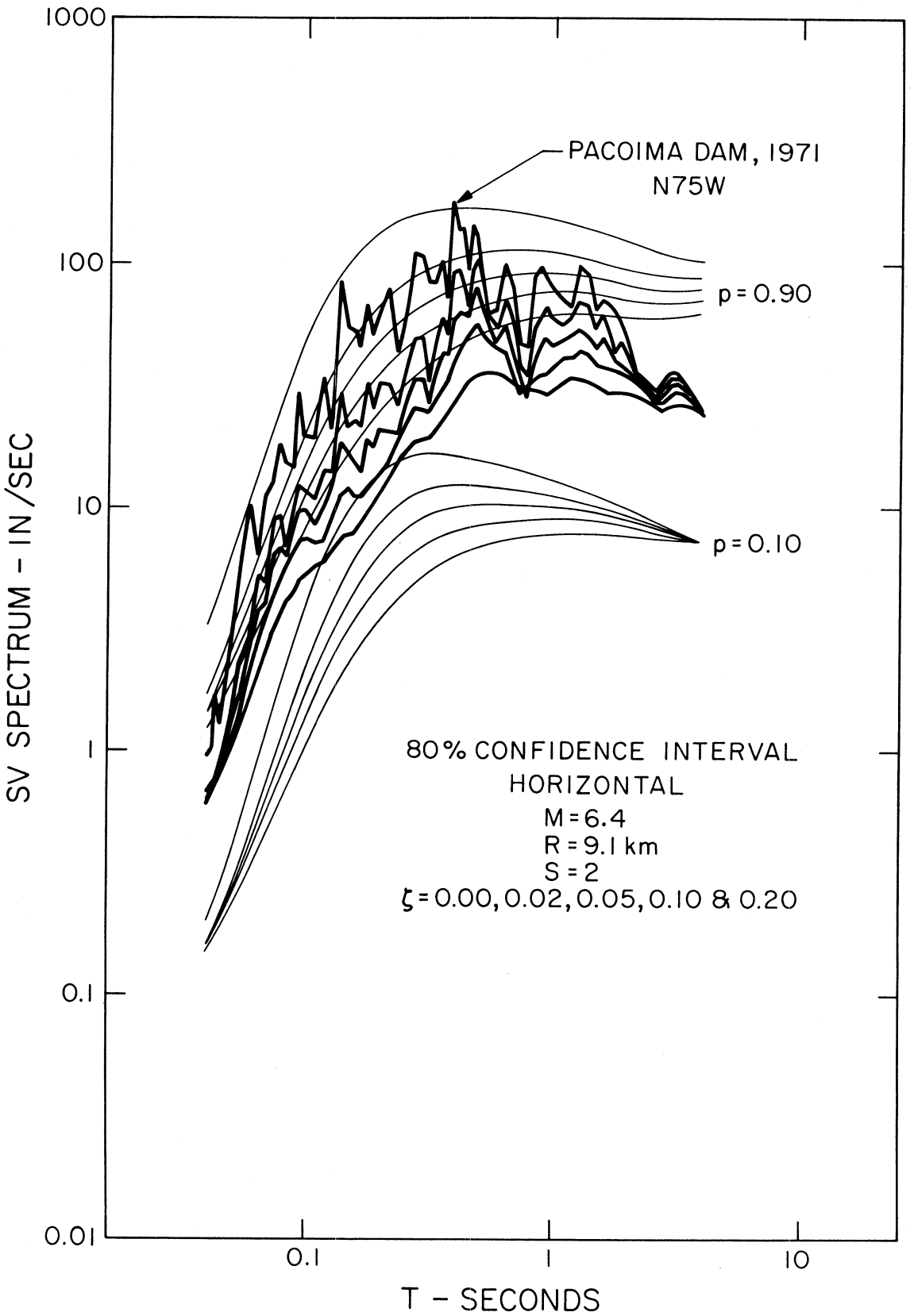
1000
100
10
1
0.1
0.01
SV SPECTRUM - IN/SEC
PACOIMA DAM, 1971
N75W
p = 0.90
p = 0.10
80% CONFIDENCE INTERVAL
HORIZONTAL
M = 6.4
R = 9.1 km
S = 2
ζ = 0.00, 0.02, 0.05, 0.10 & 0.20
0.1
1
10
T - SECONDS

FIGURE 14

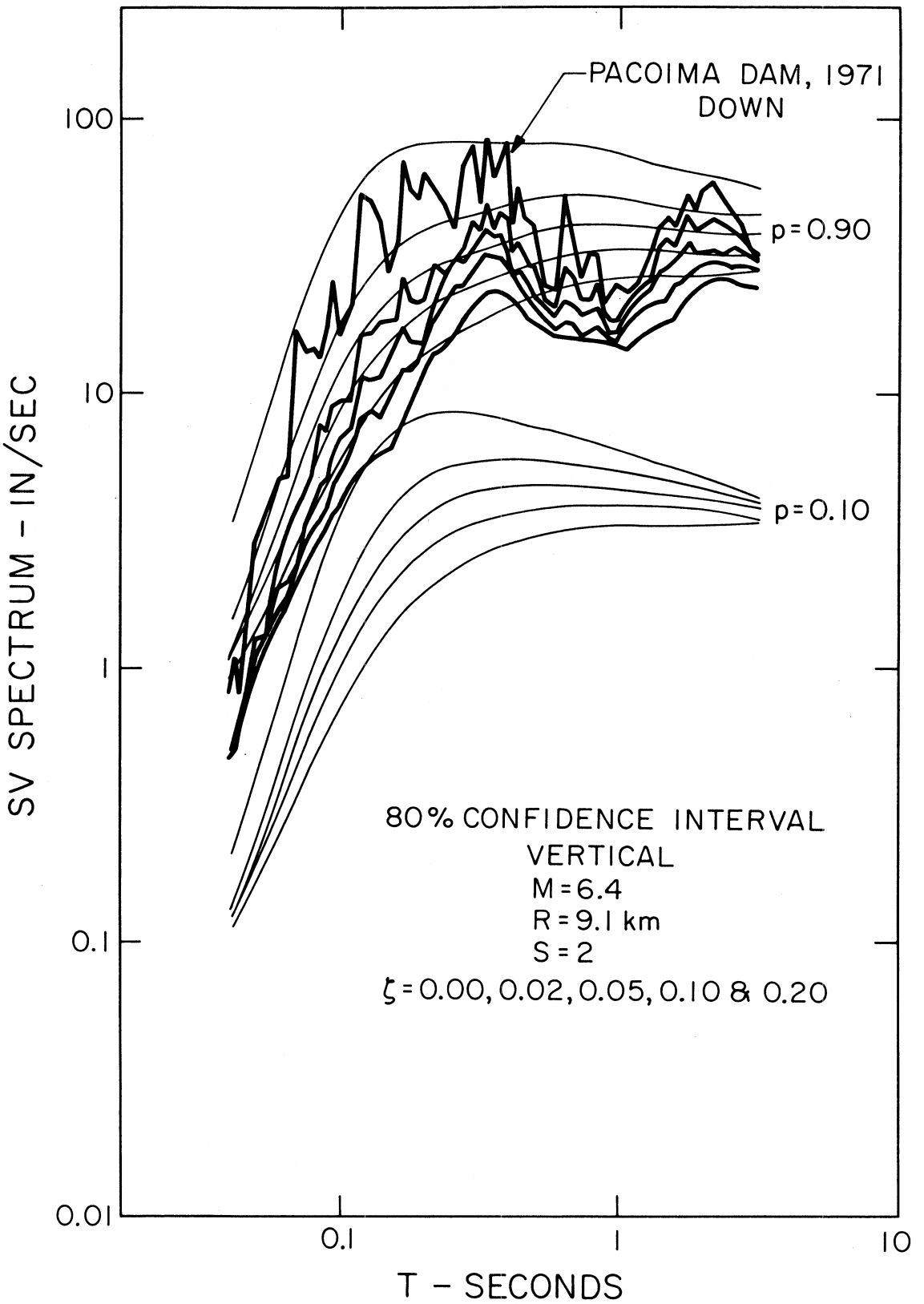
PACOIMA DAM, 1971
DOWN
p=0.90
p=0.10
80% CONFIDENCE INTERVAL
VERTICAL
M=6.4
R=9.1 km
S=2
ζ=0.00, 0.02, 0.05, 0.10 & 0.20
SV SPECTRUM - IN/SEC
T - SECONDS
100
10
1
0.1
0.01
0.1
1
10

FIGURE 15

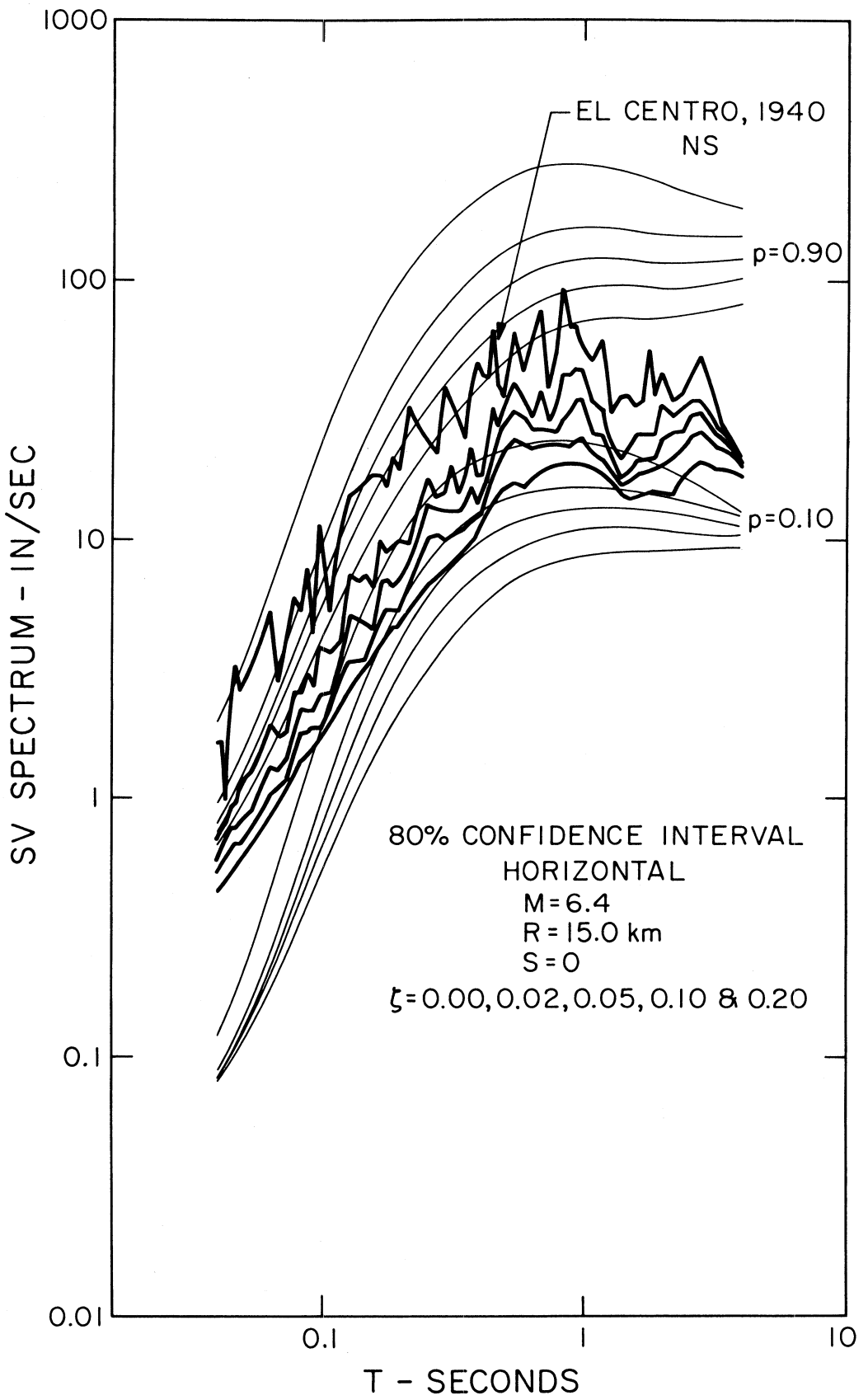
1000
100
10
1
0.1
0.01
SV SPECTRUM - IN/SEC
EL CENTRO, 1940
NS
p=0.90
p=0.10
80% CONFIDENCE INTERVAL
HORIZONTAL
M=6.4
R=15.0 km
S=0
ζ=0.00, 0.02, 0.05, 0.10 & 0.20
0.1
1
10
T - SECONDS

FIGURE 16

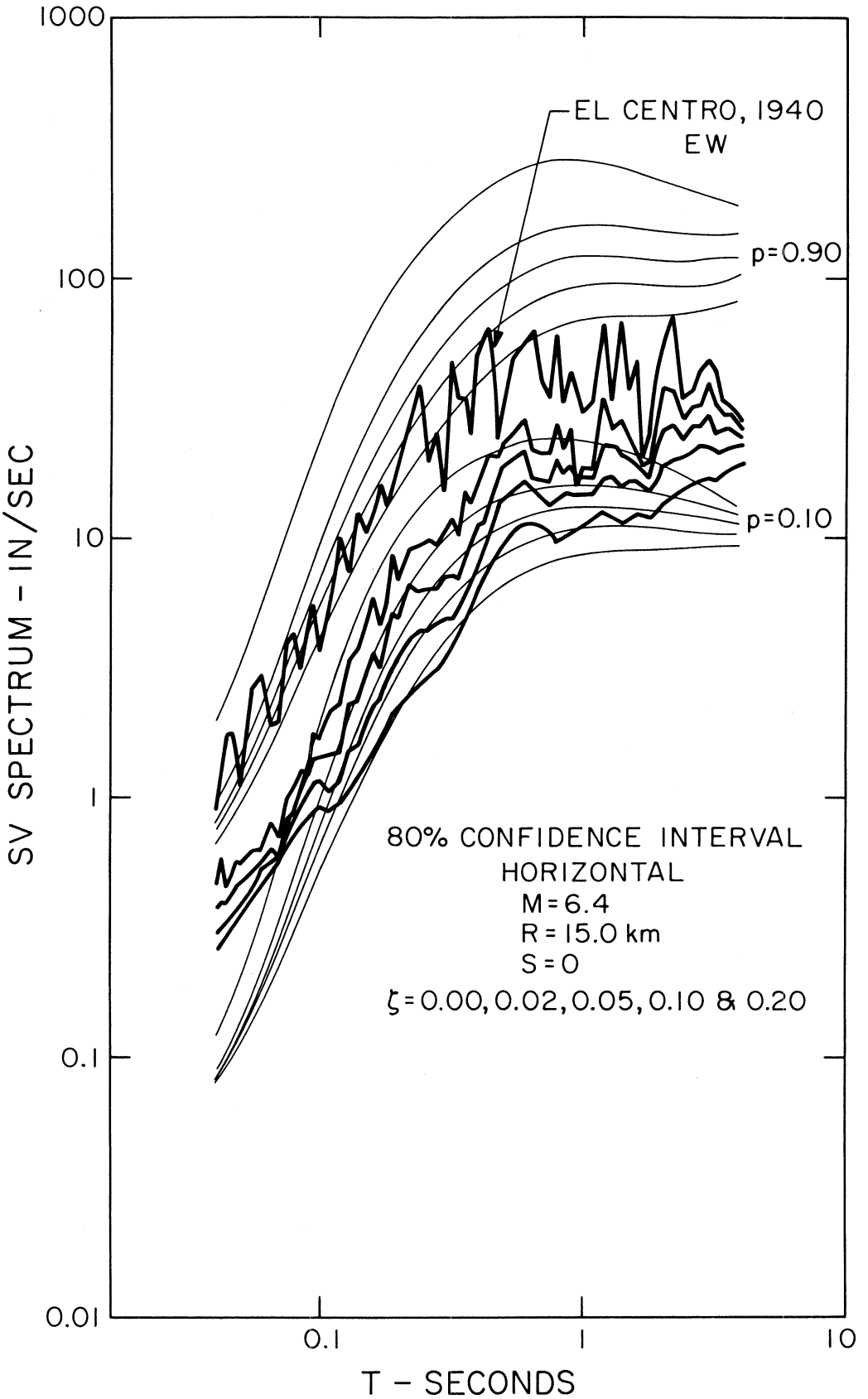
1000
100
10
1
0.1
0.01
SV SPECTRUM - IN/SEC
EL CENTRO, 1940
EW
p=0.90
p=0.10
80% CONFIDENCE INTERVAL
HORIZONTAL
M=6.4
R=15.0 km
S=0
ζ=0.00, 0.02, 0.05, 0.10 & 0.20
0.1
1
10
T - SECONDS

FIGURE 17

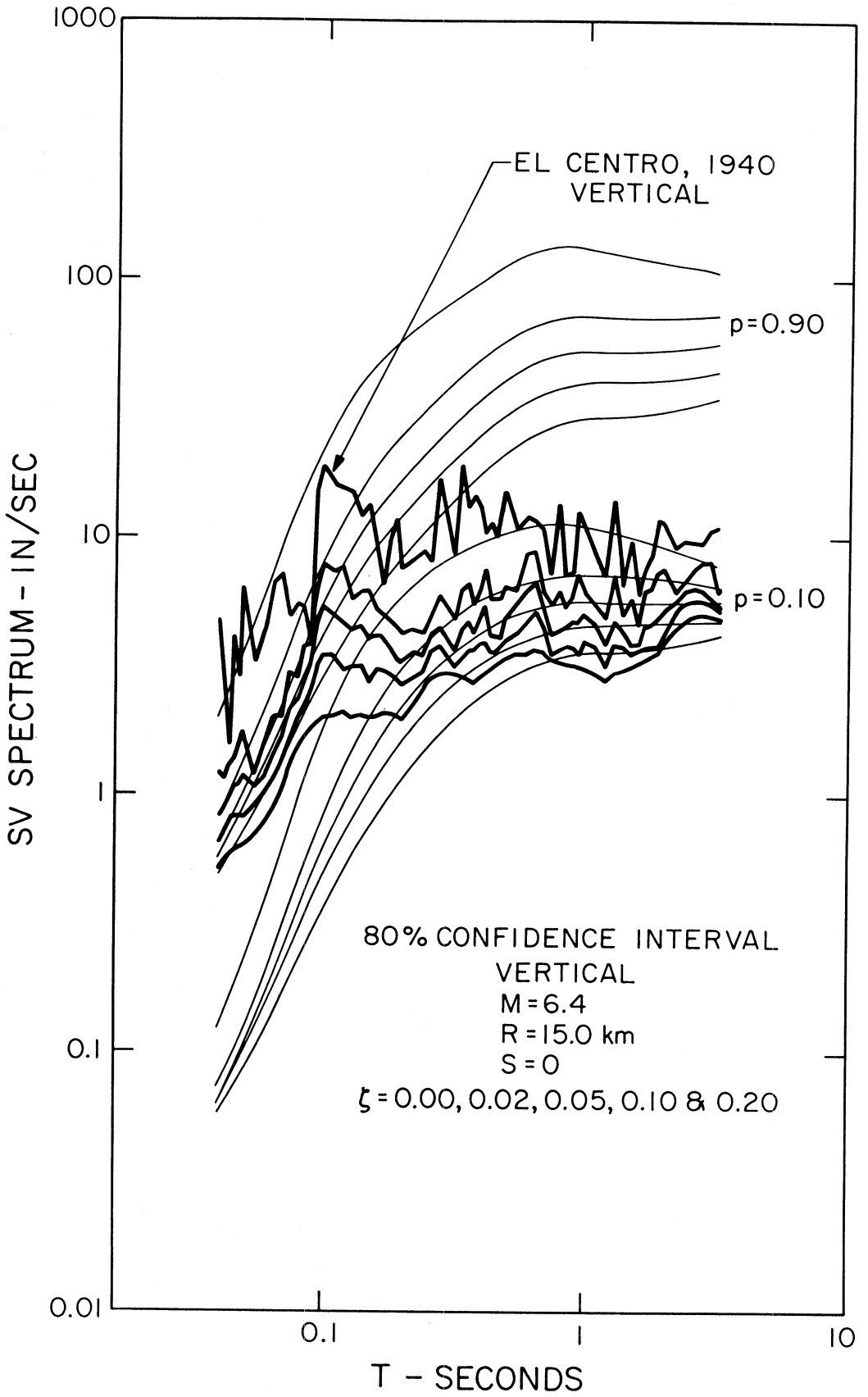
1000
100
10
1
0.1
0.01
SV SPECTRUM - IN/SEC
EL CENTRO, 1940
VERTICAL
p=0.90
p=0.10
80% CONFIDENCE INTERVAL
VERTICAL
M=6.4
R=15.0 km
S=0
ζ=0.00, 0.02, 0.05, 0.10 & 0.20
0.1
1
10
T - SECONDS

FIGURE 18

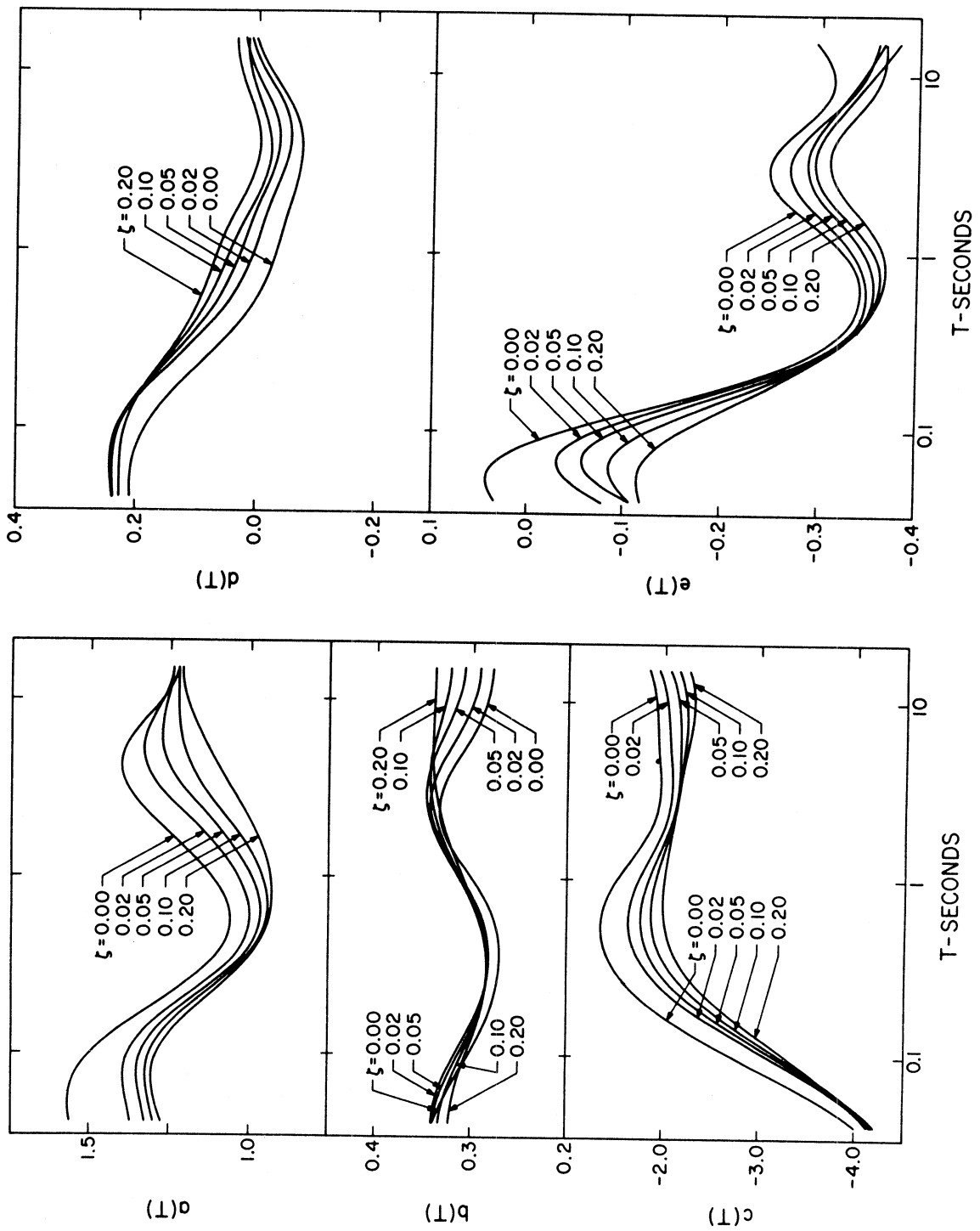
a(T)
b(T)
c(T)
d(T)
e(T)
T-SECONDS
T-SECONDS
ζ=0.00
0.02
0.05
0.10
0.20
ζ=0.20
0.10
0.05
0.02
0.00

FIGURE 19

TABLE III

Regression Parameters for Equation (2) and $\alpha(T)$, $\beta(T)$ and $N(T)^*$ at Eleven Selected Periods

$\log_{10}T$(sec)	-1.398	-1.171	-0.943	-0.716	-0.489	-0.261	-0.034	0.193	0.420	0.648	0.875
ζ = 0.0											
a(T)	1.562	1.556	1.460	1.286	1.125	1.059	1.106	1.221	1.349	1.402	1.332
b(T)	0.339	0.320	0.296	0.278	0.271	0.275	0.296	0.324	0.333	0.316	0.292
c(T)	-4.010	-3.342	-2.522	-1.859	-1.473	-1.358	-1.498	-1.774	-1.956	-1.962	-1.931
d(T)	0.208	0.203	0.173	0.115	0.049	-0.002	-0.031	-0.051	-0.070	-0.074	-0.045
e(T)	0.034	0.032	-0.074	-0.221	-0.314	-0.342	-0.331	-0.287	-0.249	-0.268	-0.308
$\alpha(T)$	2.487	2.486	2.515	2.591	2.627	3.867	3.859	3.807	3.644	3.518	3.574
$\beta(T)$	-1.066	-1.097	-1.134	-1.173	-1.177	-2.444	-2.454	-2.467	-2.401	-2.322	-2.329
N(T)	2	2	2	2	2	1	1	1	1	1	1
ζ = 0.02											
a(T)	1.371	1.393	1.358	1.222	1.066	0.999	1.028	1.113	1.240	1.329	1.308
b(T)	0.341	0.331	0.311	0.291	0.282	0.287	0.307	0.332	0.343	0.330	0.307
c(T)	-4.173	-3.640	-2.907	-2.228	-1.793	-1.644	-1.731	-1.935	-2.078	-2.083	-2.053
d(T)	0.237	0.243	0.221	0.164	0.097	0.040	0.007	-0.016	-0.041	-0.056	-0.034
e(T)	-0.077	-0.031	-0.098	-0.230	-0.323	-0.348	-0.338	-0.303	-0.270	-0.285	-0.329
$\alpha(T)$	2.516	2.498	2.535	2.618	2.649	3.872	3.820	3.758	3.613	3.528	3.625
$\beta(T)$	-1.089	-1.110	-1.157	-1.205	-1.206	-2.464	-2.445	-2.441	-2.379	-2.324	-2.358
N(T)	2	2	2	2	2	1	1	1	1	1	1
ζ = 0.05											
a(T)	1.325	1.349	1.321	1.193	1.040	0.968	0.986	1.058	1.168	1.260	1.272
b(T)	0.340	0.328	0.307	0.288	0.282	0.290	0.310	0.333	0.347	0.341	0.323
c(T)	-4.194	-3.682	-2.984	-2.334	-1.915	-1.770	-1.837	-2.005	-2.137	-2.174	-2.169
d(T)	0.238	0.241	0.222	0.171	0.110	0.061	0.029	0.004	-0.024	-0.037	-0.015
e(T)	-0.107	-0.057	-0.118	-0.241	-0.328	-0.355	-0.349	-0.319	-0.289	-0.295	-0.327
$\alpha(T)$	2.482	2.491	2.541	2.619	2.647	3.863	3.797	3.758	3.657	3.538	3.515
$\beta(T)$	-1.074	-1.105	-1.159	-1.206	-1.206	-2.461	-2.431	-2.435	-2.396	-2.328	-2.304
N(T)	2	2	2	2	2	1	1	1	1	1	1

ζ = 0.10

a(T)	1.298	1.322	1.293	1.172	1.026	0.948	0.954	1.016	1.111	1.190	1.221
b(T)	0.333	0.322	0.304	0.287	0.282	0.291	0.309	0.329	0.342	0.343	0.334
c(T)	-4.184	-3.701	-3.052	-2.441	-2.035	-1.881	-1.917	-2.035	-2.142	-2.205	-2.240
d(T)	0.237	0.237	0.219	0.174	0.119	0.077	0.048	0.016	-0.016	-0.021	0.001
e(T)	-0.107	-0.087	-0.146	-0.251	-0.328	-0.359	-0.359	-0.329	-0.297	-0.303	-0.335
α(T)	2.475	2.501	2.553	2.620	2.652	3.878	3.797	3.758	3.684	3.569	3.515
β(T)	-1.075	-1.111	-1.161	-1.203	-1.208	-2.471	-2.430	-2.429	-2.405	-2.345	-2.313
N(T)	2	2	2	2	2	1	1	1	1	1	1

ζ = 0.20

a(T)	1.274	1.304	1.268	1.148	1.015	0.941	0.931	0.964	1.031	1.106	1.170
b(T)	0.322	0.315	0.301	0.287	0.284	0.291	0.306	0.323	0.336	0.340	0.340
c(T)	-4.139	-3.708	-3.128	-2.567	-2.182	-2.014	-2.008	-2.074	-2.146	-2.217	-2.297
d(T)	0.226	0.225	0.211	0.173	0.127	0.093	0.068	0.039	0.006	-0.004	0.016
e(T)	-0.118	-0.120	-0.177	-0.260	-0.325	-0.360	-0.368	-0.345	-0.314	-0.317	-0.351
α(T)	2.511	2.555	2.594	2.634	2.651	3.889	3.800	3.738	3.681	3.586	3.495
β(T)	-1.094	-1.141	-1.182	-1.208	-1.207	-2.480	-2.433	-2.409	-2.387	-2.342	-2.293
N(T)	2	2	2	2	2	1	1	1	1	1	1

---

* See section entitled "Distribution of Spectral Amplitudes" for definition of α(T), β(T) and N(T).

that $\log_{10}[SV(T)]$ amplitudes can be approximated by a linear dependence on I_{MM}, discrete numerical levels ranging from 1 to 12 and corresponding to twelve MMI levels I through XII (Trifunac, 1978; Trifunac and Anderson, 1977; 1978). For the range between MMI = IV and MMI = VIII where the data is concentrated, this assumption appears to be adequate for approximate correlations as in equation (2).

Figures 20 through 29 present SV spectra plotted for MMI levels 4, 6 and 8 with heavy lines and for MMI levels 10 and 12 with light lines. Since data is now marginally adequate to characterize empirical models for MMI levels up to VII and perhaps to VIII, heavy lines indicate the MMI range where equation (2) should apply. Light lines in Figures 20 through 29 serve to present extrapolated SV amplitudes but outside the range where equation (2) can be tested by the data. Figures 20 through 29 further show spectral amplitudes for s=0 and 2, for ζ = 0.0, 0.02, 0.05, 0.10 and 0.20, and for p = 0.5. The average and average plus one standard deviation of SV amplitudes computed from digitization and processing noise are also shown in these figures to outline the amplitude and frequency range where equation (2) may apply. As for correlations with M, R, s, v and p, based on equation (1), low amplitude SV spectra here can be taken to be relatively free of noise only for periods and MMI levels indicated in Figures 20 through 29. Equation (2) should therefore not be used outside this range.

Examples presented in Figures 13 through 18 are repeated in Figures 30 through 35 but for scaling in terms of MMI. Strong

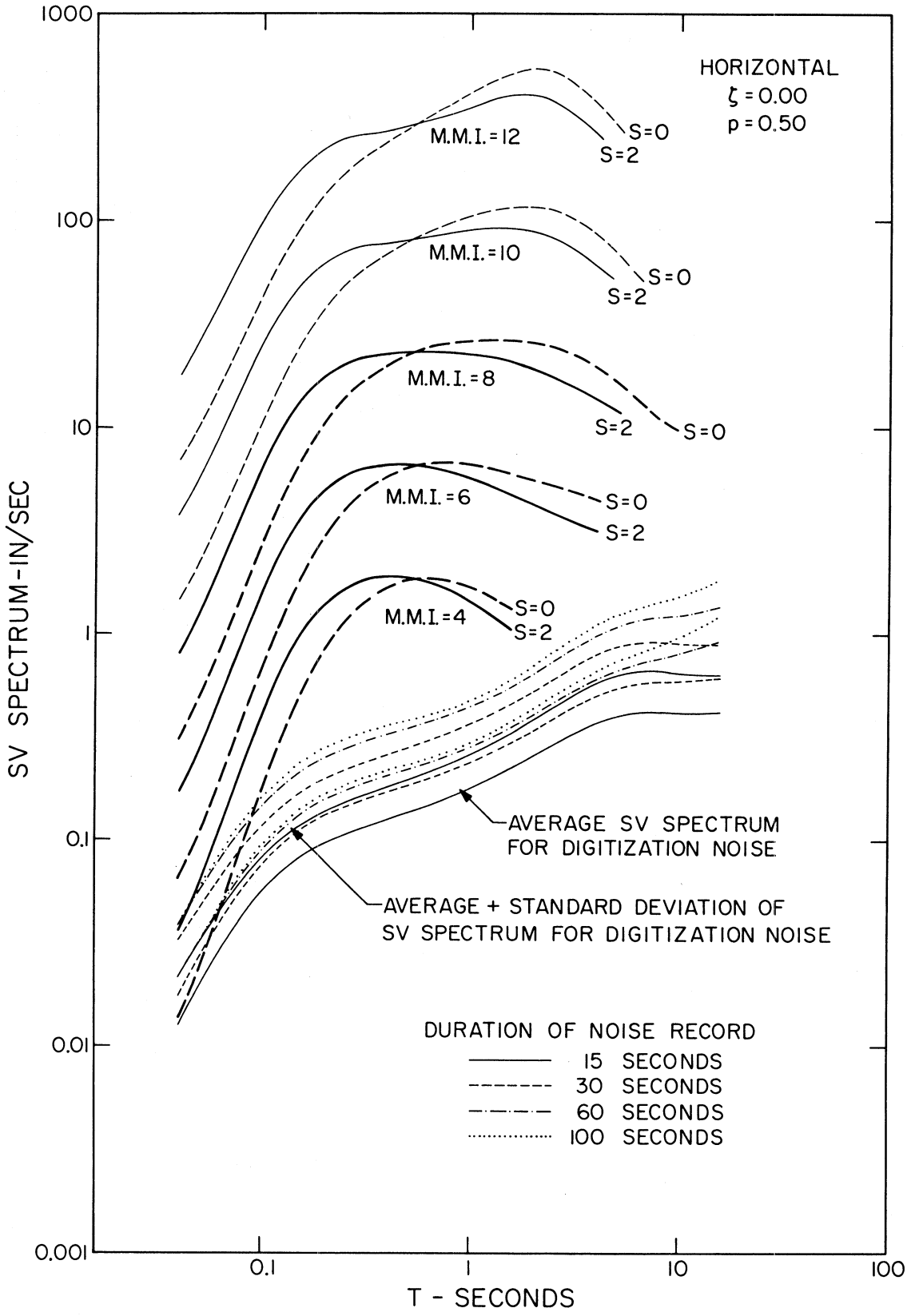
HORIZONTAL
ζ = 0.00
p = 0.50
M.M.I. = 12
S=0
S=2
M.M.I. = 10
S=0
S=2
M.M.I. = 8
S=2
S=0
M.M.I. = 6
S=0
S=2
M.M.I. = 4
S=0
S=2
AVERAGE SV SPECTRUM FOR DIGITIZATION NOISE
AVERAGE + STANDARD DEVIATION OF SV SPECTRUM FOR DIGITIZATION NOISE
DURATION OF NOISE RECORD
15 SECONDS
30 SECONDS
60 SECONDS
100 SECONDS
SV SPECTRUM-IN/SEC
1000
100
10
1
0.1
0.01
0.001
0.1
1
10
100
T - SECONDS

FIGURE 20

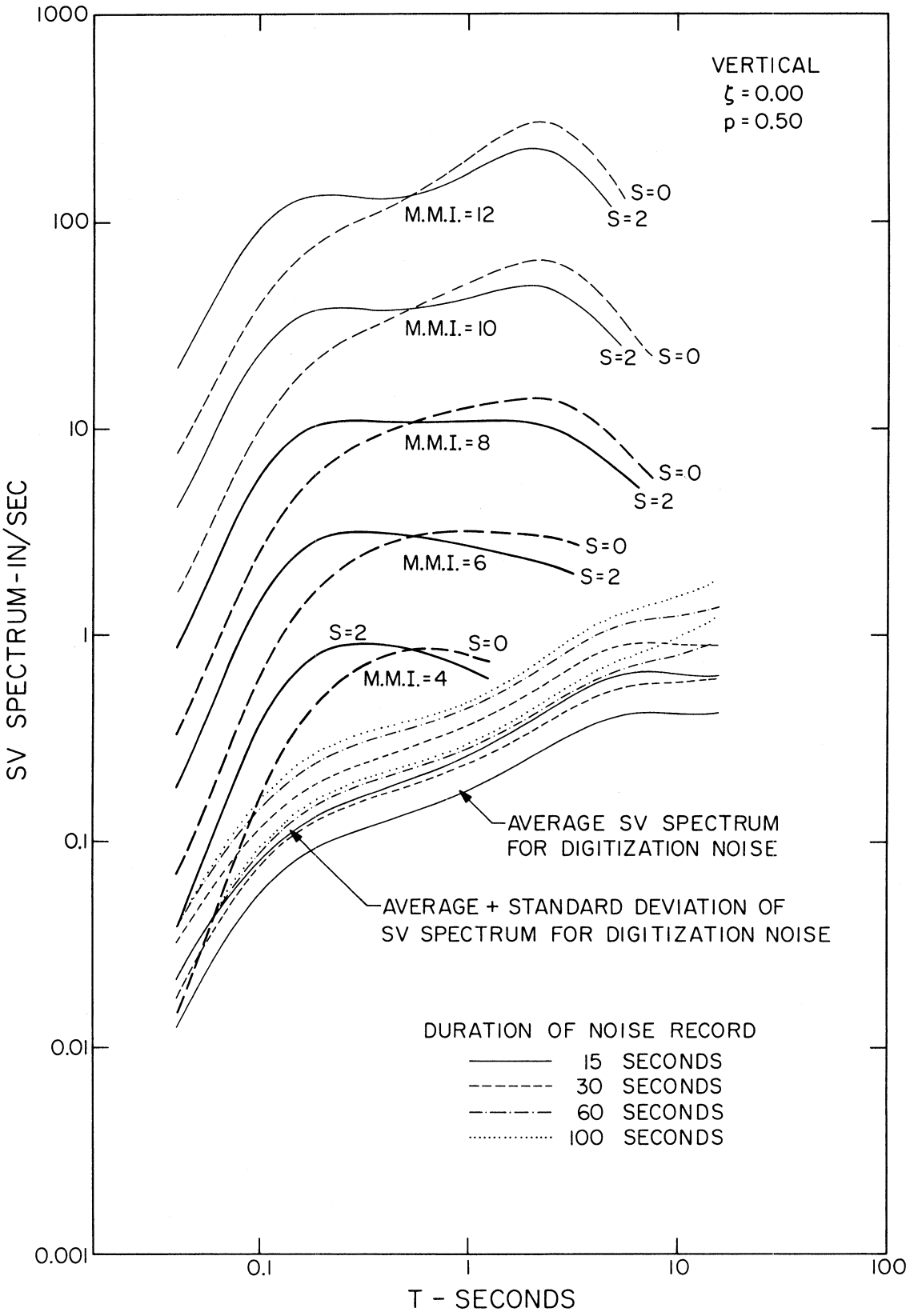
VERTICAL
ζ = 0.00
p = 0.50
M.M.I. = 12
S=0
S=2
M.M.I. = 10
S=2
S=0
M.M.I. = 8
S=0
S=2
M.M.I. = 6
S=0
S=2
S=2
S=0
M.M.I. = 4
AVERAGE SV SPECTRUM FOR DIGITIZATION NOISE
AVERAGE + STANDARD DEVIATION OF SV SPECTRUM FOR DIGITIZATION NOISE
DURATION OF NOISE RECORD
15 SECONDS
30 SECONDS
60 SECONDS
100 SECONDS
SV SPECTRUM-IN/SEC
1000
100
10
1
0.1
0.01
0.001
0.1
1
10
100
T - SECONDS

FIGURE 21

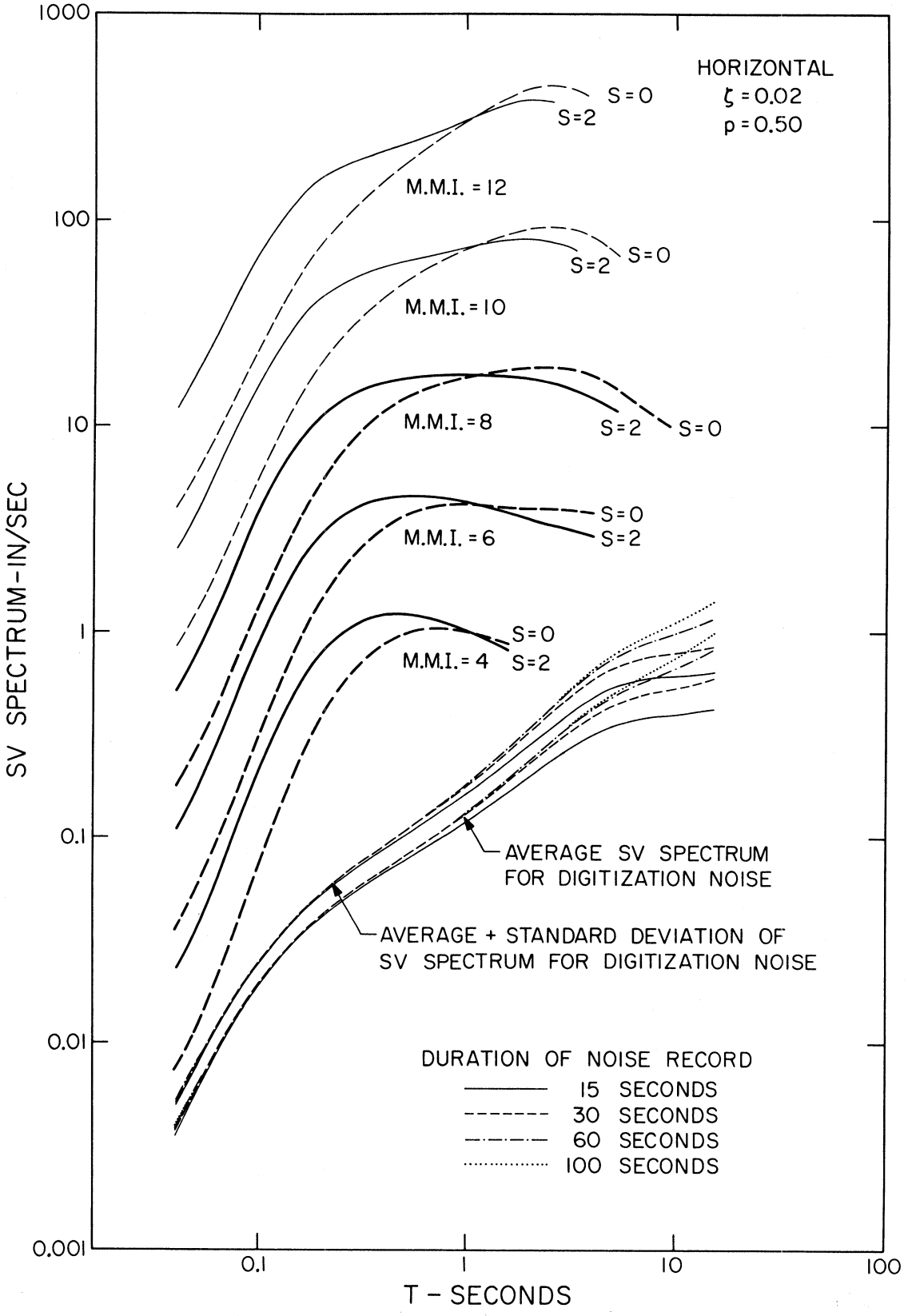
HORIZONTAL
ζ = 0.02
p = 0.50
M.M.I. = 12
S = 0
S=2
M.M.I. = 10
S=2
S=0
M.M.I. = 8
S=2
S=0
M.M.I. = 6
S=0
S=2
M.M.I. = 4
S=0
S=2
AVERAGE SV SPECTRUM
FOR DIGITIZATION NOISE
AVERAGE + STANDARD DEVIATION OF
SV SPECTRUM FOR DIGITIZATION NOISE
DURATION OF NOISE RECORD
15 SECONDS
30 SECONDS
60 SECONDS
100 SECONDS
SV SPECTRUM-IN/SEC
1000
100
10
1
0.1
0.01
0.001
0.1
1
10
100
T - SECONDS

FIGURE 22

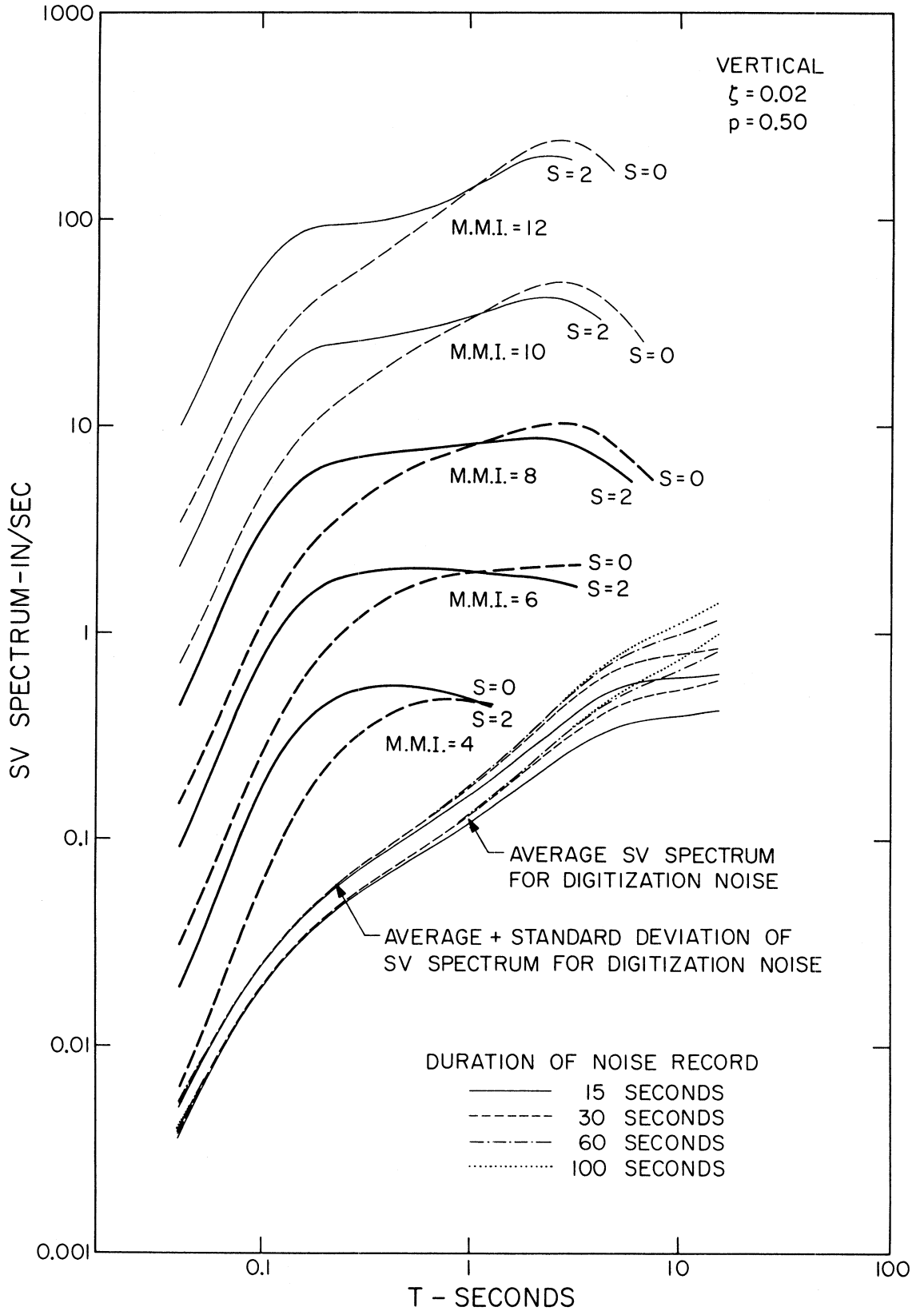
VERTICAL
ζ = 0.02
p = 0.50
S = 2
S = 0
M.M.I. = 12
S = 2
S = 0
M.M.I. = 10
M.M.I. = 8
S = 0
S = 2
S = 0
S = 2
M.M.I. = 6
S = 0
S = 2
M.M.I. = 4
AVERAGE SV SPECTRUM
FOR DIGITIZATION NOISE
AVERAGE + STANDARD DEVIATION OF
SV SPECTRUM FOR DIGITIZATION NOISE
DURATION OF NOISE RECORD
15 SECONDS
30 SECONDS
60 SECONDS
100 SECONDS
SV SPECTRUM-IN/SEC
1000
100
10
1
0.1
0.01
0.001
0.1
1
10
100
T - SECONDS

FIGURE 23

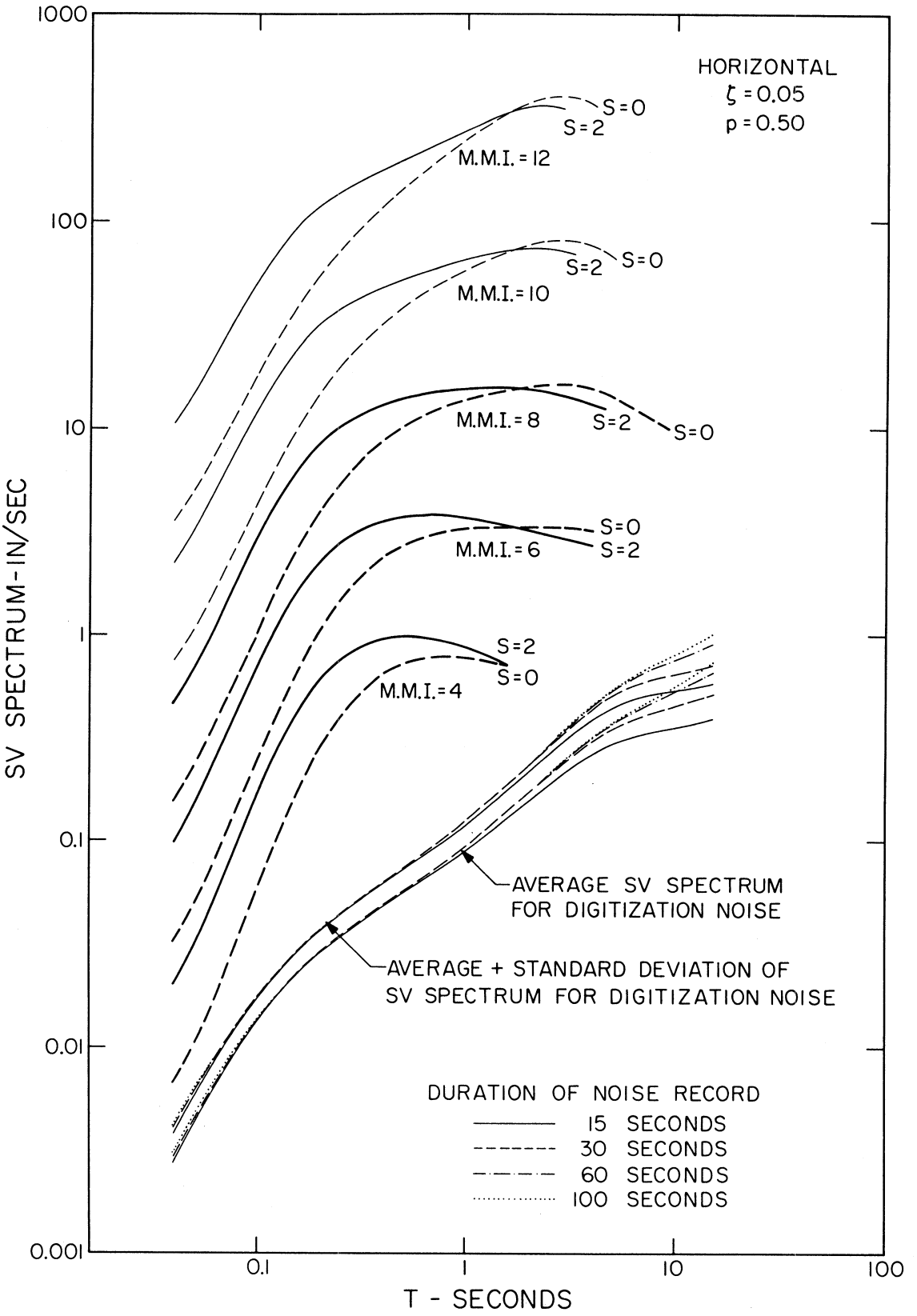
HORIZONTAL
ζ = 0.05
p = 0.50
M.M.I. = 12
M.M.I. = 10
M.M.I. = 8
M.M.I. = 6
M.M.I. = 4
S=0
S=2
AVERAGE SV SPECTRUM FOR DIGITIZATION NOISE
AVERAGE + STANDARD DEVIATION OF SV SPECTRUM FOR DIGITIZATION NOISE
DURATION OF NOISE RECORD
15 SECONDS
30 SECONDS
60 SECONDS
100 SECONDS
SV SPECTRUM-IN/SEC
T - SECONDS
1000
100
10
1
0.1
0.01
0.001
0.1
1
10
100

FIGURE 24

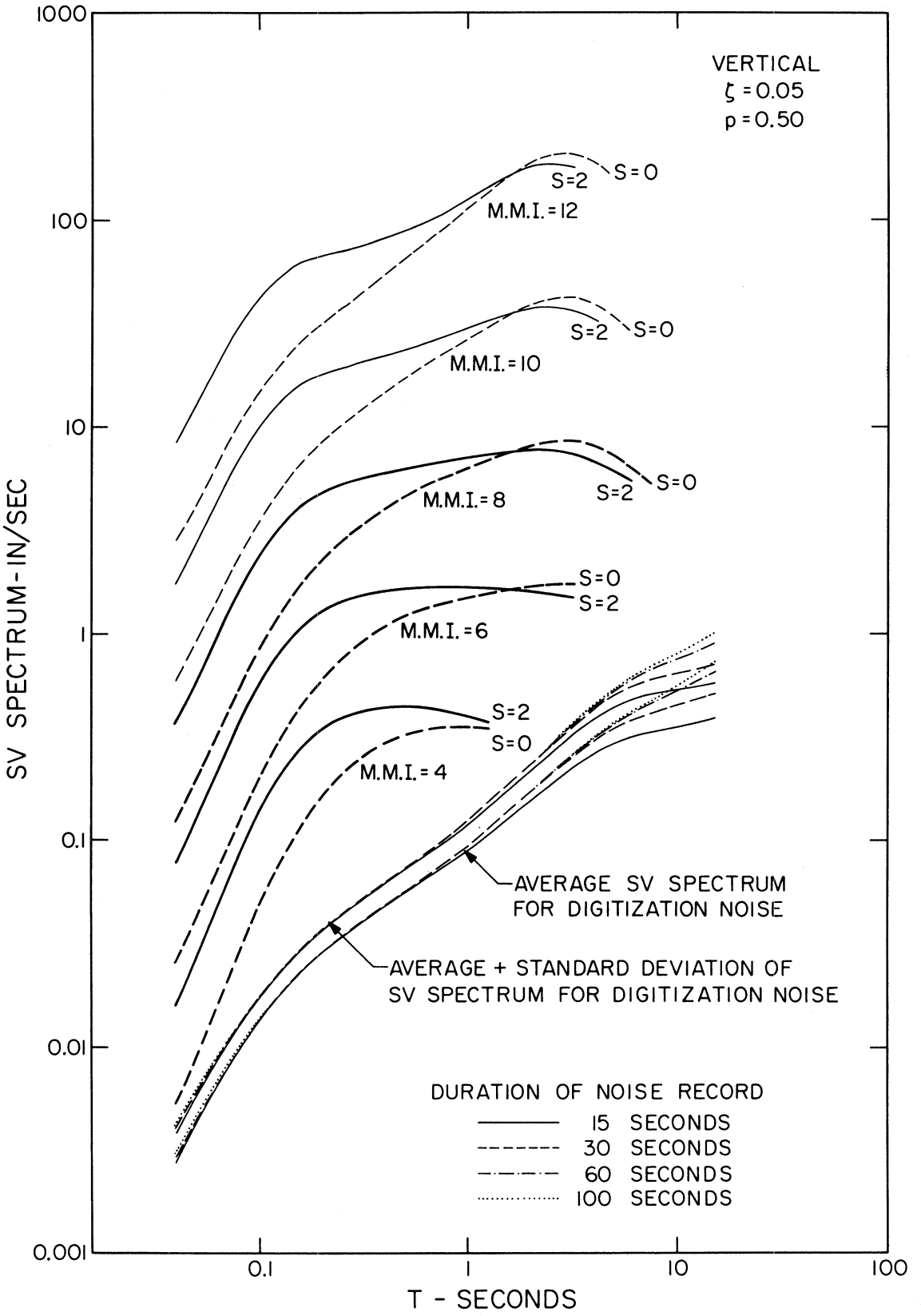
VERTICAL
ζ = 0.05
p = 0.50
S=0
S=2
M.M.I. = 12
S=2
S=0
M.M.I. = 10
M.M.I. = 8
S=2
S=0
S=0
S=2
M.M.I. = 6
S=2
S=0
M.M.I. = 4
AVERAGE SV SPECTRUM
FOR DIGITIZATION NOISE
AVERAGE + STANDARD DEVIATION OF
SV SPECTRUM FOR DIGITIZATION NOISE
DURATION OF NOISE RECORD
15 SECONDS
30 SECONDS
60 SECONDS
100 SECONDS
SV SPECTRUM-IN/SEC
1000
100
10
1
0.1
0.01
0.001
0.1
1
10
100
T - SECONDS

FIGURE 25

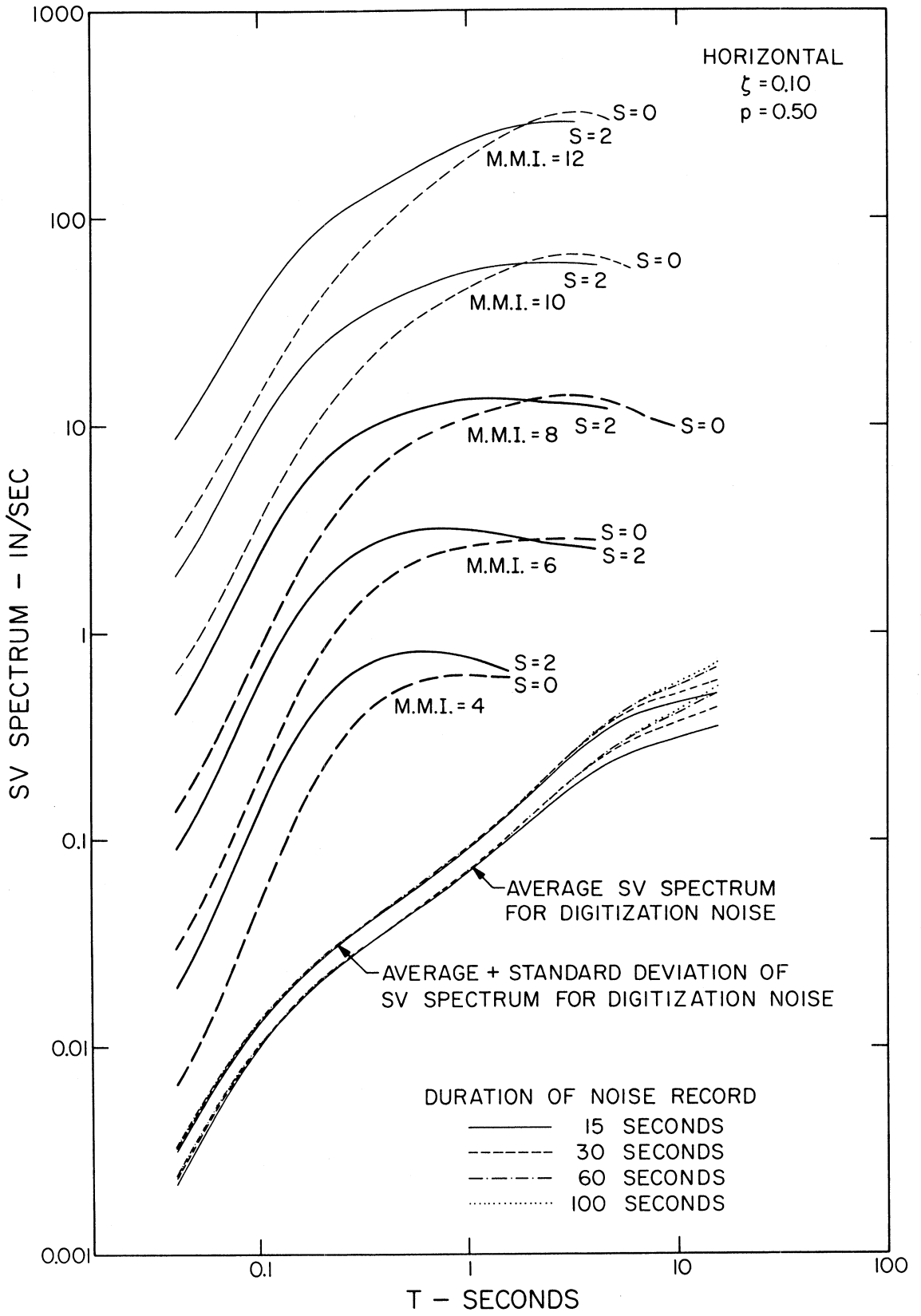
HORIZONTAL
ζ = 0.10
p = 0.50
S = 0
S = 2
M.M.I. = 12
S = 0
S = 2
M.M.I. = 10
M.M.I. = 8
S = 2
S = 0
S = 0
S = 2
M.M.I. = 6
S = 2
S = 0
M.M.I. = 4
AVERAGE SV SPECTRUM FOR DIGITIZATION NOISE
AVERAGE + STANDARD DEVIATION OF SV SPECTRUM FOR DIGITIZATION NOISE
DURATION OF NOISE RECORD
15 SECONDS
30 SECONDS
60 SECONDS
100 SECONDS
SV SPECTRUM - IN/SEC
1000
100
10
1
0.1
0.01
0.001
0.1
1
10
100
T - SECONDS

FIGURE 26

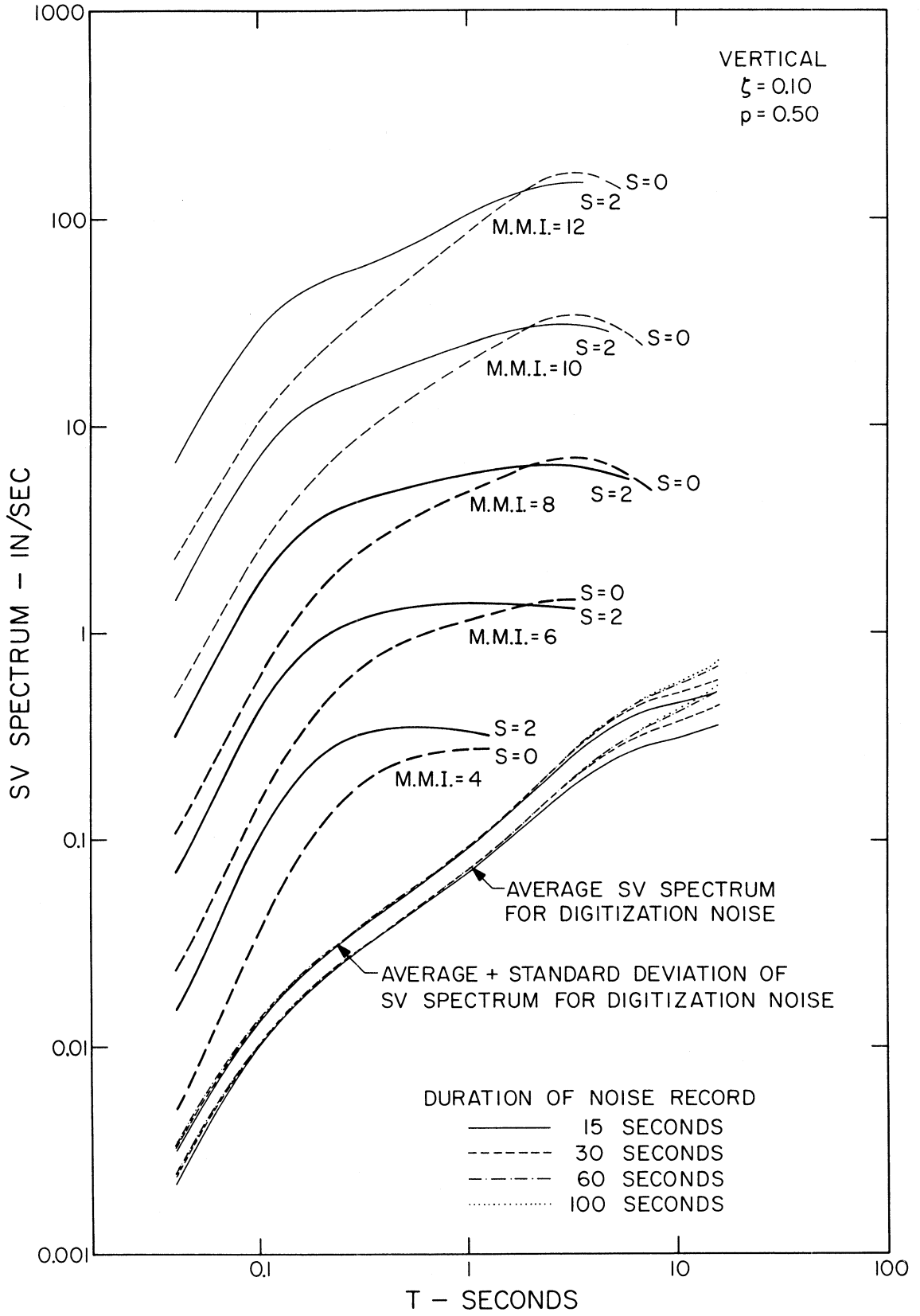
VERTICAL
ζ = 0.10
p = 0.50
S=0
S=2
M.M.I.=12
S=0
S=2
M.M.I.=10
S=0
S=2
M.M.I.=8
S=0
S=2
M.M.I.=6
S=2
S=0
M.M.I.=4
AVERAGE SV SPECTRUM FOR DIGITIZATION NOISE
AVERAGE + STANDARD DEVIATION OF SV SPECTRUM FOR DIGITIZATION NOISE
DURATION OF NOISE RECORD
15 SECONDS
30 SECONDS
60 SECONDS
100 SECONDS
SV SPECTRUM – IN/SEC
1000
100
10
1
0.1
0.01
0.001
0.1
1
10
100
T – SECONDS

FIGURE 27

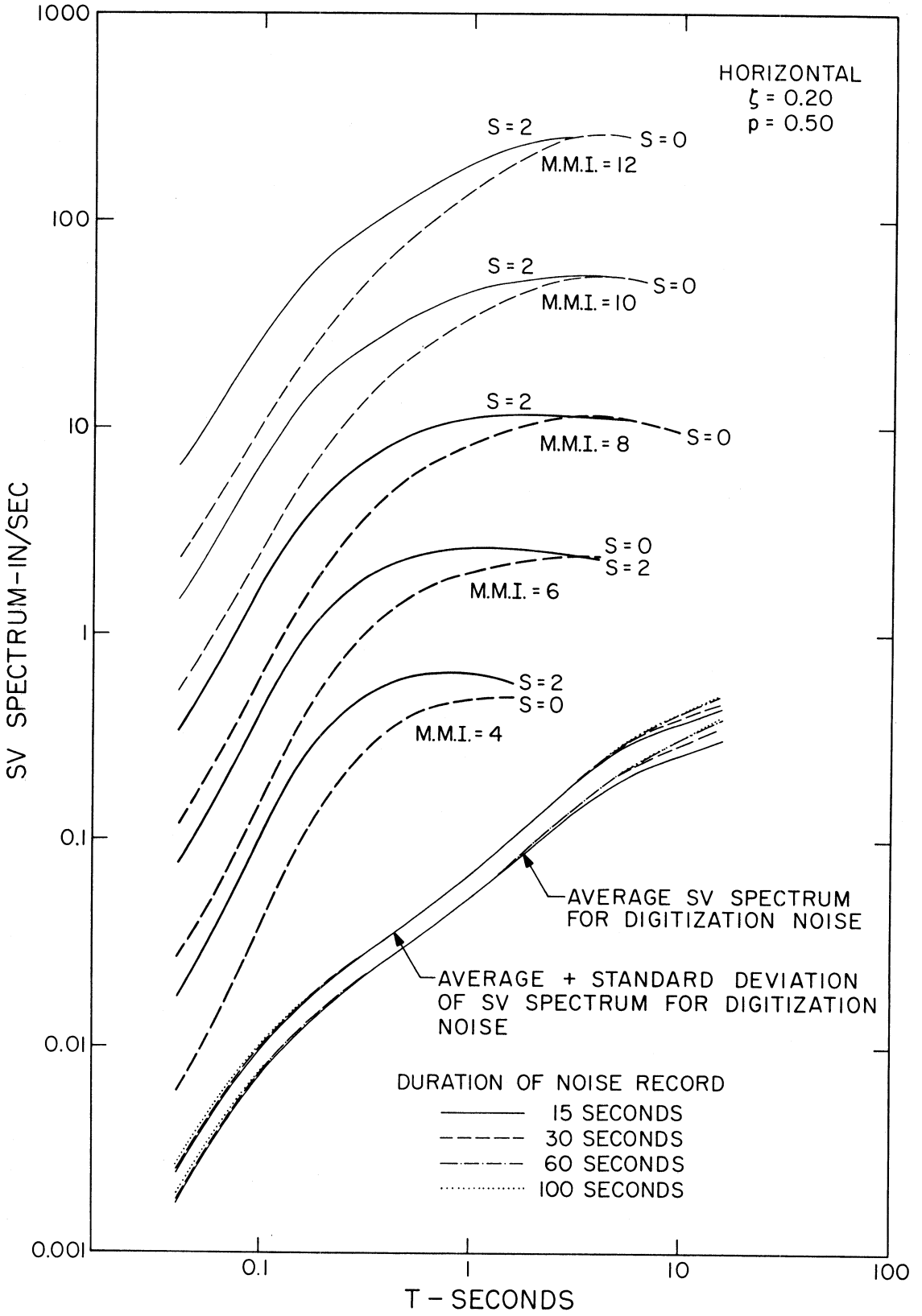
HORIZONTAL
ζ = 0.20
p = 0.50
S = 2
S = 0
M.M.I. = 12
S = 2
S = 0
M.M.I. = 10
S = 2
M.M.I. = 8
S = 0
S = 0
S = 2
M.M.I. = 6
S = 2
S = 0
M.M.I. = 4
AVERAGE SV SPECTRUM FOR DIGITIZATION NOISE
AVERAGE + STANDARD DEVIATION OF SV SPECTRUM FOR DIGITIZATION NOISE
DURATION OF NOISE RECORD
15 SECONDS
30 SECONDS
60 SECONDS
100 SECONDS
SV SPECTRUM-IN/SEC
1000
100
10
1
0.1
0.01
0.001
0.1
1
10
100
T - SECONDS

FIGURE 28

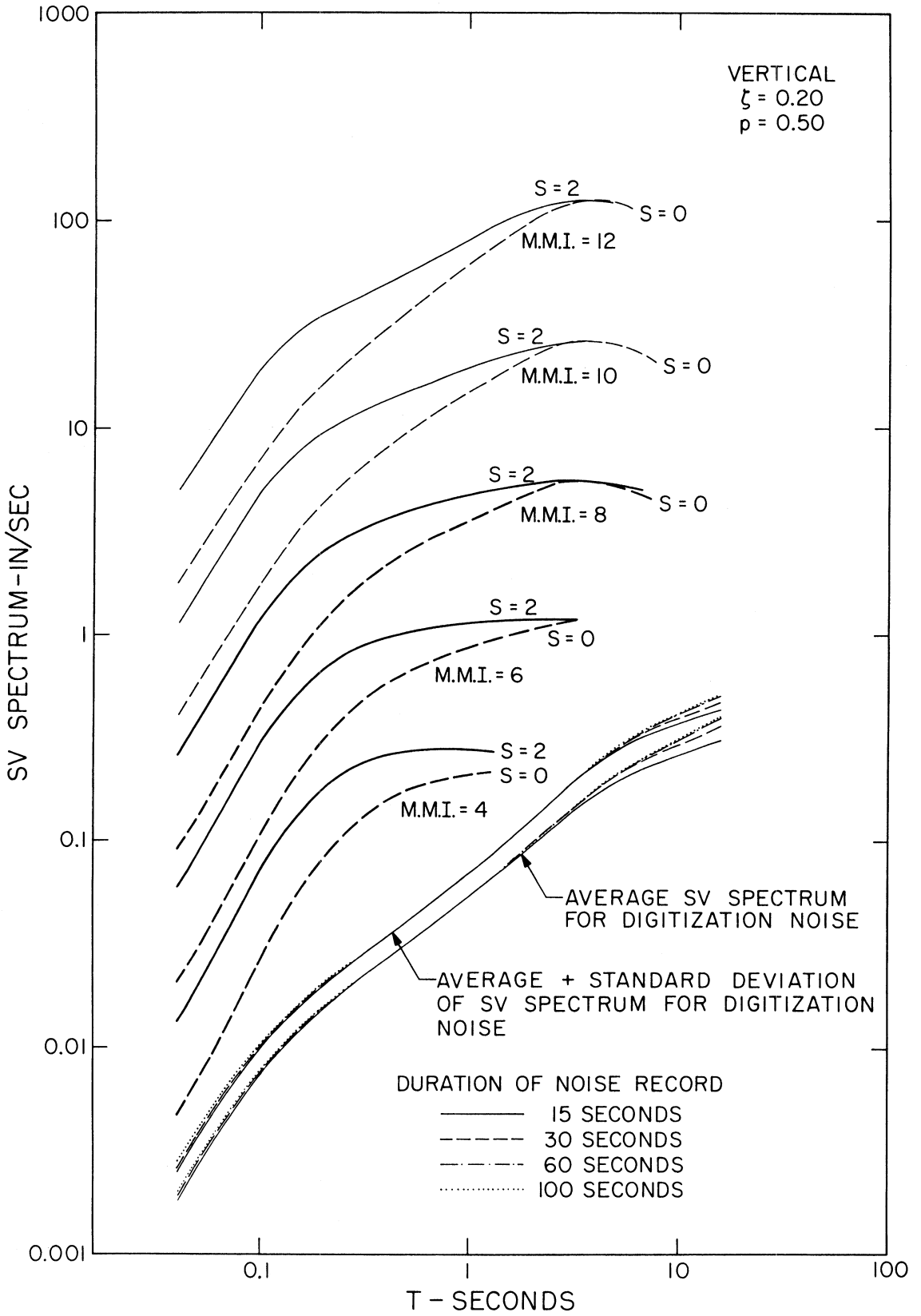
VERTICAL
ζ = 0.20
p = 0.50
S = 2
S = 0
M.M.I. = 12
M.M.I. = 10
M.M.I. = 8
M.M.I. = 6
M.M.I. = 4
AVERAGE SV SPECTRUM FOR DIGITIZATION NOISE
AVERAGE + STANDARD DEVIATION OF SV SPECTRUM FOR DIGITIZATION NOISE
DURATION OF NOISE RECORD
15 SECONDS
30 SECONDS
60 SECONDS
100 SECONDS
SV SPECTRUM-IN/SEC
T - SECONDS
1000
100
10
1
0.1
0.01
0.001
0.1
1
10
100

FIGURE 29

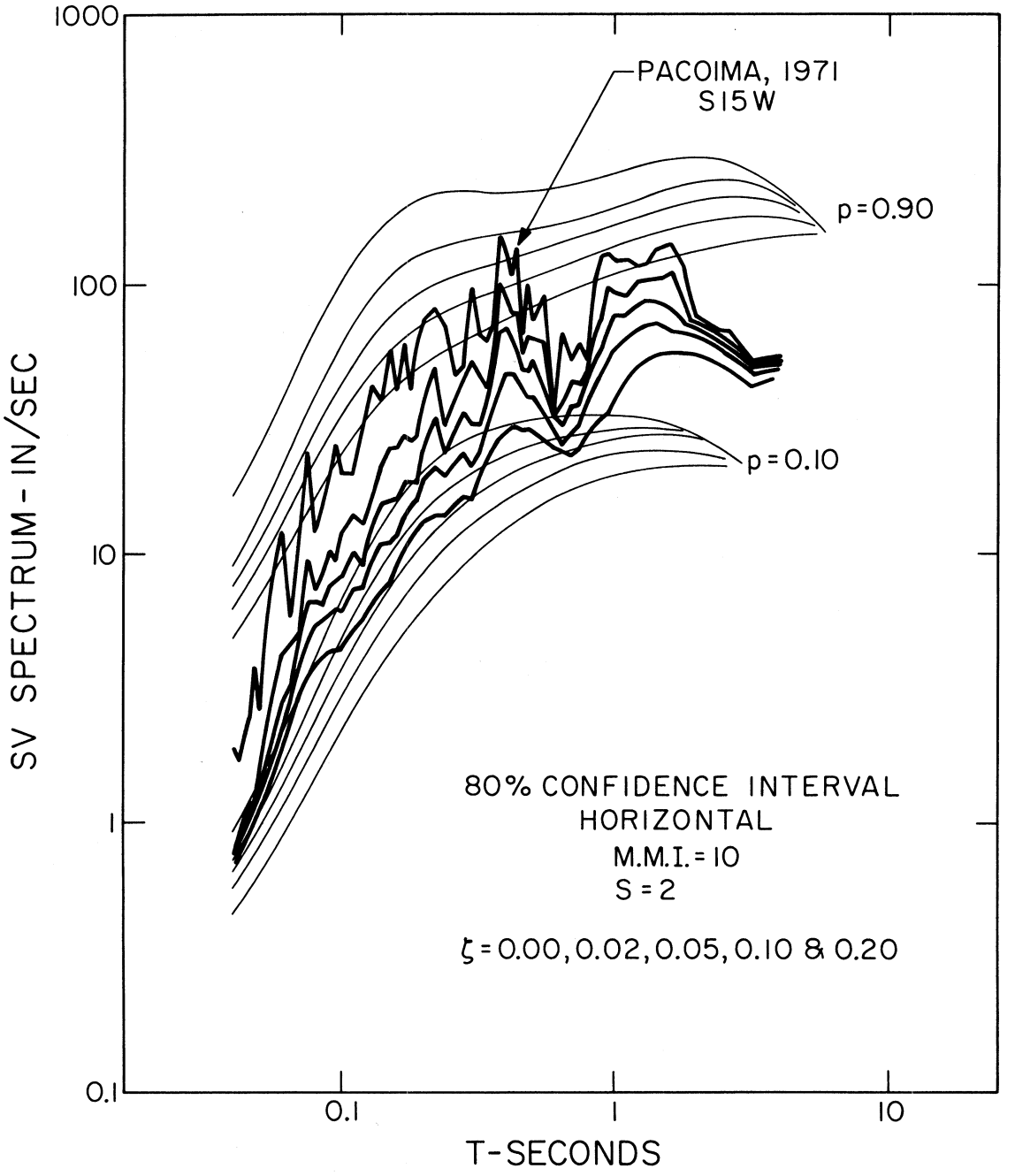
1000
100
10
1
0.1
SV SPECTRUM - IN/SEC
PACOIMA, 1971
S15W
p = 0.90
p = 0.10
80% CONFIDENCE INTERVAL
HORIZONTAL
M.M.I. = 10
S = 2
ζ = 0.00, 0.02, 0.05, 0.10 & 0.20
0.1
1
10
T-SECONDS

FIGURE 30

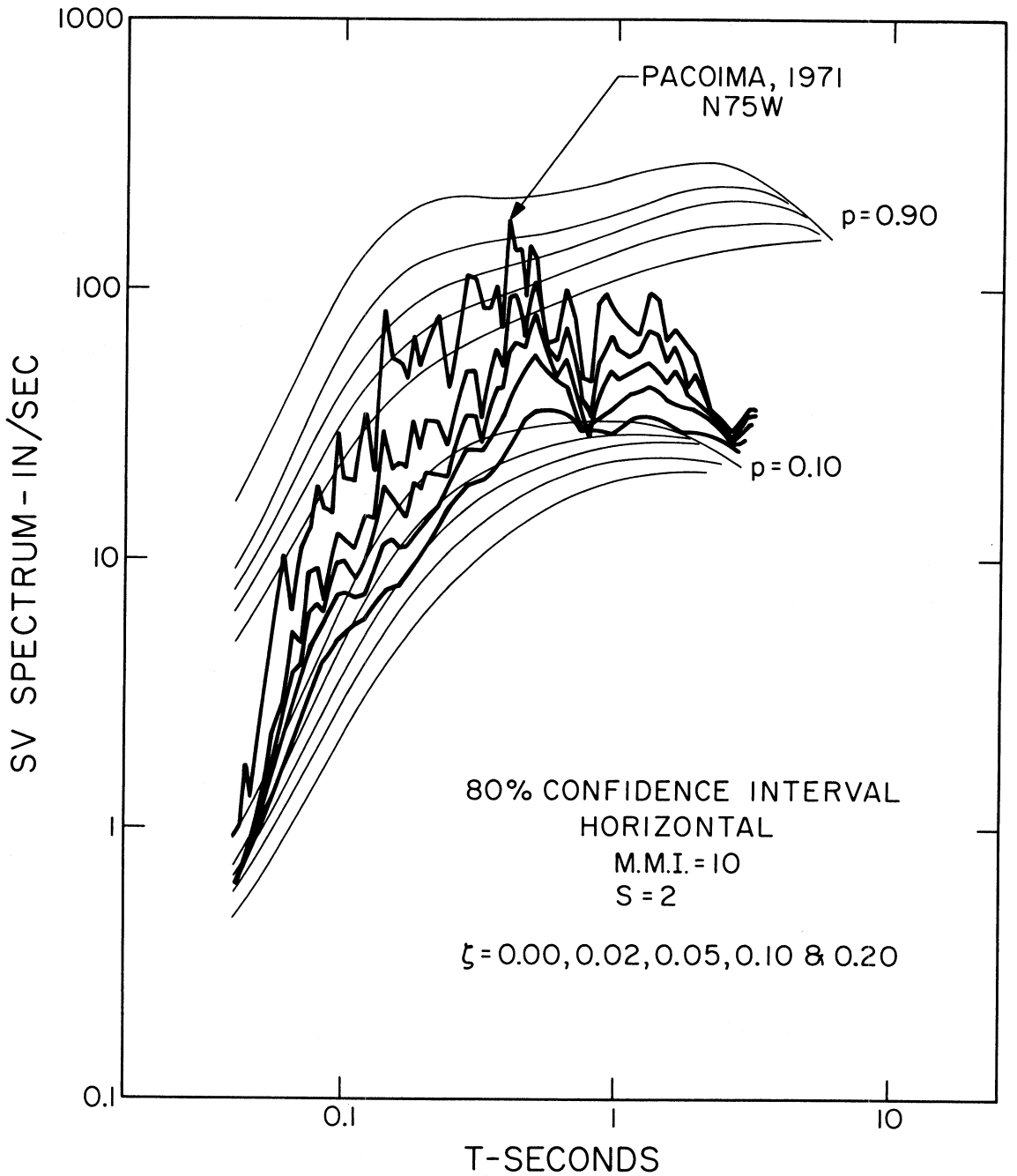
1000
100
10
1
0.1
SV SPECTRUM - IN/SEC
PACOIMA, 1971
N75W
p = 0.90
p = 0.10
80% CONFIDENCE INTERVAL
HORIZONTAL
M.M.I. = 10
S = 2
ζ = 0.00, 0.02, 0.05, 0.10 & 0.20
0.1
1
10
T-SECONDS

FIGURE 31

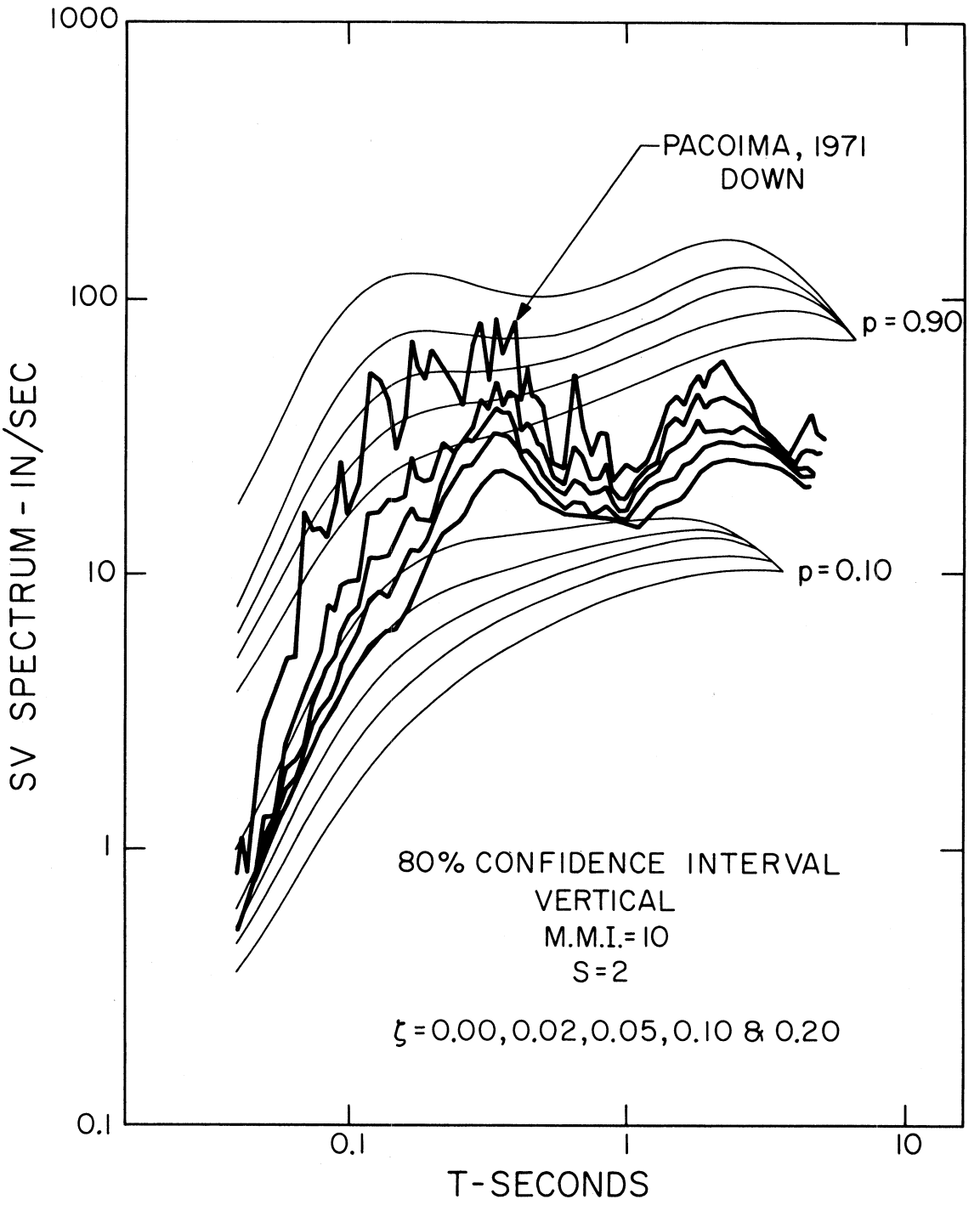
1000
100
10
1
0.1
SV SPECTRUM - IN/SEC
PACOIMA, 1971
DOWN
p = 0.90
p = 0.10
80% CONFIDENCE INTERVAL
VERTICAL
M.M.I.= 10
S=2
ζ = 0.00, 0.02, 0.05, 0.10 & 0.20
0.1
1
10
T-SECONDS

FIGURE 32

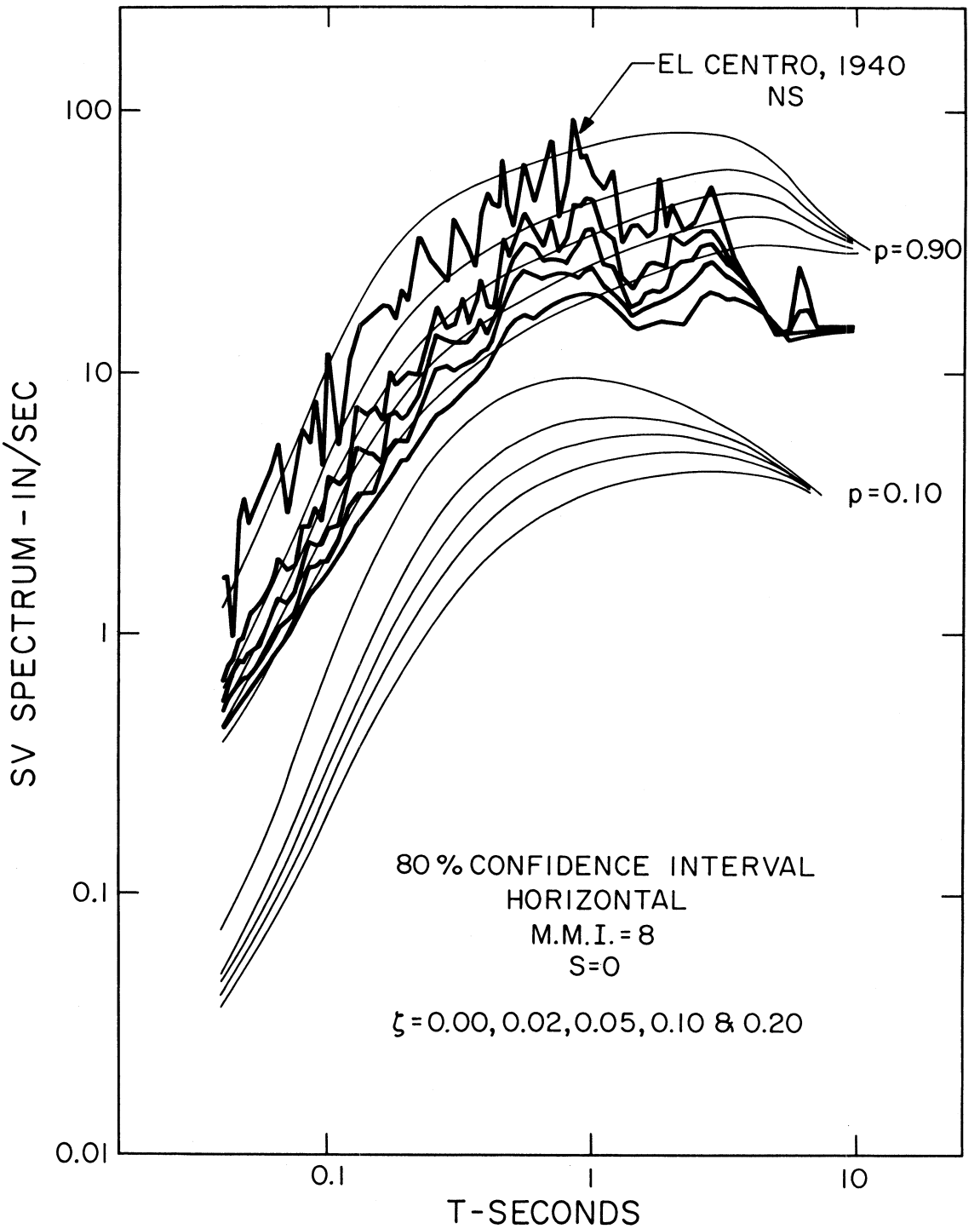
EL CENTRO, 1940
NS
p=0.90
p=0.10
80 % CONFIDENCE INTERVAL
HORIZONTAL
M.M.I. = 8
S=0
ζ = 0.00, 0.02, 0.05, 0.10 & 0.20
SV SPECTRUM - IN/SEC
100
10
1
0.1
0.01
0.1
1
10
T-SECONDS

FIGURE 33

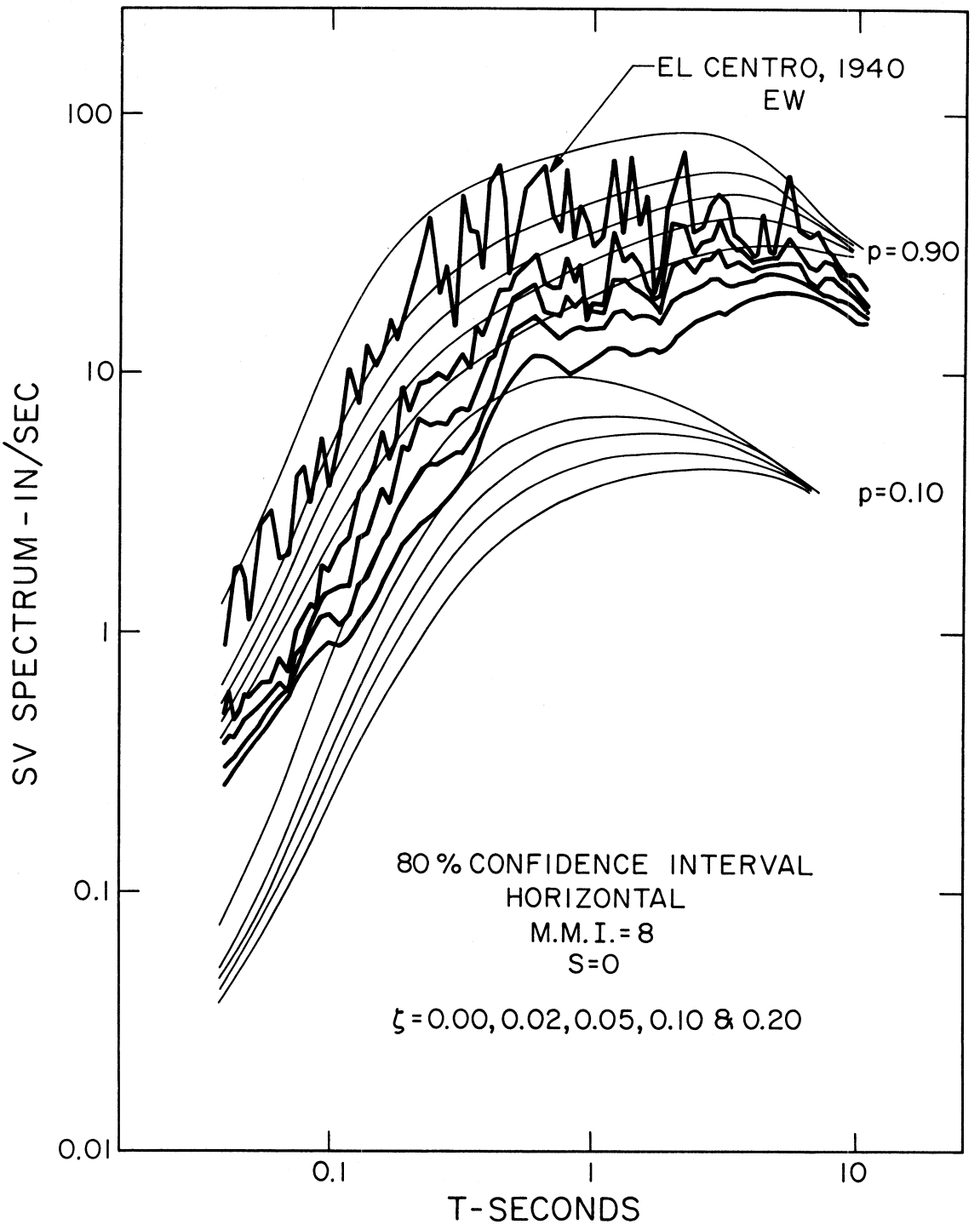
EL CENTRO, 1940
EW
p=0.90
p=0.10
80 % CONFIDENCE INTERVAL
HORIZONTAL
M.M.I.= 8
S=0
ζ = 0.00, 0.02, 0.05, 0.10 & 0.20
SV SPECTRUM - IN/SEC
T-SECONDS
100
10
1
0.1
0.01
0.1
1
10

FIGURE 34

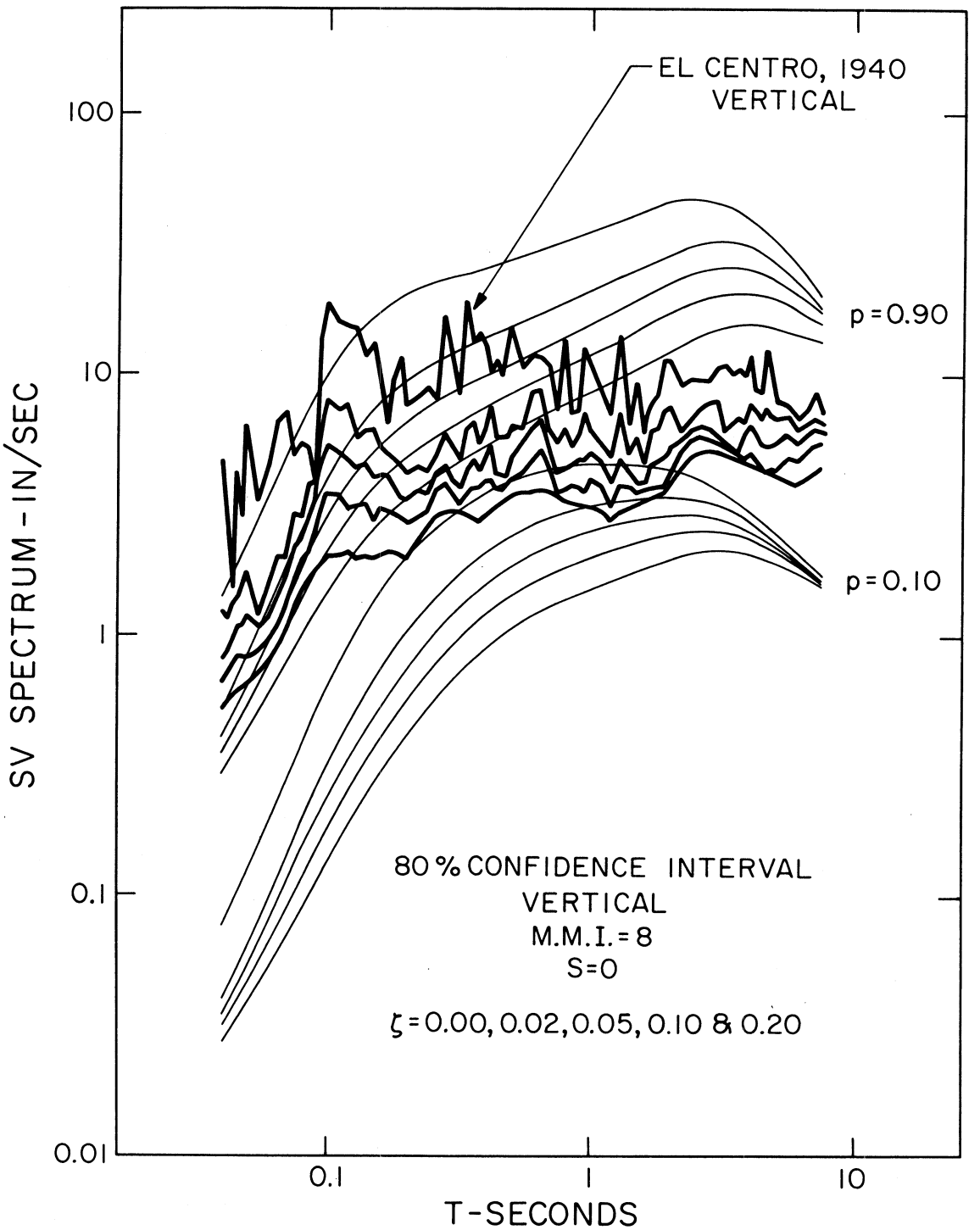
EL CENTRO, 1940
VERTICAL
p = 0.90
p = 0.10
80 % CONFIDENCE INTERVAL
VERTICAL
M.M.I. = 8
S=0
ζ = 0.00, 0.02, 0.05, 0.10 & 0.20
SV SPECTRUM - IN/SEC
T-SECONDS
100
10
1
0.1
0.01
0.1
1
10

FIGURE 35

shaking at the Pacoima Dam site during the San Fernando, California, earthquake of 1971 and at El Centro during the Imperial Valley, California, earthquake of 1940 have been characterized by MMI = X and VIII, respectively. Equation (2) has been employed to compute 80 percent confidence interval (between SV spectra for p = 0.9 and 0.1) for ζ = 0.0, 0.02, 0.05, 0.10 and 0.20, and for s=2 and s=0, respectively. It is seen from Figures 30 through 35 that the agreement between computed and calculated SV amplitudes is adequate.

We suggested in several previous studies that a consistency check between equation (1) and (2) would be to compare spectral amplitudes for the largest possible level of shaking in terms of M and MMI scaling (Trifunac and Anderson, 1977, 1978). Figures 36 and 37 show such comparison for SV spectra computed from equations (1) and (2) and for other scaling parameters as shown in the figures. It is seen that, even though equation (2) may overestimate SV amplitudes for short periods T < 0.1 sec (or equation (1) underestimate SV amplitudes in the same period range), equations (1) and (2) are virtually consistent in a way which is in agreement with our previous analyses (see Figures 51 and 52 of Trifunac and Anderson, 1977, and Figures 48 and 49 of Trifunac and Anderson, 1978). This suggests again an agreement with previous analyses on SA and PSV spectral amplitudes that the slope b(T) in equation (2) is probably not too different from the one which will be derived eventually when significantly greater body of data becomes available, especially for MMI > VIII. Finally, as we noted in our previous work,

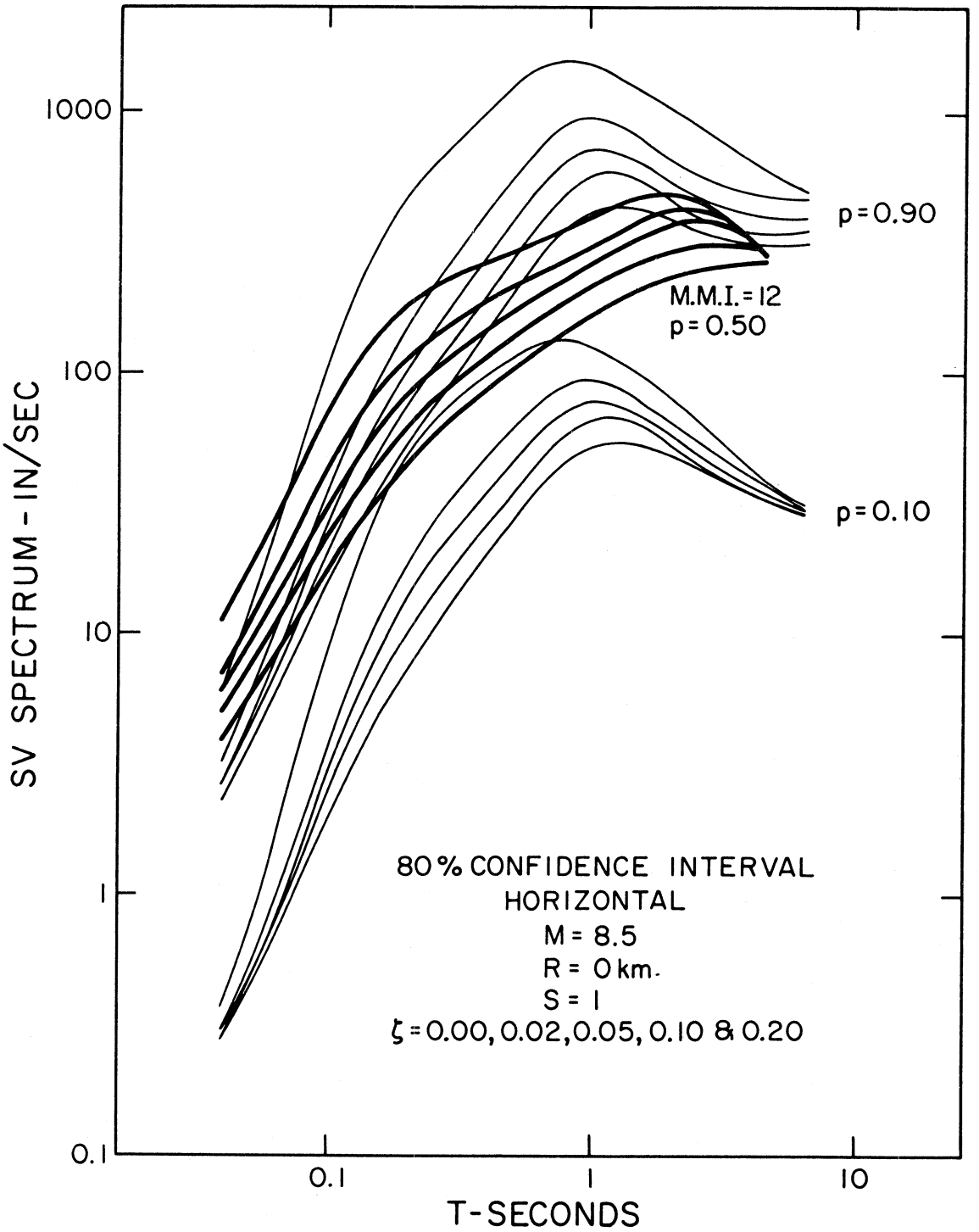
1000
100
10
1
0.1
SV SPECTRUM - IN/SEC
0.1
1
10
T-SECONDS
p=0.90
M.M.I.=12
p=0.50
p=0.10
80% CONFIDENCE INTERVAL
HORIZONTAL
M = 8.5
R = 0 km.
S = 1
ζ = 0.00, 0.02, 0.05, 0.10 & 0.20

FIGURE 36

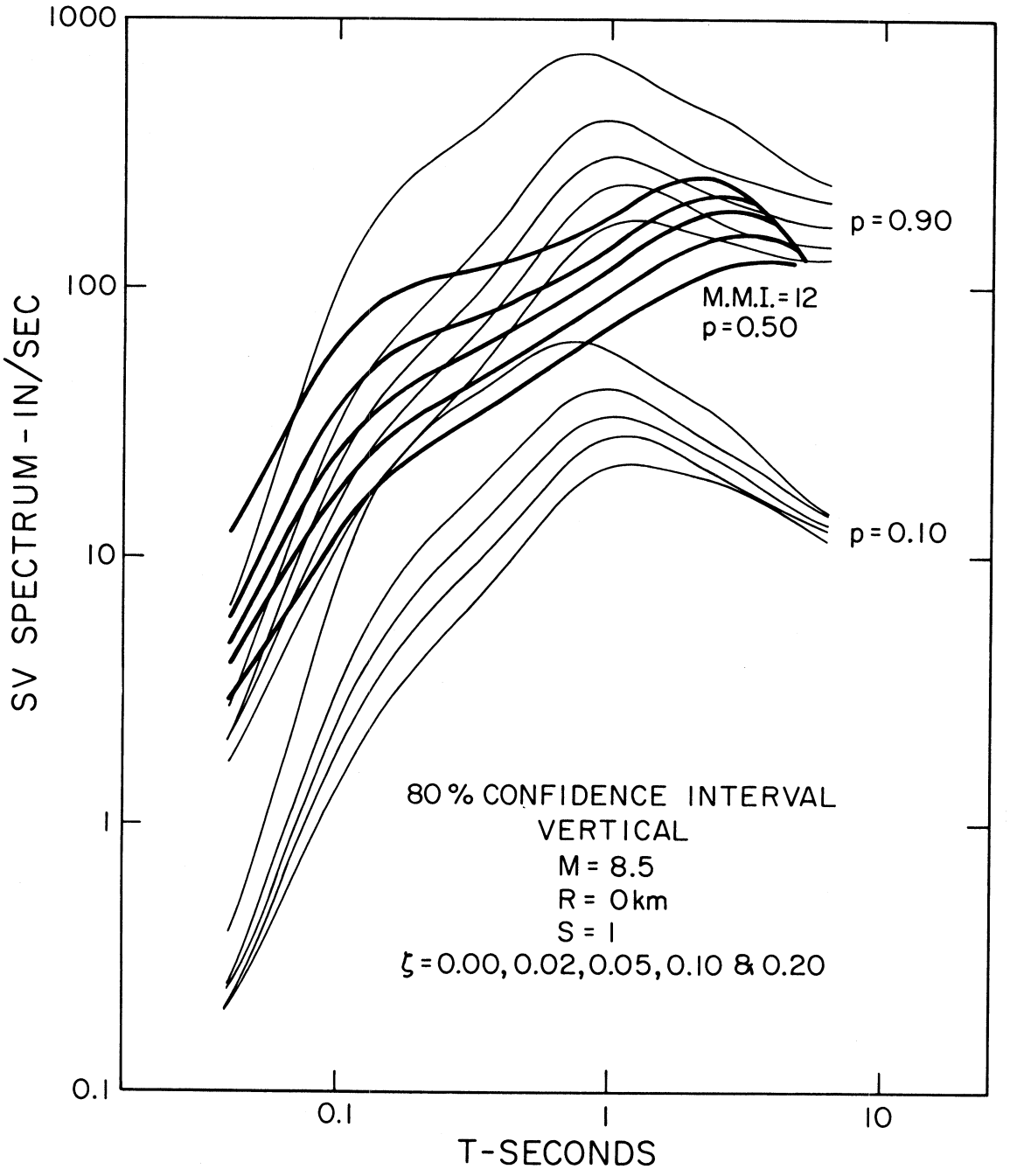
1000
100
10
1
0.1
SV SPECTRUM - IN/SEC
0.1
1
10
T-SECONDS
p = 0.90
M.M.I. = 12
p = 0.50
p = 0.10
80 % CONFIDENCE INTERVAL
VERTICAL
M = 8.5
R = 0km
S = 1
ζ = 0.00, 0.02, 0.05, 0.10 & 0.20

FIGURE 37

this also suggests that the arbitrary assumption that individual levels on MMI scale (I through XII) can be assigned to a linearly increasing numerical scale 1, 2, ..., 11, and 12, clearly does not lead to gross inconsistencies that can be detected by the data, so far recorded.

DISTRIBUTION OF SPECTRAL AMPLITUDES

The variable p in equations (1) and (2) which takes on values between 0.1 and 0.9 does not represent probability but in this interval, approximates the cumulative distribution of data with respect to equations (1) and (2). Once the smoothed functions a(T) through g(T) are known it is possible to calculate $SV(T)_p$ amplitudes from (1) and (2), for all scaling parameters corresponding to actually recorded accelerograms, and to compute actual fraction of data p_a, which are below the approximate (linear) value of p between 0.1 and 0.9. Figures 38 and 39 present smoothed results of such calculations for p = 0.1, 0.2, ... 0.8 and 0.9, for ζ = 0.0, 0.02, 0.05, 0.10 and 0.20, and plotted versus period T. From these figures it is possible then to derive an analytic continuous representation of p_a versus p (from now on, we replace p by p_ℓ) and as a function of T (Trifunac and Anderson, 1977, 1978).

In our previous work, we assumed that the distribution p_a can be derived by approximating the distribution of response amplitudes by the Rayleigh distribution. Since SV spectra result from the same physical basis as PSV and SA spectra, there seems to exist no reason to assume that the distribution of SV amplitudes cannot be approximated by the Rayleigh distribution function as well. Consequently, if N(T) is the number of response peaks during the time interval contributing significantly to SV amplitudes, it can be shown (Trifunac and Anderson, 1977) that p_a can be approximated by

$$p_a = [1 - \exp(-e^{\alpha(T)p_\ell + \beta(T)})]^{N(T)} \qquad (3)$$

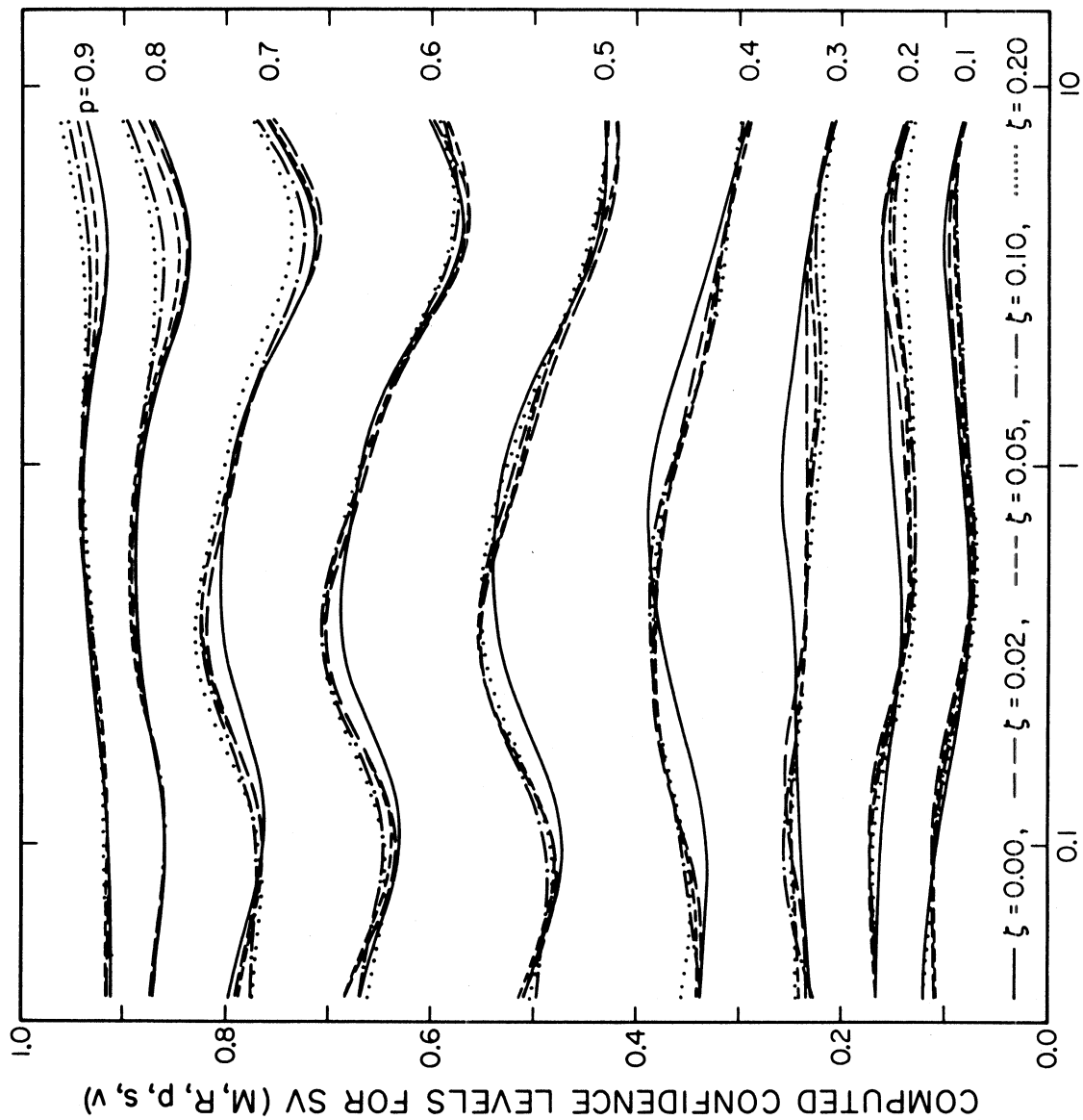
COMPUTED CONFIDENCE LEVELS FOR SV (M, R, p, s, ν)
1.0
0.8
0.6
0.4
0.2
0.0
p=0.9
0.8
0.7
0.6
0.5
0.4
0.3
0.2
0.1
0.1
1
10
T-SECONDS
ζ = 0.00, ζ = 0.02, ζ = 0.05, ζ = 0.10, ζ = 0.20

FIGURE 38

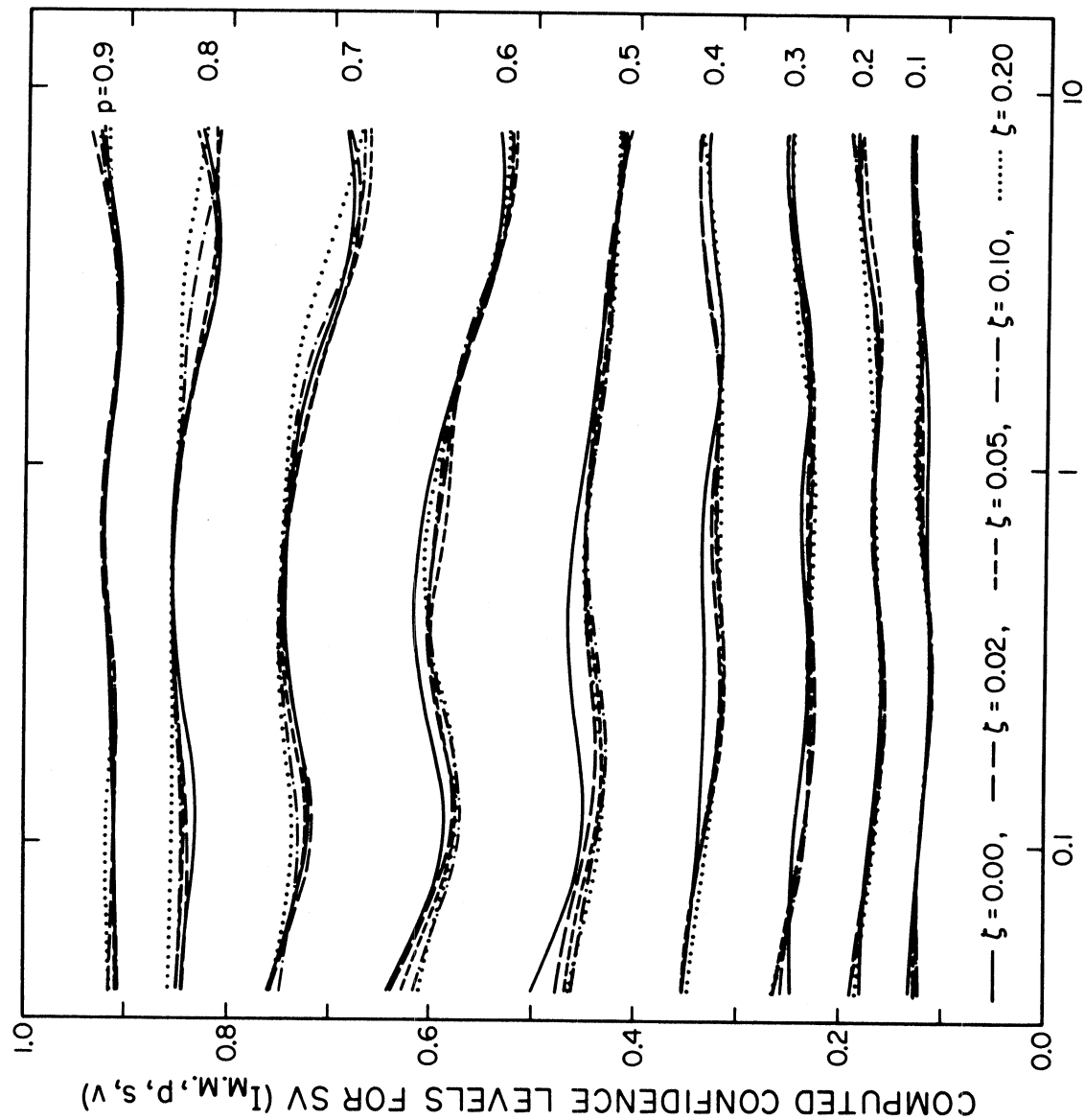
COMPUTED CONFIDENCE LEVELS FOR SV ($I_{M.M.}$, p, s, v)
T-SECONDS
p=0.9
0.8
0.7
0.6
0.5
0.4
0.3
0.2
0.1
0.0
0.2
0.4
0.6
0.8
1.0
0.1
1
10
—— ζ = 0.00, —— ζ = 0.02, - - - ζ = 0.05, —·— ζ = 0.10, ····· ζ = 0.20

FIGURE 39

In (3), $\alpha(T)$, $\beta(T)$ and $N(T)$ can be selected by fitting this equation to the data in Figures 38 and 39.

Figures 40 and 41 show the range of $N(T)$ which leads to p_a versus p_ℓ that cannot be rejected by either χ^2 or Kolmogorov-Smirnov (K-S) tests. In these figures the best values for N are indicated by integers 1 through 5. These integers also identify the fractions of critical damping as follows: 1 for $\zeta = 0.0$, 2 for $\zeta = 0.02$, 3 for $\zeta = 0.05$, 4 for $\zeta = 0.10$ and 5 for $\zeta = 0.20$.

The best values of N are smaller than what would be expected from direct use of the ratio of duration of shaking and the oscillator natural period as illustrated for $M = 6.5$, and $R = 0$ and 100 km (Trifunac and Westermo, 1976a). The best values of N are however consistent with similar analyses for SA and PSV spectra (Trifunac and Anderson, 1977, 1978) where we concluded that the "best" value of $N(T)$ is apparently more representative of a shorter time interval which contributes significantly to the maximum response only. Since the object of this analysis is also only to find a simple useful analytical model for p_a versus p_ℓ, which does not violate simple principles governing the statistics of spectral amplitudes, we choose $N(T) = 6.5/T$ for $N \leq 20$ and $N = 20$ for $\log_{10} T \leq -0.478$. These values of N have been represented by a continuous line in Figures 40 and 41 and are also tabulated in Table II.

This value of N and the best estimates of $\alpha(T)$ and $\beta(T)$ are shown in Figure 42. This figure also presents the average, μ, and the standard deviation σ of p_a versus p_ℓ (middle) and the χ^2 and largest

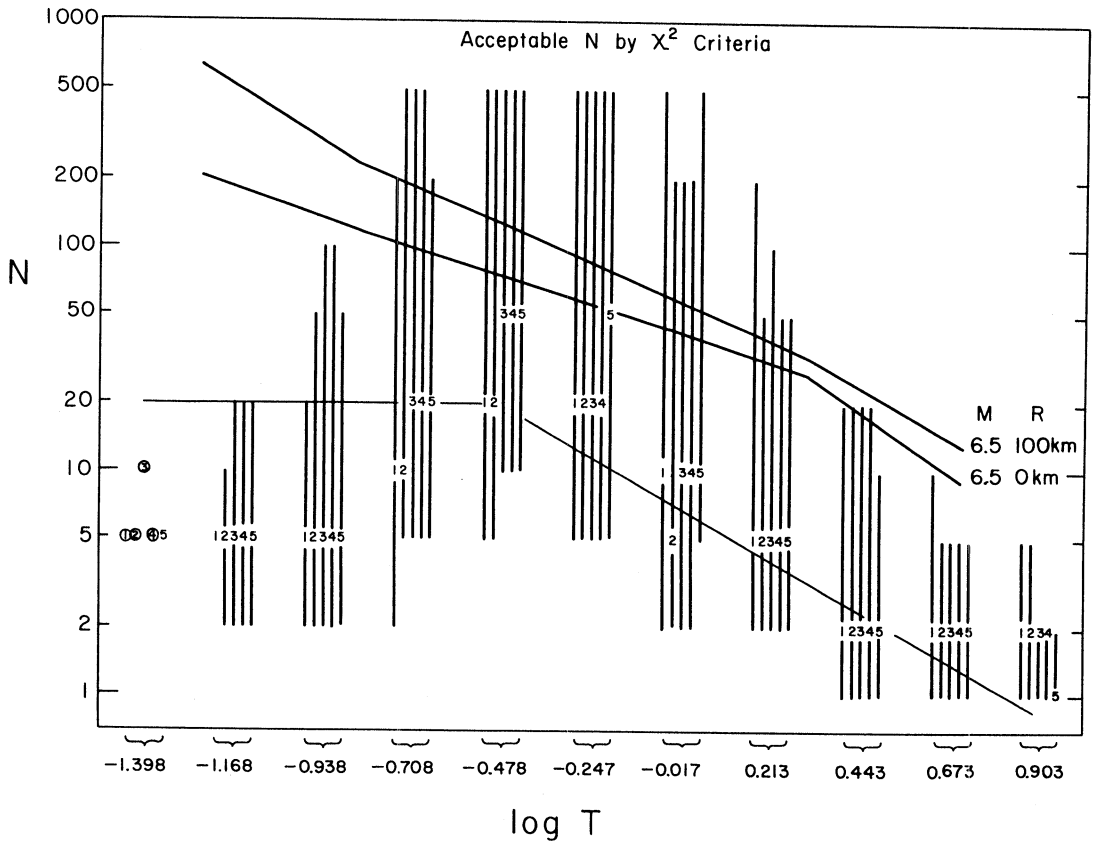

Figure 40

Summary of the results of the statistical test χ^2 for distribution of form (3) relating p_a and p_ℓ for the regression of $\log_{10}[SV]$ as a function of p_ℓ, M, R, s and v. For each of 11 periods, we have plotted an integer (1-5) at the value of N which leads to the smallest value of χ^2. The vertical line shows the range of N which leads to a value of the χ^2 statistic which is small enough that the corresponding distribution is not rejected at the 95% confidence level. Where the integer (1-5) is circled, the best value of χ^2 is rejected. The integers 1-5 refer to the value of damping: 1 for $\zeta = 0.0$; 2 for $\zeta = 0.02$; 3 for $\zeta = 0.05$; 4 for $\zeta = 0.10$; and 5 for $\zeta = 0.20$.

The values of N which might be expected from the results of Trifunac and Westermo (1976a) for a magnitude 6.5 earthquake at 0 km and 100 km are shown. We chose the value of N to be integers approximately equal to the straight line through the data, which has the equation $N = 6.5/T$, for $N < 20$ and $N = 20$ for $\log_{10}T \leq -0.478$.

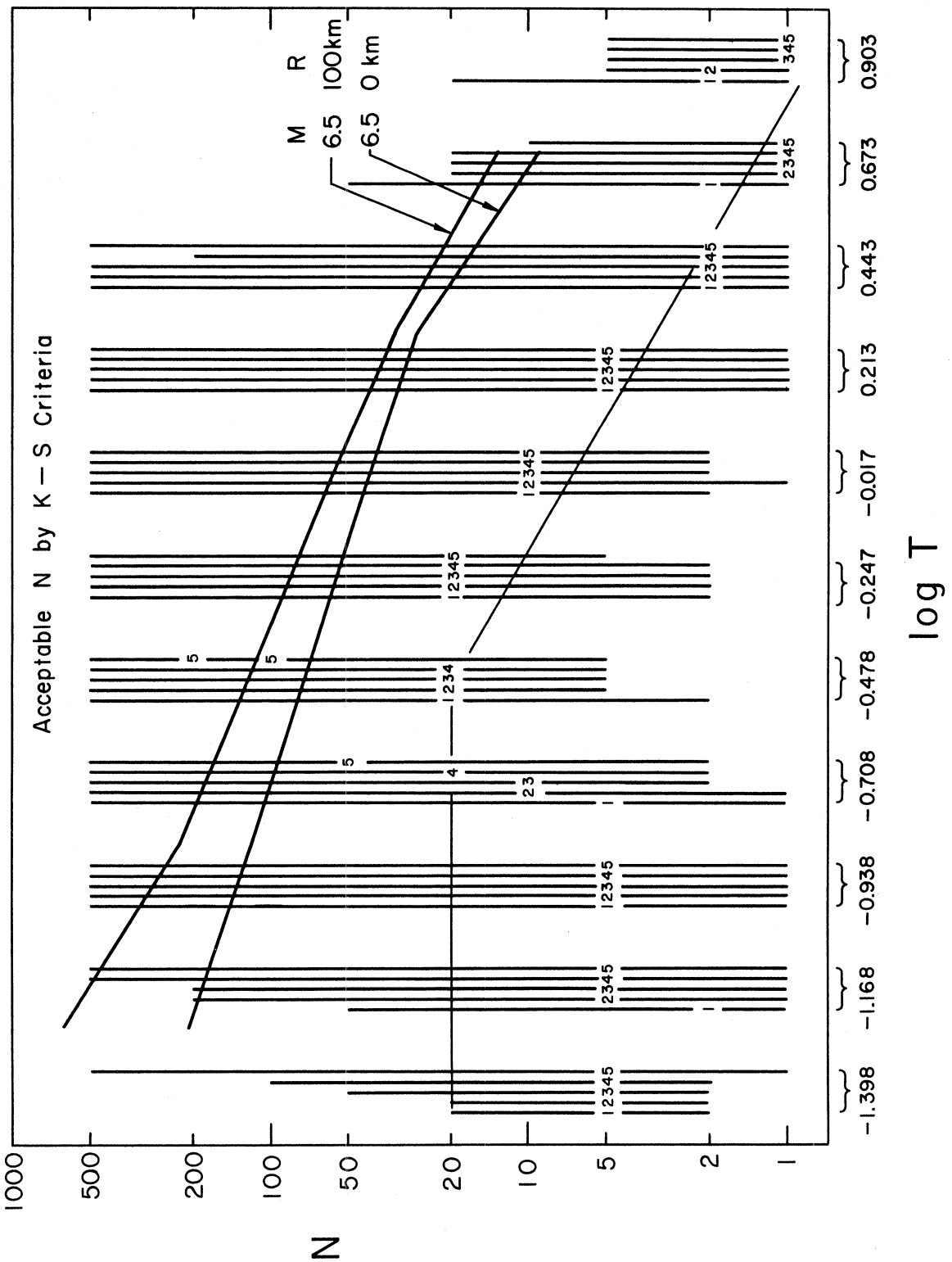

Figure 41

Results of the Kolmogorov-Smirnov statistical test to determine which values of N are acceptable to fit the data of p_a vs. p_ℓ for the regression of SV with magnitude and distance. Other symbols are as in Figure 40.

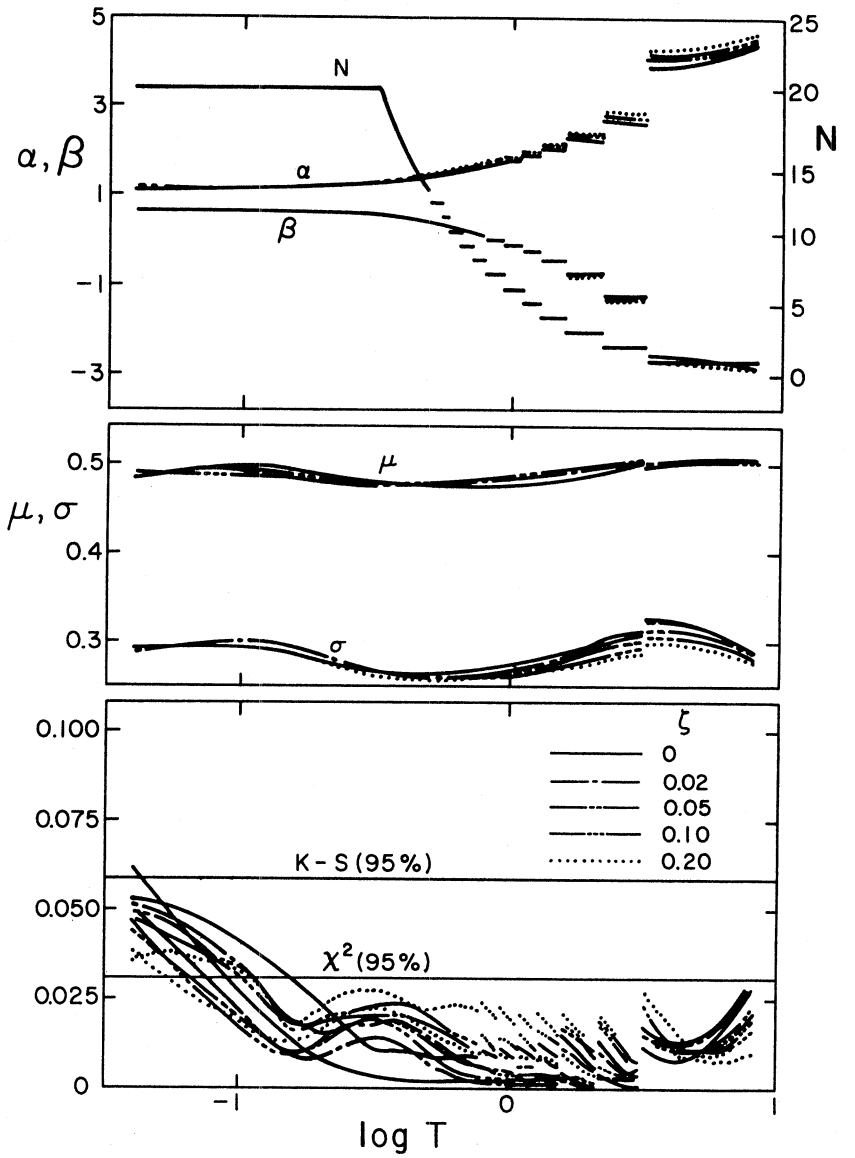

Figure 42

Parameters for one set of distributions (3) which approximately give p_a as a function of p_ℓ. The upper curves give α, β, and N (equation (3)). N is quantized, but the individual integers cannot be illustrated on this scale, so N is drawn as a continuous line.

The central section gives the parameters μ and σ derived from α, β and N using equations (6) through (9) in Trifunac and Anderson (1977). The lower section shows the statistical quality of fit by the Kolmogorov-Smirnov and the χ^2 criteria. The χ^2 test can be recognized by its smaller amplitudes for periods in the central and left portions of the graph. The levels marked K-S (95%) and χ^2 (95%) are those which, if exceeded, lead to rejection of the assumed distribution at that frequency. The five lines are for the five values of damping, as indicated.

differences between computed and assumed p_a for K-S test (bottom). It is seen from this figure that, except for $T \approx 0.1$ and χ^2 test only, the functions $\alpha(T)$, $\beta(T)$ and $N(T)$ lead to p_a versus p_ℓ which is acceptable at 95% confidence level.

Figures 43 and 44 present the values of $N(T)$ which lead to acceptable p_a versus p_ℓ in equation (3) for scaling in terms of MMI (Figure 39). Again, as in our earlier studies (Trifunac and Anderson, 1977; 1978), permissible values of $N(T)$ are much smaller than what would be expected on the basis of empirically determined duration of strong shaking (Trifunac and Westermo, 1976b). We choose $N = 2$ for $T \leq .4$ sec and $N = 1$ for $T > .4$ sec. Figure 45 then presents $\alpha(T)$ and $\beta(T)$; $\mu(T)$ and $\sigma(T)$; and the results of χ^2 and K-S tests for goodness of fit. It is seen that with these values of $\alpha(T)$, $\beta(T)$ and $N(T)$ (also see Table III), the model in equation (3) is acceptable for all T with 95% confidence level.

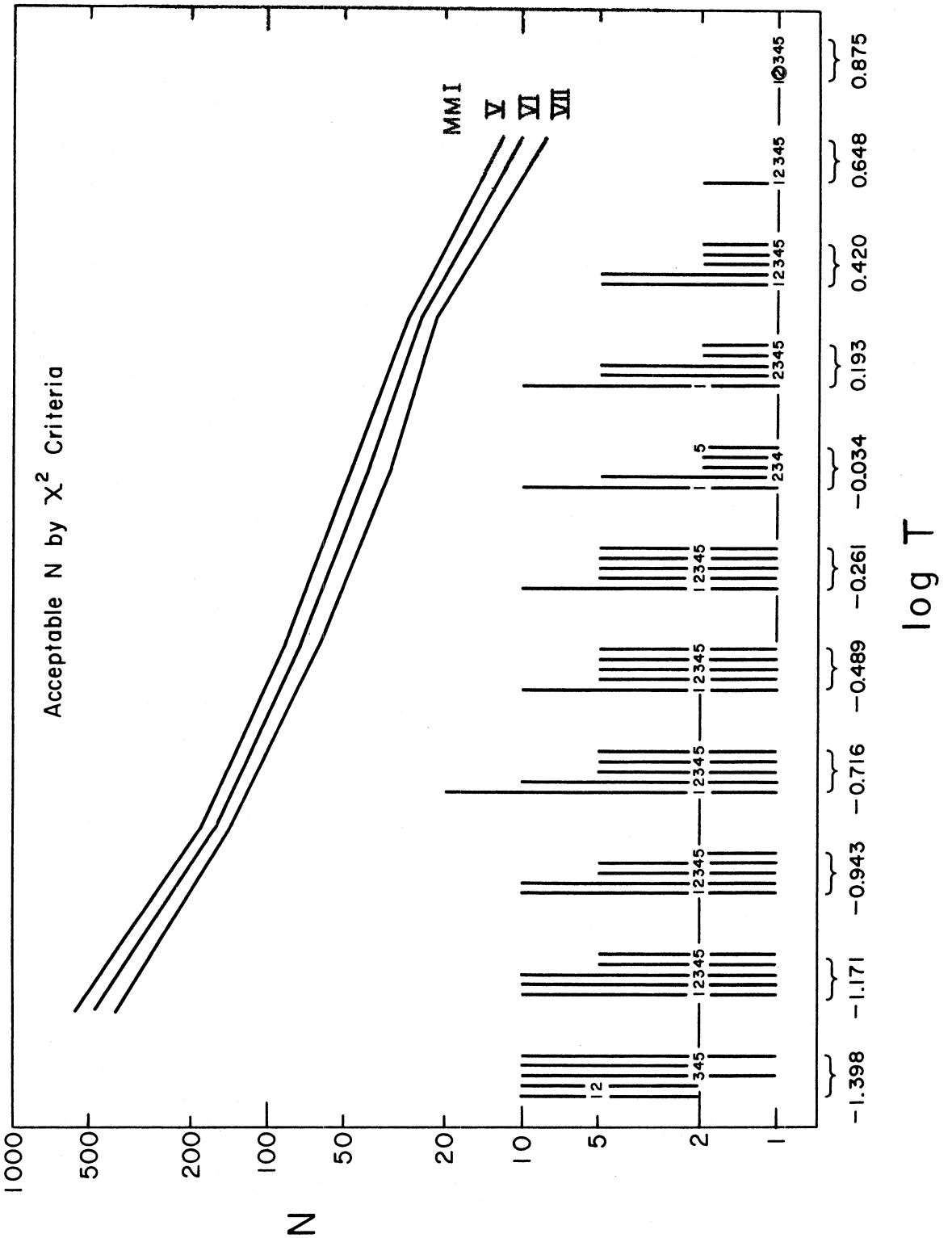

Figure 43

Results of the χ^2 statistical test to determine which values of N are acceptable to fit the data of p_a vs. p_ℓ for the regression of SV with Modified Mercalli Intensity. The upper lines show those N which might be expected on the basis of results of Trifunac and Westermo (1976b) for intensity V, VI and VII shaking. For the later regression, we chose the N indicated by the light line. Other symbols are as in Figure 40.

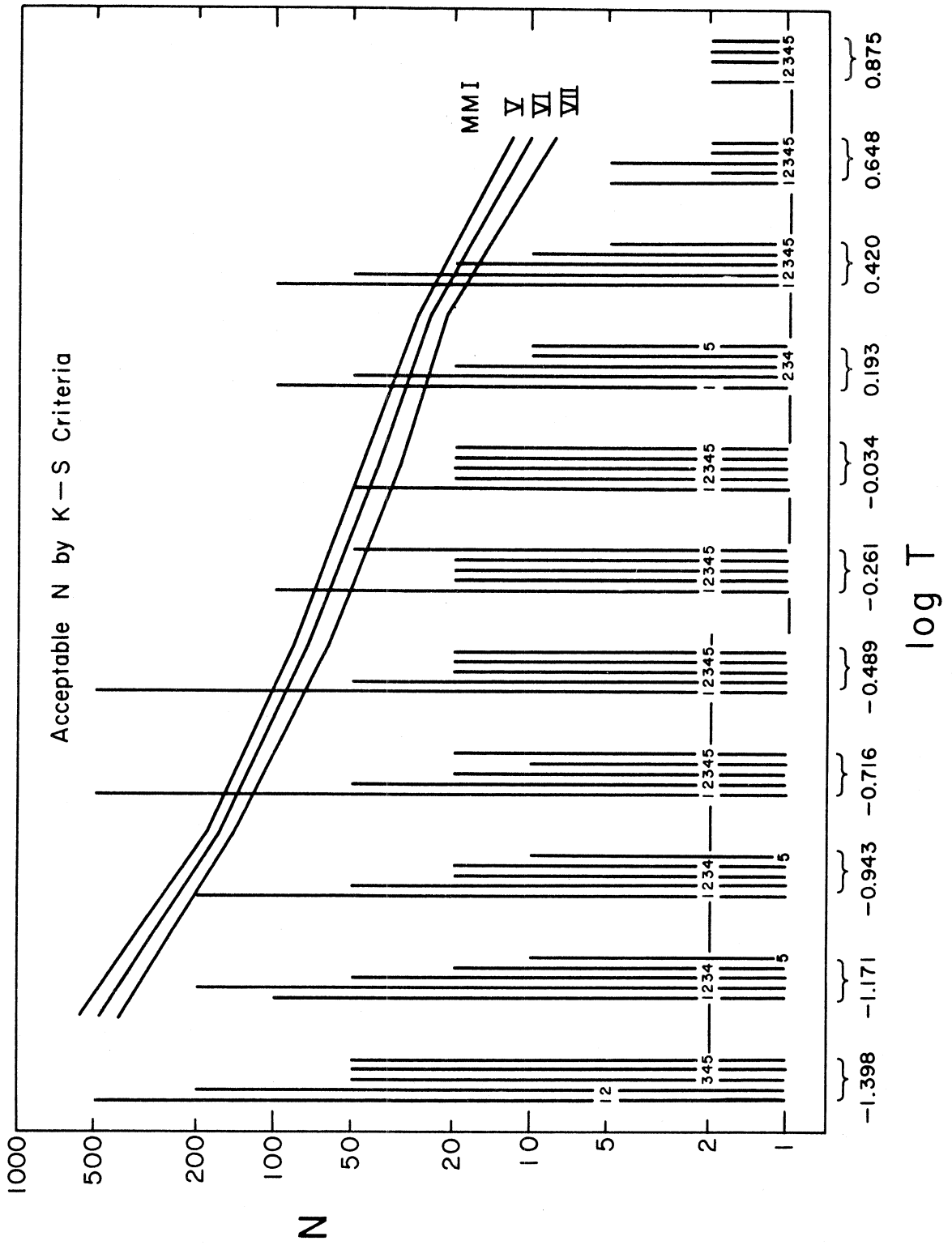

Figure 44

Equivalent of Figure 43, except that it shows the results of the Kolmogorov-Smirnov test.

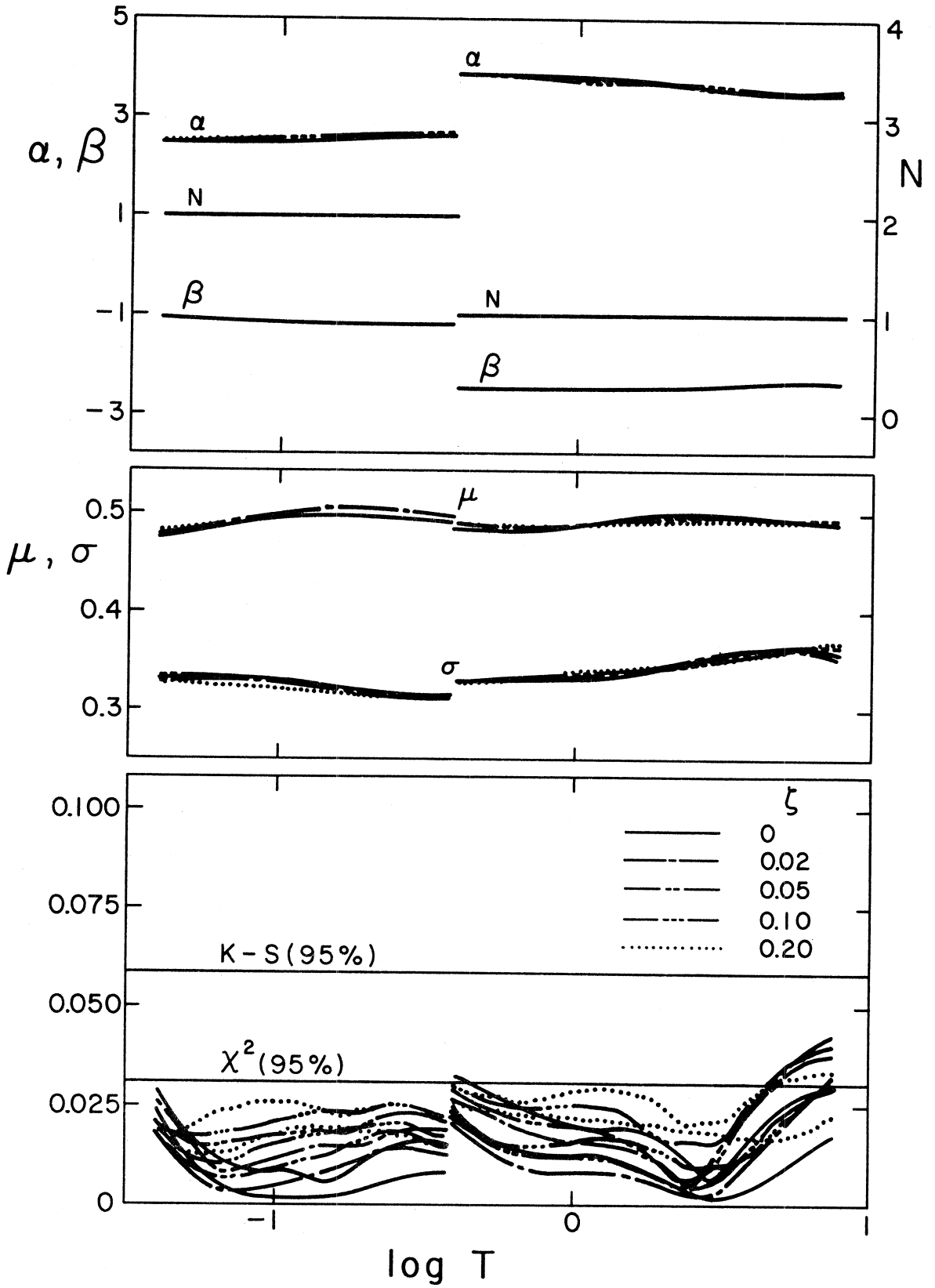

Figure 45

Equivalent of Figure 42 for the regression of SV with intensity

CONCLUSIONS

In this report, we have duplicated the empirical analyses done previously for SA and PSV spectra and applied it to SV spectra. Since essentially all methods and procedures are identical to those we used to derive models for SA and PSV spectra, only those discussions and descriptions of the procedures which are essential for the completeness of this report have been duplicated. Thus, the reader interested in details on why and how certain procedures have been developed should begin by studying our previous papers and reports (Trifunac, 1976, 1978; Trifunac and Anderson, 1977, 1978).

Conclusions regarding general properties of the empirical models are also identical to those we reported on previously. Thus, we conclude by a quote from Trifunac and Anderson (1978): "...

1. The rate of growth of spectral amplitudes decreases with increasing magnitude.
2. Spectral amplitudes at high frequencies tend to be higher on basement rock sites (s=2) than on alluvium sites (s=0). This trend is consistent in all empirical models studied, so far, but the differences in spectral amplitudes seem not to be significant at high frequencies. At long periods, this trend is reversed and becomes significant.
3. The differences in amplitudes of horizontal versus vertical SV spectra depend on the period T and cannot be approximated by a constant.

4. The scatter of SV spectrum amplitudes about the regression model (1) in terms of earthquake magnitude, M, and epicentral distance, R, is not smaller than the scatter of the same amplitudes about the empirical model (2) in terms of MMI.
5. The distribution of SV spectrum amplitudes about the two regression models (1) and (2) is not inconsistent with the assumed Rayleigh distribution of the peaks of response amplitudes.
6. For the largest possible levels of strong shaking and well outside the range where equations (1) and (2) apply, we found that these two empirical models are consistent.

Finally, it should be noted that, as for other related models, the results of this report should be considered as preliminary since when more abundant and complete data becomes available, it will be possible to develop better, more detailed and more complete empirical scaling methods. In the meantime, the models presented here may serve as an interim basis for estimation of SV amplitudes and for known or assumed parameters describing the strong shaking."

ACKNOWLEDGEMENTS

This research has been supported in part by a grant from the National Science Foundation and by a contract from the Nuclear Regulatory Commission.

REFERENCES

Richter, C.F. (1958). Elementary Seismology, Freeman, San Francisco.

Trifunac, M.D. (1973). Analysis of Strong Earthquake Ground Motion for Prediction of Response Spectra, International J. of Earthquake Eng. and Struct. Dyn., Vol. 2, No. 1, 59-69.

Trifunac, M.D. (1976). Preliminary Empirical Model for Scaling Fourier Amplitude Spectra of Strong Ground Acceleration in Terms of Earthquake Magnitude, Source to Station Distance and Recording Site Conditions, Bull. Seism. Soc. Amer., 66, 1343-1373.

Trifunac, M.D. (1978). Preliminary Empirical Model for Scaling Fourier Amplitude Spectra of Strong Ground Acceleration in Terms of Modified Mercalli Intensity and Recording Site Conditions, Int. J. Earthquake Eng. and Struct. Dyn., (in press).

Trifunac, M.D., and J.G. Anderson (1977). Preliminary Empirical Models for Scaling Absolute Acceleration Spectra, Dept. of Civil Eng., Report No. CE 77-03, U.S.C., Los Angeles.

Trifunac, M.D., and J.G. Anderson (1978). Preliminary Empirical Models for Scaling Pseudo Relative Velocity Spectra, Dept. of Civil Eng., Report No. CE 78-04, U.S.C., Los Angeles.

Trifunac, M.D., and A.G. Brady (1975). On the Correlation of Seismic Intensity Scales with the Peaks of Recorded Strong Ground Motion, Bull. Seism. Soc. Amer., 66, 139-162.

Trifunac, M.D., and B.D. Westermo (1976a). Dependence of Duration of Strong Earthquake Ground Motion on Magnitude, Epicentral Distance, Geologic Conditions at the Recording Station and Frequency of Motion, Dept. of Civil Eng., Report No. 76-02, U.S.C., Los Angeles.

Trifunac, M.D., and B.D. Westermo (1976b). Correlation of Frequency Dependent Duration of Strong Earthquake Ground Motion with the Modified Mercalli Intensity and the Geologic Conditions at the Recording Stations, Dept. of Civil Eng., Report No. 76-03, U.S.C., Los Angeles.